Master Thesis
TVVR 15/5010

Coastal evolution at Macaneta Spit, Mozambique

An analysis of longshore and cross-shore processes

Christofer Karlsson
Johan Liljedahl

Division of Water Resources Engineering
Department of Building and Environmental Technology
Lund University

Coastal evolution at Macaneta Spit, Mozambique – an analysis of longshore and cross-shore processes

By:
Christofer Karlsson
Johan Liljedahl

Master Thesis

Division of Water Resources Engineering
Department of Building & Environmental Technology
Lund University
Box 118
221 00 Lund, Sweden

Water Resources Engineering
TVVR-15/5010
ISSN 1101-9824

Lund 2015
www.tvrl.lth.s
Master Thesis
Division of Water Resources Engineering

Department of Building & Environmental Technology
Lund University

English title:	Coastal evolution at Macaneta Spit, Mozambique – an analysis of longshore and cross-shore processes
Author(s):	Christofer Kalsson Johan Liljedahl
Supervisor:	Magnus Larson Jaime Palalane
Examiner:	Hans Hanson
Language	English
Year:	2015
Keywords:	Macaneta spit, Maputo, Mozambique, overwash, erosion, breaching, cross-shore modeling, longshore modeling, EBED

LUNDS TEKNISKA HÖGSKOLA
Lunds universitet

Lund University
Faculty of Engineering, LTH
Departments of Earth and Water Engineering

This study has been carried out within the framework of the Minor Field Studies (MFS) Scholarship Programme, which is funded by the Swedish International Development Cooperation Agency, Sida.

The MFS Scholarship Programme offers Swedish university students an opportunity to carry out two months' field work in a developing country resulting in a graduation thesis work, a Master's dissertation or a similar in-depth study. These studies are primarily conducted within subject areas that are important from an international development perspective and in a country supported by Swedish international development assistance.

The main purpose of the MFS Programme is to enhance Swedish university students' knowledge and understanding of developing countries and their
problems. An MFS should provide the student with initial experience of conditions in such a country. A further purpose is to widen the human resource base for recruitment into international co-operation. Further information can be reached at the following internet address: http://www.tg.lth.se/mfs

The responsibility for the accuracy of the information presented in this MFS report rests entirely with the authors and their supervisors.

Gerhard Barmen

Gerhard Barmen
Local MFS Programme Officer

Postadress Box 118, 221 00 Lund *Besöksadress* John Ericssons väg 1 *Telefon dir* 046-222 9657, *växel* 046-222 00 00 *Telefax* 046-2229127
E-post Gerhard.Barmen@tg.lth.se

Acknowledgements

This report on *Coastal evolution at Macaneta spit – an analysis of cross-shore and longshore processes* is the final part of our master thesis project for Master of Science in environmental engineering at Lund University. The thesis has been carried out at the department of Water Resources Engineering at the Faculty of Engineering, LTH and in cooperation with Eduardo Mondlane University in Maputo. The study was performed in the spring 2015, which of nine weeks was spent in Mozambique.

First of all we would like to thank our supervisor at Water Resources Engineering at Lunds Tekniska Högskola, Professor Magnus Larson for all help and support throughout the project, especially when handling the modeling softwares. We also want to express our warmest thanks to our supervisor in Maputo; PhD student Jaime Palalane, for all the great care and support during our stay in Maputo. Despite his huge workload he spent lots of time helping us with accommodation, organizing the field study and driving us between places. Without his help the master thesis would never have been realized. We also want to show our appreciation to our examiner, Professor Hans Hanson for finding the project and introducing us to Jaime.

Our warmest appreciation goes to Omar Khan at Eduardo Mondlane University for all the valuable comments and help he gave when processing the bathymetry in ArcGIS. Moreover we would like to thank Karin Larsson at the department of Physical Geographic and Ecosystem Science, Lund University who gave some final help with the interpolation of the bathymetric grid in ArcGIS.

For all the help with the GPS and Echo sonar equipment during our field investigations we would like to thank Leovigildo Cumbe, technician at the Hidraulic lab and António Zucula, technician at the Structure lab. We also wish to say a big thank you to António Santos, technician at the Soil Mechanics lab for his help with analysing the grain size distribution of our samples.

We would also like to express our gratitude to DHI for letting us take part of their collected data from their previous study of Macaneta. The data was used frequently to validate the probability in our results.

Last but not least we give our warmest gratitude to SIDA, the Department of Water Resource Engineering and Ångpanneföreningens Forskningsstiftelse for making the thesis economically possible.

Christofer Karlsson and Johan Liljedahl
Lund, 27th of May 2015

Abstract

Macaneta spit is located about 30km north of Maputo, Mozambique, with the Indian Ocean on the east side and Incomáti River on the west side of the spit, composing an interesting and vulnerable area from a hydrodynamic point of view. Few studies regarding coastal processes are done in the area and changes of the morphology could result in breaching of the spit and thereby affect both accessibility to the spit and the water supply for irrigation in the region. This master thesis was conducted as a minor field study in collaboration between Lund University, Sweden, and Eduardo Mondlane University, Mozambique. The study investigates the coastal evolution of the Macaneta spit, with hope to provide an understanding of the hydrodynamic conditions present at Macaneta and thereby assist policy makers in setting up priorities and taking preventive measures to for example avoid breaching of the spit. The investigation includes field studies at Macaneta together with modeling of cross-shore and longshore processes for the period 2005-2015. Modeling wave propagation from offshore in EBED generated a local nearshore wave condition used as input to the cross-shore and the longshore simulations. Result from the simulations was analyzed together with historical images of Macaneta to quantify the risk of overwashing and breaching of the spit at critical sections along the spit. The result obtained indicates that there is a stable condition in the northern part of the spit, although overwash events seem to occur often. In the southern part of the spit an eastern migration is observed. Moreover, ongoing erosion at the narrow isthmus in this region can be seen from satellite images. Further studies of the area are highly recommended, in particular for coastal sections evidently more prone to the risk of breaching.

Keywords: Macaneta spit, Maputo, Mozambique, overwash, erosion, breaching, cross-shore modeling, longshore modeling, EBED

Sammanfattning

Barriärhalvön Macaneta är belägen 30km norr om Maputo, Mozambique, med Indiska oceanen i öst och floden Incomáti i väst, där utgör den ett intressant och utsatta områdena ur ett hydrodynamiskt perspektiv. Få studier är gjorda rörande kustprocesser i området och förändringar i morfologin skulle kunna resultera i genombrott av barriärhalvön och därmed påverka både tillgängligheten av barriärhalvön samt tillgången på bevattningsvatten i regionen. Denna masteruppsats har utförts som en mindre fältundersökningsstudie i samarbete mellan Lunds Tekniska Högskola och Eduardo Mondlane Universitet, Mocambique. Studien utreder kustutvecklingen av barriärhalvön Macaneta, med hopp om att ge förståelse av förutsättningarna i kustområdet och därmed bistå beslutsfattare vid fastställande om prioritering och förebyggande åtgärder. Utförda undersökningar inkluderar fältundersökningar av Macaneta samt modellering av vinkleräta och parallella kusttransporter för perioden 2005-2015. Modellering av inkommande vågors fortplantning med EBED genererade det lokala vågklimatet vilket användes som ingående data för simulering av vinkleräta och parallella kusttransporter. Resultatet från utförda simuleringar analyserades tillsammans med historiska satellitbilder av Macaneta för att kvantifiera risken för överspolning och genombrott vid kritiska sektioner längs barriärhalvön. Erhållna resultat indikerar att stabila förhållanden återfinns i de norra delarna av barriärhalvön även då överspolning verkar ske ofta. I de södra delarna av barriärhalvön har en östlig migration observerats. På denna del av barriärön indikerar satellitbilder en pågående erosion av det smalaste näset. Fortsatta studier av området rekommenderas starkt, särskilt för av kustsektionerna med större risk för genombrott.

Table of content

1. Introduction

1.1 Background

Coastal zones are among the most productive and vulnerable areas in the world. The zone where ocean meets land offers a wide variety of valuable habitats and ecosystems, and plays an important role for human settlements and activities. Coastal areas are subjects to constant morphological changes, some regions at a higher pace and more extreme than others. Erosion and accretion are acknowledged phenomenons in many coastal regions around the world and accordingly dominant processes for coastal dynamics in Mozambique where the conducted study was carried out, Figure 1.

The natural erosion represent more than 90% of the erosion of the coastline in Mozambique and is driven by natural processes that arises due to tropical depressions, cyclones and recent relative sea level rise (Moreira M. E., 2005). Moreover, longshore sediment transport generated by currents and breaking waves also make up for the natural erosion (Palalane, Larson, Hanson, & Juízo, 2015). In addition to the erosion driven by natural processes, human activities contribute to accelerating erosion rates and are in many areas responsible for transfer the problems to new coastal stretches (Fanos, 1995). The anthropogenic activities are based on the urban and tourism pressure of areas adjacent to the coastline. The removal of onshore protection such as mangroves and dune vegetation to make room for housing, construction of hotel resorts on top of the dunes or structures like harbors or piers across the coastline has changed the sediment transport pattern and lead to considerable coastal erosion (Langa, 2007; Chemane D, Motta H., Achimo M., 1997). The sediment transport is also influenced by dredging of Maputo Bay that subsequently could contribute to the coastal erosion in the region (Bird & Lewis, 2015; Ruby, Canhanga, & Cossa, 2008).

The coastal erosion leads to economic, environmental and social losses for the affected society. The nearly 2800km long coast of Mozambique (CIA, 2014) possesses associated vulnerability, and a deeper knowledge of the governing coastal processes is crucial to secure future development along the coastline. The coast plays an important role for the fishery, agriculture, and tourism and is one of the most valuable

assets in the country with potential to contribute significantly to the national income and at the same time provide social and economic benefits to the population in the coastal areas. Around 40% of the population in Mozambique lives in the coastal districts, which by area represents less than 23% of the country, and most of the major cities are located close to the sea (Chemane, Motta, & Achimo, Vulnerability of coastal resources to climate changes in Mozambique: a call for integrated coastal zone management, 1997).

The coastal stretch of Macaneta spit is located about 30km north of Maputo, Mozambique, and constitutes the coastal area of our study. The spit is known for its attractive and clean beach. Macaneta offers several resorts and is a popular tourist destination for visitors and residents of the southern Mozambique and South Africa. Moreover there are also some local residents at Macaneta living mainly off what the sea offers. Few studies regarding coastal processes are done in the area and changes of the morphology could have significant impact on the entire region of Maputo.

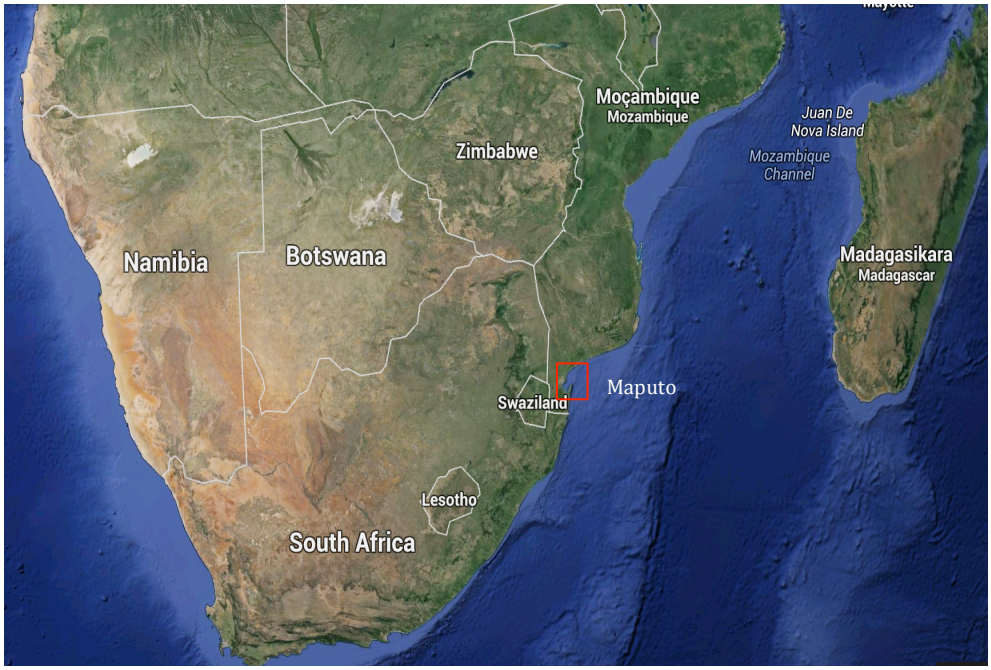

Figure 1. Geographical location of Mozambique and Maputo *(Google Earth, 2014).*

1.2 Objectives

Coastal regions are heavily exposed to natural and anthropogenic effects causing great consequences for national economic development. However, few scientific studies exist in the subject of coastal development in Mozambique (Palalane, Larson, Hanson, & Juízo, 2015). The main objectives of this study are to investigate and quantify the processes governing sediment transport and coastal evolution of the Macaneta spit in Maputo, Mozambique, Figure 2. With the hope to provide an understanding of the conditions present at Macaneta and thereby assist policy makers in setting up priorities and taking preventive measures. The effects of both longshore and cross-shore transport processes on the spit evolution will be studied using available historical data together with numerical models for wave transformation, sediment transport, and wave runup. A particular topic of interest is the probability for overwash and breaching of the spit from the ocean side, which is most at risk during storms events with strong waves coinciding with high sea water levels.

Figure 2. Overview of Maputo Bay together with the location of Macaneta spit and Inhaca Island *(Google Earth, 2014).*

1.3 Procedure

A literature review was performed of previous coastal evolution studies related to Macaneta Spit and surrounding coastal areas. Emphasis has been on the hydrodynamics, sediment transport and coastal evolution of the spit. However, general literature on nearshore waves, currents, sediment transport, and morphological processes was also performed.

Existing data related to nearshore processes (e.g., waves, currents, water levels, shorelines, beach profiles, and sediment characteristics) was collected from universities, government agencies and private companies with interests related to the coast. The data was thereafter compiled and analyzed. Additional field data collection was carried out during two weeks in March/April of 2015, focusing on mapping the general morphology, measuring shoreline positions, recording beach profiles, performing sediment sampling, and measuring nearshore bathymetric.

Mathematical models were applied to simulate the coastal processes at the spit, focusing on both the longshore and cross-shore transports. In the modeling, the regional wave transformation model EBED was first used to obtain realistic nearshore wave climates, taking into account the shadowing effects of the Inhaca Island Figure 2. Based on the modeled wave climates, the variation in the longshore sand transport along the spit was calculated, as well as the associated gradients to assess spit evolution. The wave climate was also used to determine dune erosion, overwash, and the likelihood of breaching at particularly exposed cross sections. The models were calibrated and validated, to the extent possible, against field data collected at the site and findings from previous studies.

1.4 Limitations

Due to lack of records regarding wave and tidal data the offshore wave data and tidal data was collected from reanalysis data provided by the Wavewatch III model and WXTide32, respectively. Although, these data are simulated they have been assumed correct. Due to lack of equipment no complementary measuring during the field study has been made for validation.

The report mainly focuses on the coastal processes on the seaside of the spit. To fully evaluate risks of overwash and breaching the riverside should be evaluated as a dynamic process working parallel with the ocean side processes. The effects from river are important but were considered to be outside the scope of this study.

2. The South Coast of Mozambique

The south coast of Mozambique stretches from Ponta de Ouro by the South African border 600km up to Inhambane. The climate in the southern region of Mozambique consists of a dry winter and rainy summer period. The area is classified as an equatorial desert according to the Köppen-Geiger climate classification (Köppen, 1936). The rainfall is mainly restricted to the rainy season October to March, and the dry season from April to September. The average precipitation is 800mm/year and the average annual temperature at the coast is 23°C. The predominant winds in the area are from southeast (Windfinder, 2015).

In the southern part of Mozambiqe the ground is composed of unconsolidated Quaternary rock mixed with younger recent sediments of sandy dune and plains. In the area around the large river mouths denser composed soils, alluviums, are also found. Sandy beaches with recent dunes characterize the coastline. The coastal area is typical low lands at the shore and rising landwards to above 200m above sea level at the distance of 15 to 140km from the coast (Chemane, Motta, & Achimo, 1997).

2.1 Macaneta Spit

The area for the study is Macaneta spit, located about 30km north of Maputo, **Fel! Hittar inte referenskälla.**. The northern boundary is the Macaneta Holiday Resort, the most southern located resort at Macaneta, and the southern boundary is formed by the tip of Macaneta spit, Figure 5. On the eastern side of the spit the Indian Ocean is found and to the west the estuary of Incomáti River. Focus of the study was put on the coastal processes of the ocean side of the spit. The survey area is about 12km long and has a width varying from 50 to 600 m. The studied spit demonstrates varying states of shoreline stability. In some parts of the area the distance between ocean and river is very short and the height difference between sea level and top of the dune is small. At these places it is of great importance to study the risk of breaching and overtopping. One of the narrowest sections with highest risk of overwashing is located just south of Macaneta resort, at this section only 50m of beach is separating river and ocean, Figure 4.

The bottom slope of northern part of Macaneta spit is quite large close to the beach and then becomes gentler further off coast. In the southern

part of the spit the bottom profile is more flat compared to northern part. At a distance of 15km east of the Macaneta spit is the Danae shoal located and south of the shoal is the Inhaca island Figure 3. These two features will have a huge impact on the wave climate at Macaneta spit as Inhaca island will protect Macaneta from waves in a southeast direction and the Danae shoal will reduce the wave energy from east, especially during low tide.

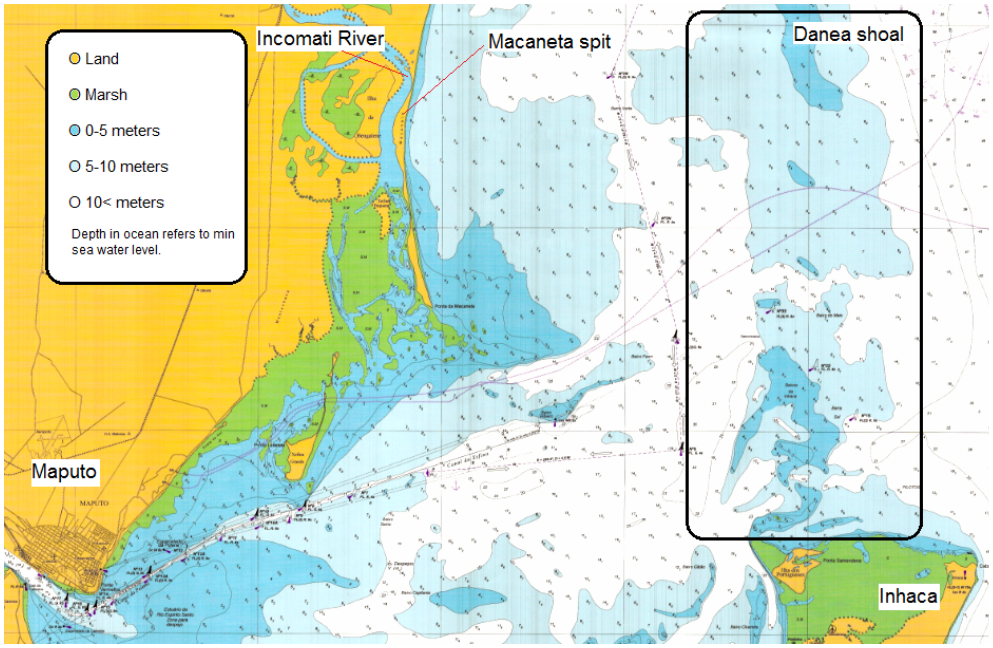

Figure 3. Sea chart over Macaneta spit and its surroundings (INAHINA, 2010).


Figure 4. The most northern part of the study area at Macaneta beach at the most narrow isthmus where breaching and overwash are of highest risk.

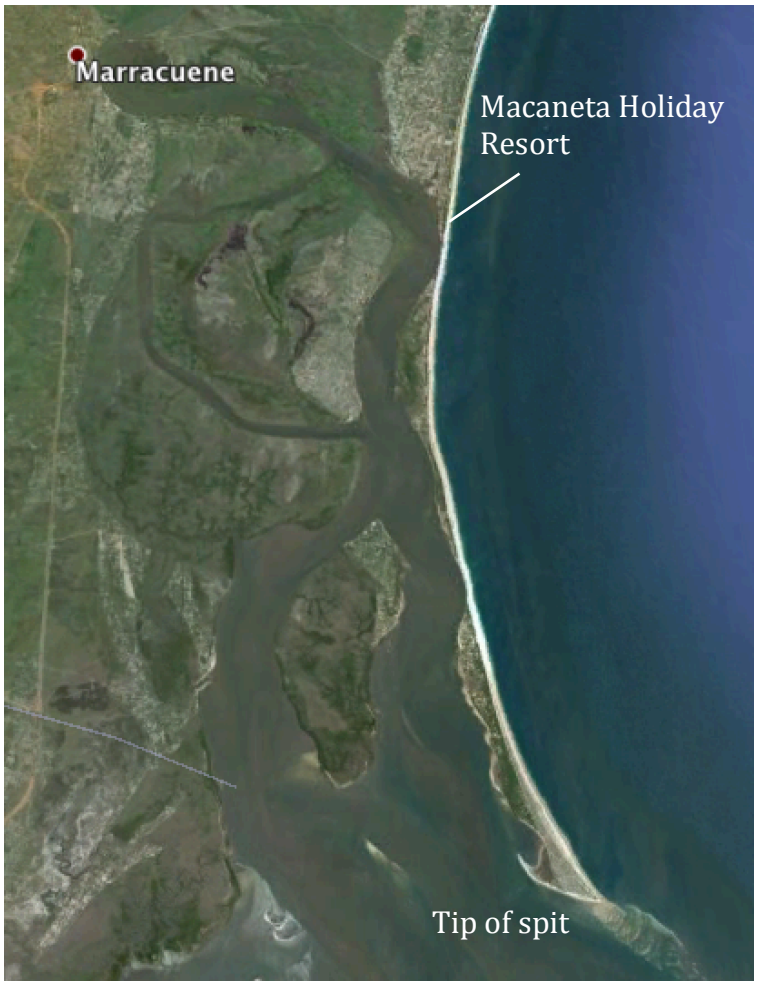

Figure 5. The study area at Macaneta beach , from Macaneta Holiday Resort in north to tip of the spit in south *(Google Earth, 2014).*

2.1.1 Activities in the area

Macaneta spit is an attractive recreational destination for tourists. Many people from Maputo and other areas visit the area, especially during the weekends. The recreational value is high due to the long, beautiful and clean beach. However, since there is lack of natural nearshore shelter of for example coral reef or sand banks the swimming conditions are quite rough making it unsuitable for families with children.

Macaneta beach also play an important role for the local fishery in the area. Many of the fishermen live north of the resort but have their boats and nets south of the resort and therefore have to cross at least one of the extremely narrow parts of Macaneta spit in order to access their boats, Figure 6.

Figure 6. Activities at Macaneta with fishermen pulling nets at the beach (left) and boat transporting tourists from Marracuene to Macaneta spit (right).

2.1.2 The future of Macaneta

Today most of the visitors at Macaneta arrive with the ferry from Marracuene on the opposite side of Macaneta. The ferry has a low capacity and can only carry a maximum of 4 cars each turn, causing long queues to the ferry during the weekends. In an effort to increase accessibility of Macaneta construction of a bridge have been initiated. When the bridge is completed the accessibility of Macaneta will be much higher and most probably also the touristic values of Macaneta. Increased tourism will lead to higher pressure of the spit with more people and possibly also vehicles on the beach and dunes interfering with the natural beach processes. Today there are some houses located along the spit Figure 7, but when the bridge is finished it will be easier to transport construction material to the spit and more houses will probably be built on the beach. Consequently the interference between the development of dunes and human settlements will increase.

Figure 7. Aerial photograpy of the peninsula with houses built on the dunes.

3. Coastal evolution processes

Understanding and being able to estimate hydrodynamic processes are of great importance as it principally determines the geometry of beaches and the evolution of a coastal region. Estimation of the wave climate is essential in nearly all coastal engineering studies and needed in order to design shore protection, hydraulic structures, marinas and other coastal structures.

The purpose of this chapter is to give a brief theoretical review of hydrodynamic and sediment processes with focus on the ones most important for the study at Macaneta.

3.1 Coastal hydrodynamics

3.1.1 Wind

Wind is the foremost abundant force for wave generation at sea. As the wind is acting on the boundary layer between air and sea, kinetic energy is transferred between the medias causing the water surface to move. The energy transferred to the sea, causing the movements on the sea surface, is limited by either the duration of the wind event or by the fetch over which the wind energy is accumulated (CEM, 2008).

The turbulent wind flow has small fluctuations in speed that create pressure variations over the sea surface that produce small ripples called capillary waves. This can be explained by the Bernoulli equation, stating that in order to maintain a constant energy head at a certain elevation an increase in velocity head must be equivalent to a decrease in pressure head and vice versa. The capillary waves add a roughness to the sea surface, which enables increasing strong winds to make the waves grow bigger (Herrington, 2012) Figure 8.

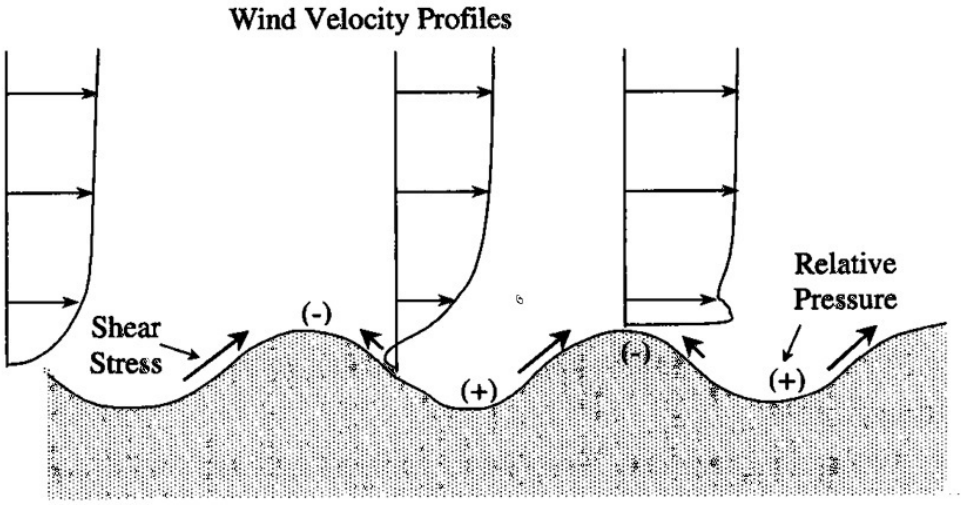

Figure 8. The mechanism of wind generated ocean waves. Displayed are the wind velocity profiles, relative pressure distribution and acting shear stresses (Warwick, 2011).

Pressure fluctuation amplifies the wave height. The wind velocity profile passing over the crest is considerably higher than the velocity profile over the trough. Consequently atmospheric pressure over the crest decreases while the pressure over the trough increases. Moreover the winds generate share stresses on the windward side of the crests, due to friction, pushing the waves forward (CEM, 2008).

In order to estimate the direction and size of wind generated waves the origin of the wind most be identified. Winds are influenced differently by the earth surface and its rotation depending on altitude (CEM, 2008). Within the atmospheric boundary layer winds are split into three regions depending on the level above earth surface, Figure 9.

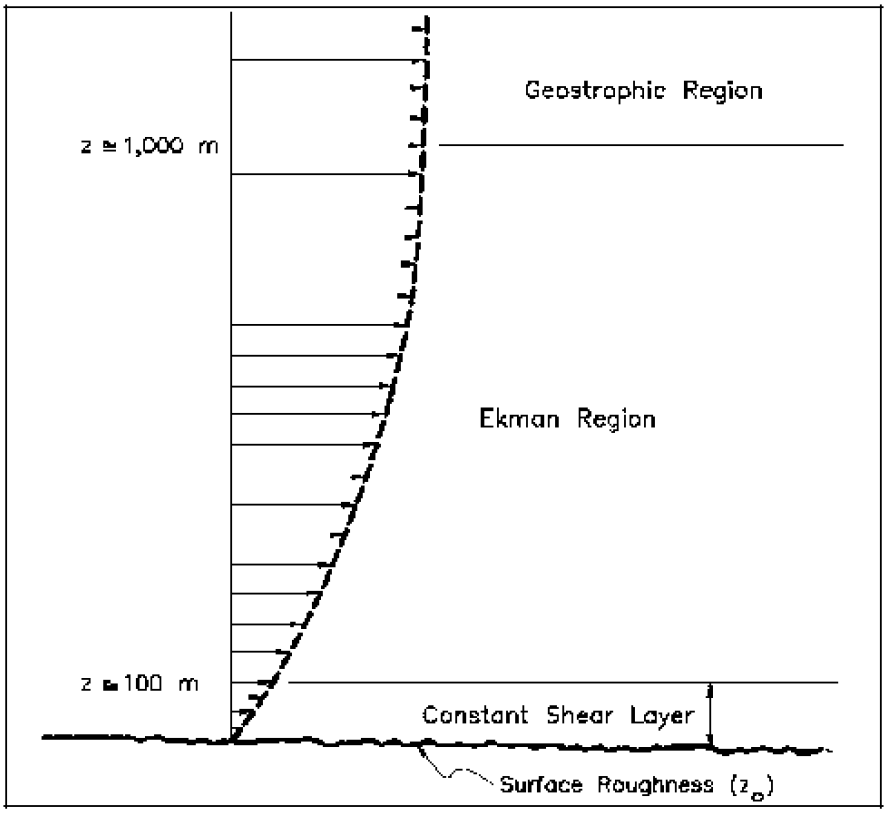

Figure 9. Wind velocity profile within the atmospheric boundary layer (CEM, 2008).

The bottom region closest to the water surface is called constant stress layer. The wind directions within the layer essentially remain constant as the Coriolis force has little or no effect in this region. Above this layer the Ekman region is found. The winds at these altitudes are more affected by the Coriolis force and winds at the top of the boundary layer deviate tens of degrees to the right of near surface wind directions. The top region is called the geostrophic layer. At this altitude the planetary surface are considered to lack influence on the winds and the wind variations are caused by mechanisms other than existing in the atmospheric boundary layer (CEM, 2008).

Given that the atmosphere is neutrally stable, the velocity profile for near surface winds within the constant stress layer can be expressed as:

$$U_z = \frac{U_*}{k} \ln \frac{z}{z_0} \quad (3.1)$$

where
U_z = wind speed at height z above the surface
U_* = friction velocity
k = van Kármán's constant (approximately equal to 0.4)
z_0 = roughness height of the surface

The international reference level for wind measurement is 10m above surface. For measurements carried out at other elevations a correction for the wind speed must be accounted for. Moreover correction for temperature difference between air and sea, position of the gauge and duration of the wind event has to be considered in order to estimate the effective wind speed of the winds generating the waves (CEM, 2008).

3.1.2 Waves

Ocean waves are primarily generated by wind but long waves may also originate from tides, atmospheric variations and geological activity. A substantial amount of wave energy is dissipated in the nearshore region; responsible for forming beaches, transporting sediment cross-shore and longshore and exert force on coastal structures (CEM, 2008).

The wave propagation is determined by a number of different processes affecting the wave energy and thus the direction, size and frequency of the waves. Waves will gain energy from a boosting wind or current while interference with structures or bottom will cause dissipation of wave energy. In the studied region Danae shoal act as a typical sink for dissipation of wave energy and constitutes the calmer wave climate at Macaneta.

3.1.2.1 Linear wave theory

The simplest mathemathical wave theory is a first order model called linear wave theory. The representation assumes that ocean waves are two-dimensional, small in amplitude, consistent, sinusoidal and that the fluid is homogenous and ideal with constant density and no viscosity. Furthermore, the Coriolis effect and surface tension are neglected and

the ocean floor is assumed to be a horizontal boundary with no vertical transport. A high order theory might give a description of higher satisfactory regarding the waves behaviour. However due to simplifications the linear wave theory is easy to apply on numerous of different problems within coastal hydraulics and presents results with reasonable accuracy of wave characteristics for a wide range of wave parameters (CEM, 2008).

A sinusoidal wave is often described by three basic characteristics: wave length (length between corresponding points on two successive waves), wave period (time it takes for the crests of two successive waves to pass a fixed point) and wave height (elevation difference between trough and following crest) (CEM, 2008).

The progressive waves move forward with a steady velocity. However, it is only the form of the wave moving forward, the water particles themselves more or less orbits during the wave motion and end up in the same position after one wavelength has passed. The movement of the water particle depends on the interaction with the bottom, Figure 10. To describe the interaction between wave and bottom relative depth is introduced. The expression is defined as the relationship between the water depth (d) and the wave length (L) (CEM, 2008).

$$Relative\ depth = d/L \tag{3.2}$$

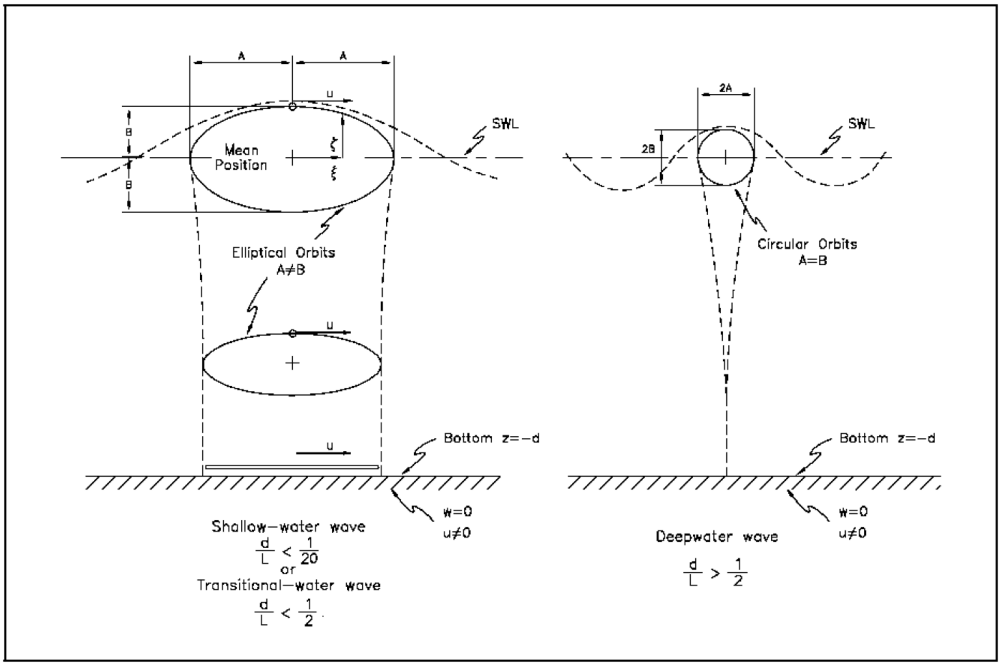

Figure 10. Water particle movement for a deep water wave and a shallow or transitional water wave (CEM, 2008).

The wave motion affects the water down to half a wavelength beneath the surface. As seen in Figure 10, a deep-water wave has a relative depth greater than 1/2 and does not affect the bottom, thus the complete motion of the water particle is a circle. On the contrary shallow water waves with a relative depth less than 1/20 and transitional water waves with a relative depth between 1/2 and 1/20 interact with the seafloor and the orbit of the water particles are more elliptic (CEM, 2008).

The motion of shallow water waves has a strong interaction with the bottom, affecting both wave and seafloor, stirring up and displacing sediment. The orbit of the water particles are consequently flat elliptic for these waves with a large horizontal displacement at both surface and bottom and a high net transport of both water and sediments. By feeding nearshore currents and contribute to the nearshore water circulation the resulting transporting force of the water account for sediment transport onshore, offshore and alongshore (CEM, 2008).

3.1.2.2 Wave transformation

When waves approach the shore and enter shallower water interactions with the bottom and coastal structures will affect the waves and have impact on wave setup, runup, nearshore currents and sediment transport. Processes causing wave transformation when approaching shore are among others refraction, shoaling, diffraction and reflection, all further explained below.

Shoaling is the process deforming the waves. The process starts as waves enters transitional water depth by reducing the wave propagation velocity. The transported energy will thereby be transformed within the wave and cause shortened wavelength and increased wave height. As the waves approach the shore with decreasing water depths wave amplitude grow gradually higher, the crest steepens and shortens and the troughs become longer and flatter. The process will progress until the point where the wave can no longer propagate, causing it to break.

The refraction process alters the wave direction at shallow water, causing the incoming waves to align with the depth contours and consequently approach the coast perpendicularly to the shoreline. Refraction is caused by the velocity difference in wave propagation between shallow and deep water. A difference in water depth along the wave crest will thereby cause the wave portion above deeper water to move at a higher velocity than the other part and the wave will turn accordingly. At the tip of the Macaneta spit refraction is significant, the complicated bathymetry causes waves to alter the direction considerably.

Diffraction is the phenomena describing the lateral energy transmittance along the wave crest, perpendicular to the direction of wave propagation. It will act to even out variation in wave height over a wave crest, transferring energy from points of higher to lower wave height. The process is also prominent when considering sheltering coastal structures such as breakwaters, causing the waves to spread into the lee zone behind the structure and thereby also reduce the force of the wave. In the study Inhaca island was found to cause considerable diffraction of offshore waves affecting the direction of the wave field at Macaneta.

As waves propagate parts of the waves will be reflected due to changing water depths or interference with coastal structures and landforms, thereby reducing the force of the propagating wave. How much of the

wave that will reflect depends on the slope of the structure, how impermeable it is and the stability of it. A vertical concrete caisson will reflect almost the entire wave energy while a flat beach, where the energy from the wave breaking is well dissipated, will generate a low reflection.

In the study of the coastal hydrodynamic processes at Macaneta shoaling, refraction and diffraction has been considered. However, in the wave modeling at Macaneta the process of reflection was not included.

3.1.2.3 Wave breaking in the surf zone

Within the surf zone wave breaking is the dominant hydrodynamic process. Shoaling causing the shore-approaching waves to grow steeper until reaching their limit at which they will brake. Breaking of waves occurs approximately at a depth equal to the wave height. However, the breaking depends on both wave, and shore characteristics whereupon several studies have been carried out to define a relationship to predict the incipient breaking height for waves. From the studies a parameter known as the breaking index (γ_b) was introduced. It is defined as the relationship between the breaking height (H_b) and the breaking depth (d_b), Figure 11.

$$\gamma_b = \frac{H_b}{d_b} \tag{3.3}$$

From laboratorial studies of smooth and uniform slopes the expression for the non-dimensional breaking index was developed. Apart from breaking height and depth, breaking index was derived to be depending on the wave steepness described by the relationship between breaking height, gravitational acceleration (g) and wave period (T) and the bottom slope represented by the empirically determined functions (a) and (b).

$$\gamma_b = a - b\frac{H_b}{gT^2} \tag{3.4}$$

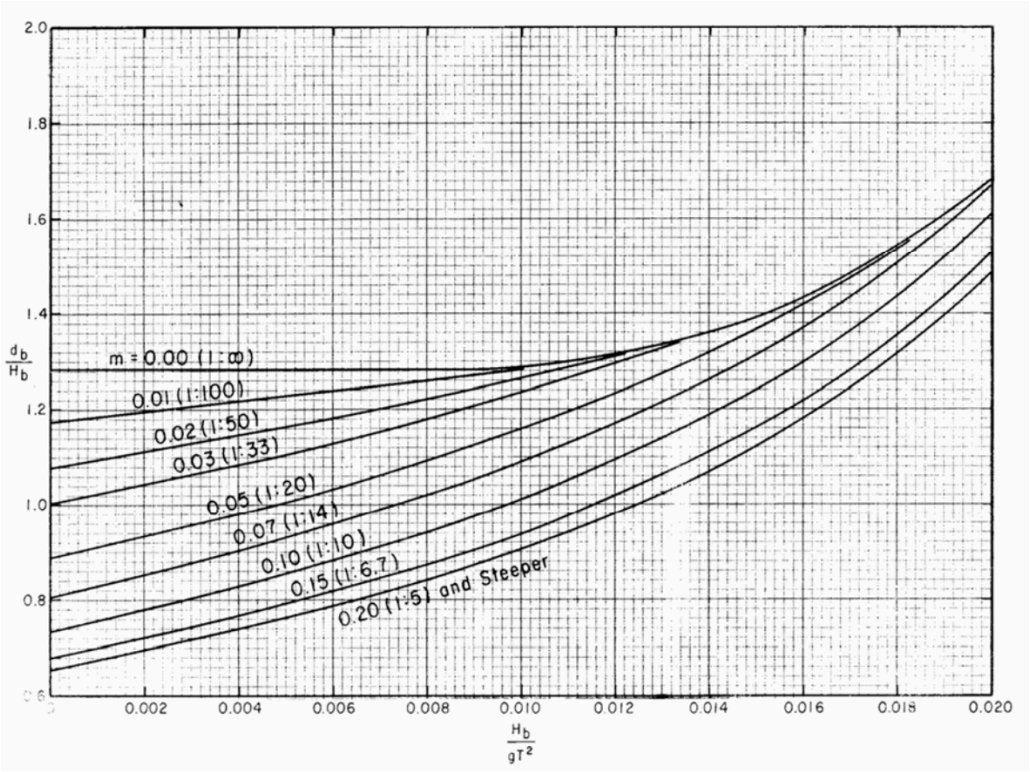

Figure 11. Relationship between breaking index, wave steepness and slope (CEM, 2008).

As the slope approaches zero the breaking index will receive the theoretical value of 0.78, while a slope that approaches infinity will generate a doubled value of 1.56. For nonuniform beach slopes the average bottom slope from the breking point to a point one wavelength offshore should be used.

If the waves break or not at shore have a big impact on the sediment transport at the beach. Waves breaking will create more turbulence and act with a bigger force on the bottom than non-breaking and thereby both scour troughs in the bottom and stir up and displace sediments. From field investigations at Macaneta it was concluded that the waves are breaking at shore.

3.1.3 Nearshore currents

The water circulation taken place in shallow and transitional waters represents nearshore currents. Breaking waves, tidal motion, wind and gravitational forces induces the currents (CEM, 2008).

In the surf zone the most dominant current is the longshore current, Figure 12, induced by the breaking of oblique incident waves. Perpendicular to the shoreline towards sea the undertow current is found. It acts as the compensating fluid transport to cross-shore propagating waves. The undertow acts along the bottom, transporting suspended sediments offshore and causing erosion of the shore. The rip current acts, just as the undertow, perpendicular to the shoreline and is induced by waves with a small approaching angle, which inhibit stable longshore currents. Instead of a continuous unidirectional flow, the longshore current will alternate in both directions forming strong cross-shore currents along the shoreline. The occurrence of rip currents may both be caused by and lead to the formation of a bowl shaped shoreline. Moreover man-made structures redirecting the longshore flow could also cause rip currents (CEM, 2008).

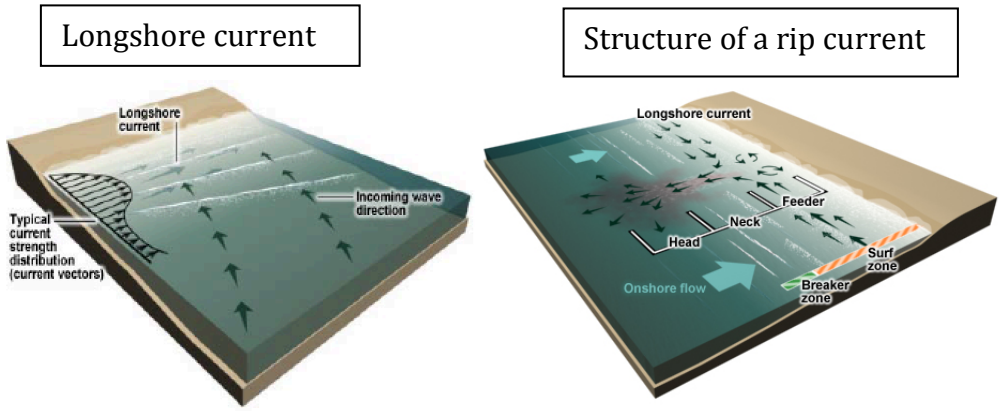

Figure 12. Longshore current distribution and structure of rip current (The Comet Program, 2012).

3.1.4 Water level variations

The water level has a major impact on the nearshore processes. Both wave transformation and point of breaking is dependent on the depth, hence the water level will determine the section of the shoreline affected by the incoming waves (CEM, 2008).

Tidal variations are short-term water level changes generated by the gravitational attraction by primarily the moon. The tidal range is at its maximum during new moon and full moon, when the alignment with the sun boost the tidal force. The tides at this time of the month are called spring tides. The weakest tides are called neap tides and are found when the sun and moon are right angled (CEM, 2008).

Short-term variation in water levels could also be the result of air pressure and winds. During low air pressure and strong winds the water surface could generate a short-term increase in the water level. This phenomenon is called a storm surge and if coinciding with a high spring tide it could lead to serious erosion and flooding of coastal areas (CEM, 2008). In the case for Macaneta these events are associated with the highest risk for breaching.

3.2 Sediment transport

Hydrodynamic processes controlling the wave activity, water level variations and currents presented in the section above will interact with sediment in the nearshore region. The sediments will suspend in the water column when the turbulence created by these physical properties is strong enough and thereafter displace the sediments with the motion of the fluid. The flow conditions are however not the only controlling variable for the coastal evolution of a shore. The transport rate is also dependent on fluid and sediment properties. Grain size distribution of sediments play an important role as it defines the amount of energy needed to suspend the sediments. To be taken into consideration are also the fall velocity, grain density, volume concentration and angle of repose. The effect of the transport may vary widely. Sometimes the only impression left is a limited redisposition of sand into bar, troughs, or rhythmic embayments cut into the beach. While other times the displacement of sediments along and perpendicular to the coast may add

up to hundreds of thousands or even millions of cubic meter each year (CEM, 2008).

The threshold values for sediment motion is determined by the function of orbital velocity under the waves, wave period and grain diameter, see Figure 13. During short wave periods with coarse grain a higher fluid velocity is needed to move the sediment (Komar P. , 1976). Do to this reason course sediment form steeper beach slopes while fine sediment are found at gentler slopes on beaches of more erosive nature (CEM, 2008).
The steep slope of Macaneta corresponds with the coarse sediment found at site.

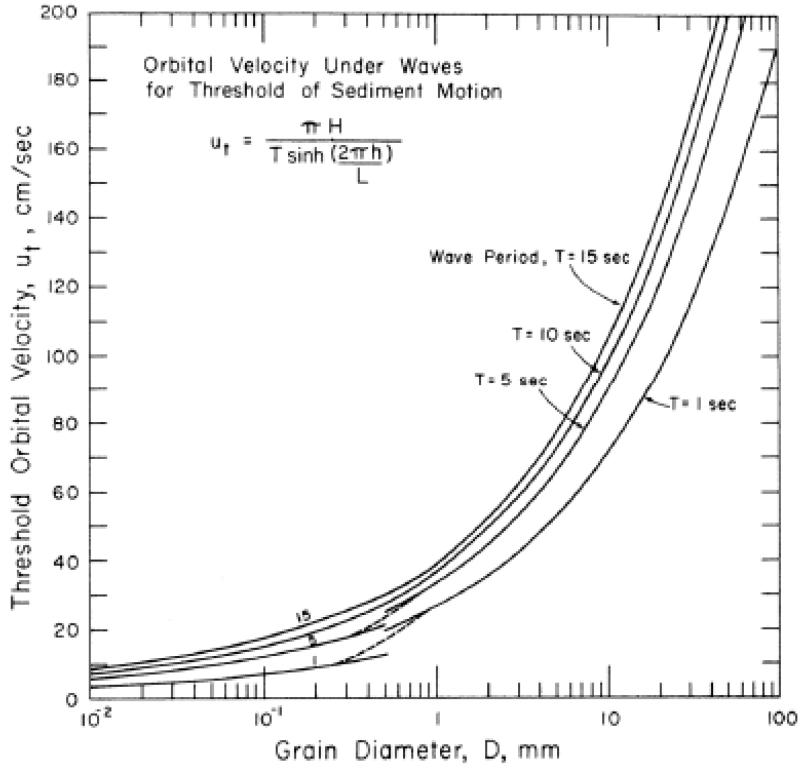

Figure 13. Orbital velocity under waves needed to reach threshold for sediment motion (Komar P. , 1976).

The transport of sediments in coastal areas is very complex and the underlying physics are not well understood.

Erosion takes place when the sediment transport leaving a control region is higher than the transport entering the region. At a reverse transport relationship accretion take place. Cross-shore processes, longshore processes or a mixture of them both affects the sediment transport. The evolution of the coastline is highly dependent on which of the two being the dominant one. The time scale of shoreline changes induced by cross-shore sediment transport is typically shorter and more seasonally bound than the longshore transport. Moreover the position and shaping of beach features are more dependent on the cross-shore transport while the long term eroding or accreting process of a certain beach section is dependent on the longshore sediment transport (CEM, 2008).

3.2.1 Longshore sediment transport

A longshore current is induced by the breaking of oblique incident waves and is the main factor for the longshore transport of sediments. The current may continue parallel to the shoreline for a great distance and has a major role controlling the eroding and accreting processes as a result of littoral drift over time (CEM, 2008).

Due to seasonal and daily variations in wind and wave directions the sediment transport might vary over the year. To be meaningful, the rate of longshore transport must therefore be calculated over a longer time, ranging up to over a year. Two transport rates are used to quantify the sediment displacement; gross transport and net transport. The net annual transport is calculated as the difference between the opposite directed transports, where the right directed transport is positive while the left directed is negative. The annual net transport can vary widely in magnitude between different location depending on the hydrodynamic processes in the area and the variation period. The gross annual transport is defined as the sum of total longshore sediment transport (CEM, 2008).

$$Q_{NET} = Q_R + Q_L \tag{3.5}$$

$$Q_{GROSS} = Q_R + |Q_L| \tag{3.6}$$

3.2.2 Cross-shore sediment transport

The cross-shore transport is transporting sediment perpendicular to the shore. The transport includes both the onshore accreting sediment transport and the offshore eroding sediment transport. Changes in wave condition may result in a varying onshore and offshore transport over the coastal profile and may cause a change in the beach profile. In most cases these changes are reversible and will not cause long-term erosion/accretion. However extreme storm events may result in loss of beach material and cause erosion. During extreme weather with high waves sediments close to the shoreline will be transported offshore and deposited on a bar towards the ocean. This movement of sediment will flatten the slope of the shoreface while the foreshore will become steeper and the shoreline will recede. When the weather and wave condition change back to the original the displaced sediment will slowly be moved back towards the shoreface and extend the shoreline (Mangor, 2012). Moreover the offshore sediment transport is considerably more rapid than the onshore transport, consequently long period of calm wave conditions are needed in order to recover sediment lost during a storm event. The beach profile response to storm events is displayed in Figure 14.

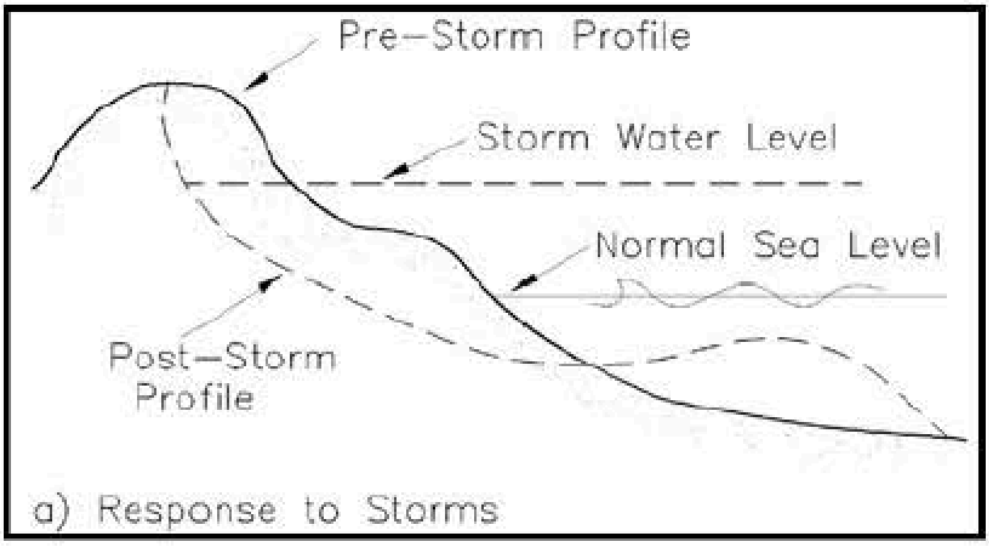

Figure 14. Cross-shore beach profile variation due to storm events (CEM, 2008).

The cross-shore transport is often seasonally bound. Typically during winter strong storm events expose the beach to larger destructing waves with shorter wave period causing erosion of the beach resulting in a

concave beach face. While the summer brings calm weather and constructing waves with a net onshore transport of sediment resulting in a slightly convex beach face, Figure 15.

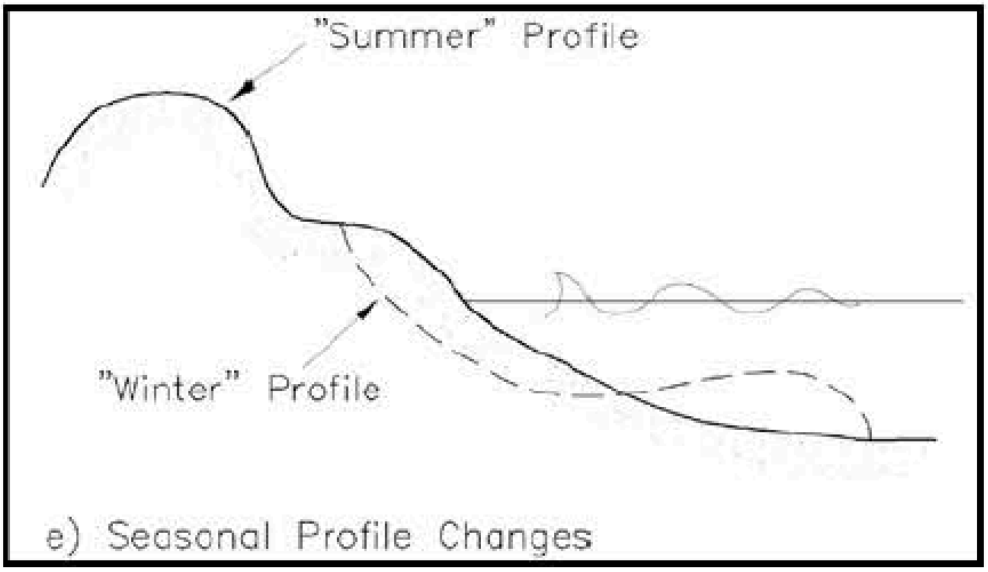

Figure 15. The cross-shore seasonal variation (CEM, 2008).

3.3 Beach terminology

The beach is the part between offshore and the coast, Figure 16. It extends from the upper landward part limit of effective wave action, with or without vegetation line, down to low tide level. The characteristics of the beach depend on many elements e.g. waves, winds, tides and grain size at the beach.

The upper part of the beach is normally only affected by waves during periods of high waves particularly when spring tides and storm events coincide. The slope mainly depends on sediment composition while the width of the cross-shore section depends on tide magnitude. (Sverdrup, Johnson, & Fleming, 1942)

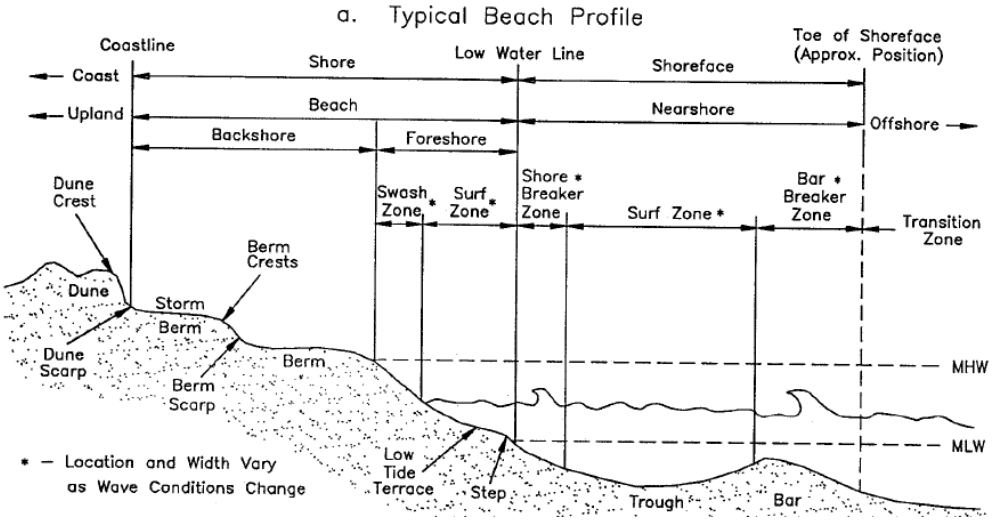

Figure 16. Beach terminology in the nearshore applied on a typical beach profile (CEM, 2008)

The nearshore zone is a very dynamic area, and beaches composed of unconsolidated material are almost in constant motion due to external forces (Nam P. , 2010). Every single wave breaking at the beach disturbs the sediments and sediment becomes suspended in the water. Currents at the beach have a huge impact on the beach profile as suspended sediment get trapped in the currents and transported away. Gradients in the transport rate inducing differences in the net transport can cause deposition or erosion of sediment, affecting the local topography (Sverdrup, Johnson, & Fleming, 1942). The direction and size of propagating waves together with nearshore currents are not constant but depend on prevailing weather conditions and seasonal changes. Moreover these fluctuations normally affect the beach profile. (Sverdrup, Johnson, & Fleming, 1942)

Beach features and dynamic beach zones used when conducting the field measurement included:
Berm, the almost horizontal part of the beach or backshore is formed by deposition of sediment by waves. Berms are not present at all beaches while some beaches can have more than one. Beaches with more than one berm are separated by a berm crest and a berm scarp (CEM, 2008).
Swash zone, the zone reached by the runup from broken waves (CEM, 2008).
Breaker zone, the nearshore region where waves become unstable and break. The area is dependent on wave height and depth. At flat beaches more than one breaker zone can be present (CEM, 2008).
Dune, zone above the highest water level, unaffected by the sediment transport by waves. Distribution of sediments is controlled by the wind (CEM, 2008).
Beach face, upper part of the foreshore down to the point of deviating slope.
Tidal plain, starting at beach face down towards surf zone until deviating slope.

3.4 Evolution of spits

Typical spits consist of sand or gravel and are common morphological features found at inlets, river mouths and at the down-drift ends of a barrier islands. Spits are of great interest to study as they could for example expand into river mouths and inlets and form a restriction of the flow or form a barrier island and decrease the accessibility of the spit. Moreover the evolution of spits could cause problem for navigation and cause dramatic change for the environment.

An early definition of spits (Johnson, 1919) state that they are “An embankment that has its distal end terminating in open water”. Another, later definition of spits provided by (Kraus, 1999) is “an organized surface-piercing accumulation of sediment that grows by transport directed from landmass or sediment source toward a water body”.
Some general characteristics of spits are: (1) major elongation in one direction; (2) consists of a long, low and narrow bank; (3) are attached at a sudden change of the coastline; (4) developed in a direction parallel to the coastline trend; (5) leaving a protected bay behind as it growths. (Johnson, 1919)

Spits are normally divided into two different groups; spits with unrestricted growth and spit with restricted growth. Spits with unrestricted growths are developed under a predominant wave generated longshore transport with low interference with other currents (Kraus, 1999). Restricted growth applies to spits that are affected by more currents than the longshore current and have a transport of sediment offshore the spit. These spits will reach an equilibrium over time, where the amount of sediment transported to the spit become equal to the amount of sediment leaving the spit, thus the length of the spit stay approximately constant (Kraus, 1999).

Spits can also be classified according to their shape, which is closely linked to the formative processes, and geomorphological constrains to their development. Some common shapes of the spit are linear, recurved and a mix of both. A linear spit develops if the longshore transport is dominant compared to other transport mechanism. However at some spits the effect of tidal or wind-induced variations in the wave climate together with refraction around the tip could alter the sediment pattern and force the spit to recurve during growth. As transport mechanisms governing the growth of the spit are changing over time the spits shape will change.

3.4.1 Evolution of Macaneta spit

No information was found about the evolution of Macaneta spit and the evolution of the spit can only be estimated. The growth of the spit is most likely governed by longshore transport from north to south providing sediment to the spit, see Figure 17.
As described in section 4.4, the Incomáti River is also of great importance for the formation of Macaneta spit. One theory is that a previous breaching episode could have caused the river to adjust the flow path forming the Xefina islands and thereby flow along the morphological feature that today is Macaneta spit. Over time sediment disposed on the seaward side and eroded from the riverside could partly be responsible for the south- eastward drift and elongation of the spit. Moreover, the discharge at the river mouth probably has a major influence for the deposition of sediments, both supporting and counteracting the seawards longshore transport. In the southern part of the spit the shadowing effect of Inhaca generates a wave climate with more southwards directed waves. This process together with the river

discharge and refraction around the tip of the spit could cause the spit to recurve.

Figure 17. The estimated longshore transport that formed Macaneta spit (Google Earth, 2014).

4. Hydrodynamic conditions at Macaneta

4.1 Currents

Offshore Maputo is the source region for the incipient Agulhas Current. At this location the northerly Mozambique Current, flowing through the Mozambique Channel, meets the easterly East Madagascar Current, from the southern cape of Madagascar. The maximum current speed found in the coastal region of Maputo is between 100cm/s and 150cm/s. (Saetre, 1985). In the Mozambique channel the southward current are affected by the narrow passage between Mozambique and Madagascar and cyclonic and anti-cyclonic eddies are formed, which continues moving south until reaching the South African coast. As a consequence of the eddy movements counter currents are generated. Offshore Maputo the Delagoa Bight eddy is found, when the south moving eddies of the Mozambique Current are passing by the bight northward counter currents along the coast are induced (Quartly & Srokosz, 2004; Lutjeharms & da Silva, 1988). These countercurrents are responsible for the formation of Inhaca, near the Maputo Bay (Suoto, 2014).

The Delagoa Bight eddy appear to be quasi-stationary and several studies indicate that it is topographically induced. From the circulation patterns it is hard to determine an exact seasonal variation of the Mozambique current. By analyzing the studies it is however plausible to assume that the current is strongest during the southern summer as a result of the baroclinic character at that time (Saetre & da Silva, 1984). Although the currents offshore Maputo have a big effect of sediment distribution and the coastal formation of the region it has a small effect on the nearshore conditions at Macaneta.

4.2 Tide

No studies were found analyzing the tidal characteristics of Macaneta spit. There are however numerous surveys examining the tidal variations of Maputo Bay and Inhaca island (Canhanga & Dias, 2005; de Boer, Rydberg, & Saide, 2000).

Tides on the coast of Mozambique, are of semi-diurnal type, meaning there are two low waters and two high waters a day occurring 12h and

25min apart, with a daily deviation of around 10-20cm in Maputo (Sete, Ruby, & Dove, 2002). The Maputo Harbour has a range of 3m between flood and ebb during spring tide, at Ponta Torres, Inhaca, the spring and neap tidal ranges are 2.2m and 0.7m respectively (de Boer, Rydberg, & Saide, 2000). In a study at Macaneta conducted by DHI a model regarding tidal characteristics was set up. It was concluded that the spring tidal range varies between 2 and 3m and that neap tidal range varies between 0.6m and 1m (DHI, 2013).

4.3 Wave climate

Due to lack of continuous measurement regarding wave climate for the Mozambican coast it is extremely hard to give the exact wave condition around Maputo and Macaneta spit. Several studies have been carried out implementing numerical modeling to determine the wave climate. However, shortage of exact bathymetric data off the coast limits the ability to determine wave propagation in the shoaling water with sufficient satisfaction. DHI has carried out a study at Macaneta spit implementing numerical modeling using wave data from the NOAA Wave Watch III (WW3) model (NWS, 2010)), developed by the U.S. National Center for Environmental Prediction (NCEP). By recording the waves breaking point at several location along the seawards side of the isthmus during both average and extreme wave conditions it was concluded that the waves are mainly NEE to SEE and rarely above 1,5m (DHI, 2013). The offshore wave height is considerably bigger than at the spit and those often exceeds 3 m. As a result of the Danae shoal, a sandbank located a few kilometers off the coast almost visible at low tide; the wave height is reduced accordingly when approaching Macaneta.

The waves offshore Maputo most often origin from the south or the east (Viola, Grifoll, Palalane, & Oliveira, 2014). The largest waves are induced by storms frequenting the Southern Ocean south of the African continent. The wind speed in this area is highest during the southern hemisphere winter and consequently the largest southern waves propagating towards Maputo are most common during this time of year (Young, 1999). The easterly waves are generated by eastern trade winds passing south of Madagascar. These winds are prominent throughout the year but strongest during the southern hemisphere summer (Jury & Pathack, 1991).

4.4 Rivers

Three water bodies enter Maputo Bay; the Maputo River, the Incomáti River and the Espírito Santo Estuary. The two major rivers are the Maputo River entering the south part of the bay and the Incomáti river flowing into Maputo Bay in the north, both with a mean monthly flow of around 80 m^3/s (de Freitas, 1984).

The Umbeluzi and Incomáti basin borders the Maputo River Basin in the north, all three originates in South Africa and discharge in to Delagoa Bay. The main tributaries of Maputo River are the Usutu River flowing through the southern part of Swaziland and the Pongola River that rises in the Drakenberg mountainous region, part of the great escarpment on the border between Lesotho and South Africa (SADC, 2010). The mean annual discharge of the Maputo River is $2\,555 \times 10^6$ m^3, the estuary has a total area of 20.4km^2 whereof 10.4km^2 are mudflats built up by river and tide deposits and exposed during spring ebb tides (de Freitas, 1984).

The Incomáti River rises in the western part of the basin in the eastern South African mountain region, on the great escarpment, at an altitude of approximately 2000m above sea level. The river flows through the north part of Swaziland before entering Mozambique and discharge at the Maputo Bay (Khalili, 2007). The mean annual discharge of Incomáti River is $2\,425 \times 10^6$ m^3 (de Freitas, 1984). The mouth of the river is located on the west side of the Macaneta peninsula that deflects the river from the Indian Ocean for the last 10km of its course (Moreira M. E., 2010). The estuary stretches about 13km south of the mouth and consists of two arms separated by the island of ilha Xefina Pequena. The eastern arm is currently the main watercourse while the west side of the island is very shallow (de Freitas, 1984). Southwest of ilha Xefina Pequena the ilha Xefina Grande is located. It is believed that the two landmasses were once one and part of the Macaneta Peninsula, at that time located further to the west, Figure 18. A breakthrough event plausible formed ilha Xefina Grande and littoral drift along the remaining peninsula together with clockwise drift of sediment discharge from the river can explain the eastward drift of Macaneta Spit (DHI, 2013; Böhlmark, 2003).

A new breaching of the peninsula is predicted at some stage in the future implying that the river will flow straight out to sea. The ecology of the estuary together with the whole of Maputo Bay will thus be deprived the influence of the Incomáti River and an increased salt water intrusion from sea would at some locations make the river water unsuitable for irrigation (de Freitas, 1984; Makoye, 2012).

Figure 18. A possible historical course of the Incomáti river and formation of the Macaneta coast. (DHI, 2013).

5. Coastal effects at Macaneta

The nearshore zone is a hydrodynamic area of continuous change. The evolution of Macaneta spit could involve risks of negative consequences for the area. The main risk at the spit is permanent breaching. In this chapter processes possessing potential risk for breaching of the spit and how such morphological change would affect the region of Macaneta are presented.

5.1 Erosion

The erosion of the beaches recorded on the southern coast of Mozambique range from 0.11 to 1.10m/year over the last 31 years (1973-2004) (Moreira M. E., 2005). According to aerial photography analysis between the 60's and 90's the Macaneta spit has been building up sediments (Hoguane & Meulen, 2010). Furthermore, it has both been displaced and stretched southeast-wards as a result of littoral drift and accretion processes were sediments from the coastal erosion in the Limpopo Bight are being deposited along the Macaneta Peninsula (Hoguane & Meulen, 2010; DHI, 2013; de Freitas, 1984).

The margins of the river delta have been observed eroding, mainly due to clearing of mangroves and vegetation over the dunes along with heavy storm events and river discharges. To limit erosion, coastal defense was constructed in the 1960's, but they are insufficient in the current situation (Hoguane & Meulen, 2010).

5.2 Overwash of barrier islands

The shape of a beach profile depends primarily on the grain size of the sediments and the dissipating effect of incoming waves. Steep beaches tend to be found in coastal areas where coarser sediment are abundant while finer sediment usually is found on beaches with more gentle slopes. Breaking waves will then contribute to the shaping. Small waves with longer wave periods generally increase the beach slope while storm waves with high wave height and short wave periods often flatten the beach (DHI, 2013).

The wave conditions will in most regions not be the same throughout the year, often there are two typical wave seasons creating a "summer" beach profile and a "winter" profile. For the case of Macaneta and Mozambique, the winter with stronger waves is prominent from April to September, resulting in flattening of the beach profiles (Nagle, 2000).

Storm event are shorter periods of harsh weather with strong waves causing the beach profile to flatten by moving beach sediment backwards against the backdune. Naturally the runup during these events is higher compared to normal conditions, due to both larger waves and the storm surge. At the narrow section of Macaneta spit the beach is not backed by high dunes stopping the ocean waves, but instead by Incomáti river. The limited width of the peninsula implying a risk that there is not enough sand to accommodate the change needed during a storm event. Meaning that the profile might not be able to prevent the ocean swell from overwashing the isthmus. The overwashing water will transport significant quantities of sediment from the dune towards the river when running down the backside of the dune. Creating washover channels in the dune and washover fans on the riverbank (Schwartz, 1982).

After an overwash event when the wave conditions return to calmer conditions the beach profile start to re-establish its normal state. Wave carrying sediment onto shore and wind-blown sediment will steepen the beach profile and fill overwash channels with sediment. However, during periods of frequent overwashing events the isthmus might never recover, leading to a constant breaching of Macaneta spit separating the landmass from the mainland (DHI, 2013).

Episodes of overwash at the narrow stretches of Macaneta spit have occurred earlier. One such episode occurred in 2002 and was documented by Magos (2002) and cited by DHI (2013), see Figure 19. Mentioned in the report is also an overwash episode of the isthmus that ocurred either in November 2000 or in November 2001. From the photos it is seen that a washover channel approximately 2m deep was dug during the overwash event. However after a few days of calmer conditions waves and wind transported sediments had filled the channel and re-established the height of the dune.

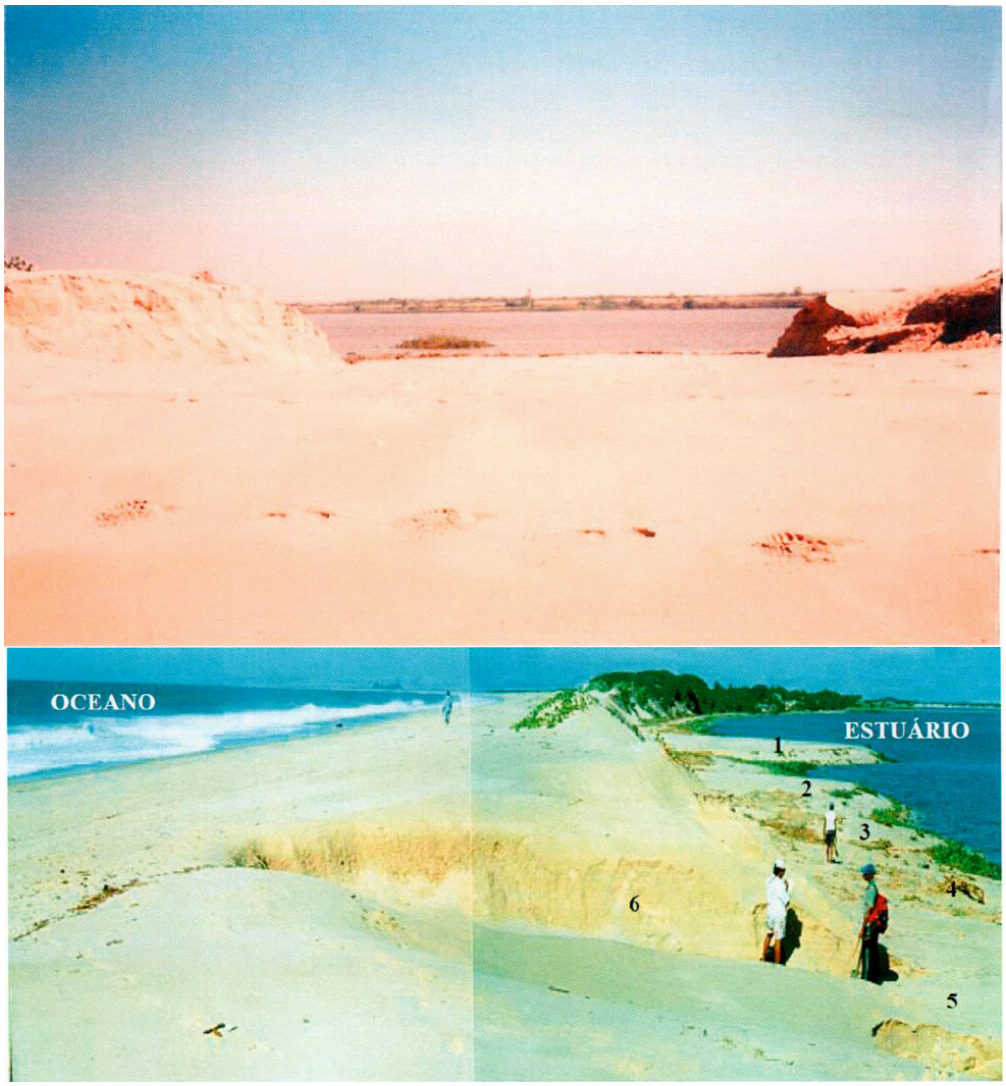

Figure 19. Photos after an overwash event at the isthmus just south of Macaneta Holiday resort. The upper photo display the created washover channel and the lower one an overview of the cross-shore profile (Magos, 2002).

5.3 Salt water intrusion

Saltwater intrusion in estuaries is essential for ecological reasons as well as water extraction purposes. The distance salt intrudes upstream depends on a number of factors including; river discharge, tidal and wind mixing and gravitational circulation.

Saltwater intrusion poses a serious problem in many rivers affecting both ecology and water extraction characteristics in the area. Salty seawater contaminates the river making the water unfit for irrigation and drinking (Aerts, Hassan, Savenije, & Khan, 2000). The problem is relatively new to the Incomáti estuary and has aroused during the last century as tributary rivers feeding the Incomáti River are being dammed and agricultural land make greater use of the river water for irrigation. As a consequence the discharge of the estuary is decreasing resulting in salt water intruding further up the river. As a direct economic and social effect agricultural land adjacent to the estuary, relying on the river for irrigation, has already been abandoned (Hoguane A. M., 2000).

In the case of an overwash event leading to a constant breaching of the spit the intrusion will affect the estuary even further. The river water would be exposed to seawater further upstream the estuary and subsequently salt intrusion will spread further up the river estuary.

It is hard to predict exactly how far the salt intrudes upstream since it depends on a number of factors, including river discharge, tidal and wind mixing and gravitational circulation. The Incmoati estuary is funnel-shaped with a cross-section decreasing inlands, meaning that the river flow speed towards sea increases with distance to the sea and the salt meets greater resistance the further it penetrates upstream. A breaching event 10km up the estuary is not likely to lead to a salt intrusion reaching 10km further up the river (Brockway, Bowers, Hoguane, Dove, & Vassele, 2006).

6. Coastal zone management

6.1 Overview of integrated coastal zone management, ICZM

Coastal zones are among the most productive and vulnerable areas in the world. The zone where sea meets land offering a wide variety of valuable habitats and ecosystems, and play an important role for humans and human activities. This is the reason why the Council of Europe concluded a resolution on the Protection of the Coastline in 1973. The aim of integrated coastal zone management, ICZM, is to provide a tool to develop a sustainable coastal zone where human activities have a minimum impact on the coastal environment. (European Commission, 2015)

One definition of the ICZM concept made by the World Bank in 1996 was;
"A process of governance that consists of the legal and institutional framework necessary to ensure that development and management plans for coastal zones are integrated with environmental (including social) goals and are made with the participation of those affected. The purpose of ICZM is to maximize the benefits provided by the coastal zone and to minimize the conflicts and harmful effects of activities upon each other, on resources and on the environment." (Post & Lundin, 1996).

The concept of integrated coastal zone management was spread all over the world and used for many countries with coastal problems. The concept of ICZM is stated above but the meaning is different depending on every countries need. The implement depends on the present status of the coastal zone, what the activities in the area are, present framework and interests of the coast. Many guidelines have been made to succeed with the transform from international concept to regional level.

Following guideline is a summary of concepts proposed to be able to implement ICZM on regional levels. (Johansson, 1997)

- Formulate objectives of the coastal management considering the national and regional priorities and mandates.
- Establish a planning organization where relevant politicians, organizations, stakeholders and public are represented.
- Identify the main development option and long-term conservancy claims and decide if these are within the objectives stated.
- Determine the current status of the coastal zone by collecting data and undertake necessary surveys.
- Analyze who is responsible for activities in the coastal zone and their future plans.
- Draft necessary action plans and maintenance for each coastal area.
- Initiate a public discussion about the coastal zones and the future development and management.
- Implement action programs and maintenance.
- Modify the action programs continuously and take complementary actions to let the program proceed.

There are many definition of coastal zone, but a commonly used definition of the coastal zone is the zone where land area is affected by sea together with the part of sea affected by land (Portman & Fishhendler, 2011). The coastal zone host many different activities which make the planning of the coastal zone complex to organize. The dynamic nature of the coast line with erosion, accretion, temporally flooding and natural movement of dune areas add further complexity to the coastal management (Mangor, SHORELINE MANAGEMENT GUIDELINES, 2004).

6.2 Integrated coastal zone management in Mozambique

The concept of ICZM was on the Agenda 21 at the Earth Summit *(UNCED)* in Rio de Janeiro, Brazil, in 1992. One year after the conference in Rio de Janeiro at the *Policy Conference on Integrated Coastal Zone Management in Eastern Africa including Island States,* held in Arusha, Tanzania (the Arusha Resolution) in April 1993, governments in the southeast of Africa agreed to implement the ICZM in their countries (World Bank and Sida, 1997).

The ICZM was launched as a part in the National Environment Management Program, NEMP that was approved 1994 by the government of Mozambique. The NEMP put focus on three main areas; urban, rural and coastal. They stated that the coastal management should be based on coordination between relevant stakeholders (institution and communities), and that they should set a plan accepted by the stakeholders. The main issues for the ICZM in Mozambique are; fisheries, coastal and marine ecosystems management, coastal and marine protection, marine parks and tourism. According to NEMP each issue should have a strategy and an action plan in short-, medium- and long-term (Chemane D, Motta H, Achimo M, 1997).

The ongoing international work of ICZM is carried out by arranging meetings and workshops between international and national experts of the coastal zone, relevant stakeholders and other interested groups. The aims of these meetings are to raise important issues for the coastal zone and increasing the knowledge among the members of the government and policy-makers in order to increase political actions at the coastal zone (World Bank and Sida, 1997).

There are many different institutions that need to collaborate in order to establish a good coastal management. Currently the coastal management is not working properly as the communication between the institutions in Mozambique is not good. In order for the work to be improved a well developed plan describing the area of responsibility between the institutions has to be formed (Chemane D, Motta H, Achimo M, 1997).

Ministry for Coordination of Environmental Action, MICOA are mainly handling works for the environmental management in Mozambique and is one of the most important institutions to implement the concept of ICZM in Mozambique. The CZN Unit is a subunit within the MICOA,

consisting of a team of professionals from different disciplines. This unit is responsible for all the activities related to coastal management including reach, planning for actions and coordination between other institutions and stakeholders (Chemane D, Motta H, Achimo M, 1997).

A huge problem with the legislation in Mozambique is the lack of enforcement. This is a problem in nearly all aspects of the country´s legislative process and without an effective enforcement is it almost impossible to secure that laws are followed. It is especially hard to control the coastal zone when the coast in Mozambique is one of the longest in the world (2500km) and the resources very limited. For example, many cases of illegal fishing and usage of inappropriate fishing techniques are known by the Maritime Administration Authorities but since they do not have the resource it is impossible to control or prevent (World Bank and Sida, 1997).

7. Field measurements

7.1 Overview

The Macaneta spit was surveyed during March 2015. The main aim during the field studies was to collect data to analyze the coastal evolution of the peninsula due to hydrodynamic processes. Field data collection was carried out with focus on mapping; general morphology, shoreline positions and cross-shore profiles. Moreover sediment sampling and a nearshore bathymetric survey was performed. A particular topic of interest was the probability for overwash and breaching of the spit at narrow sections. Whereupon beach sections vulnerable to breaching were identified, the beach profiles recorded and sediment samples collected.

7.2 Experimental setup and procedure

7.2.1 Cross-shore profile measurements

The cross-shore condition at Macaneta was investigated by analyzing the beach and sea bottom profile at selected locations along the shoreline. Emphasis of the cross-shore profiles was put on the two narrowest stretches of the spit where the risk of breaching is considered the highest. However, in order to get representative data for Macaneta spit it was important to spatially spread the cross-shore profiles along the peninsula and include both narrow sections, only consisting of a berm and wider parts with a prominent foredune. In total six beach profiles were recorded. For the two most vulnerable sections the beach profile was recorded across the dune to include both sea and river side of the spit. On the four wider sections the beach profile was recorded solely on the seaward side, from breaking zone up to dense vegetation. The locations of the measured profiles are displayed in Figure 20.

In order to survey as much of the cross-shore profiles as possible, the beach survey was carried out at the time of low spring tide during three consecutive days.

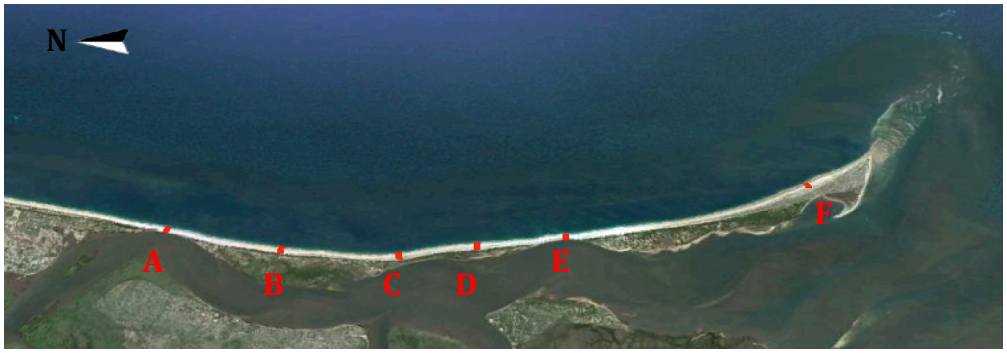

Figure 20. A satellite image of Macaneta spit displaying the six sections where cross-shore profiles were recorded (Google Earth, 2014). Section A and E are the two narrowest sections where the risk for breaching and overwash are investigated.

7.2.1.1 Operating the GPS device

The beach profiles were measured from breaking zone to foredune or river. They were recorded with a differential GPS consisting of a base station placed at a fixed location and a mobile rover unit on a pole attached to a wheel, Figure 21. The setup with a base station and rover provide a high precision as the base station has a static location correcting satellite information and transmit this information to the rover. The rover was set to automatically log points, coordinates and relative altitude, during a fixed time step. Moreover the locations of breaker zone, swash zone, berm and foredune were logged manually. The precision of the rover used together with the base station had an error margin of 4mm.

In order to access the biggest part of the bottom profile the survey was carried out during low spring tides. When using the GPS in water the force of the waves make it hard to keep the pole vertical. Consequently, in order to ensure measurement data as correct as possible and to protect the equipment from seawater, the pole was lifted to the waist before entering the water. The cross-shore beach profiles were measured out to the point of where the waves were breaking at a depth of about 1m.

Figure 21. Differential GPS instruments used during the field survey. To the left the rover unit on wheel, to the right the base station and in the center an external antenna connected to the base station.

7.2.2 Longshore profile measurements

Cross-shore and longshore transport affects the features of the spit by transporting sediment from one place to another. By mapping the shoreline position it is possible to observe the evolution of the shoreline position over time and detect ongoing trends.

The beach feature used to determine the shoreline position of Macaneta spit was the position of the berm. The survey was conducted along the entire spit, from the southernmost point of the spit up to Macaneta Holiday Resort. Recordings of the shoreline position was carried out with a differential GPS set to automatically log points at a fixed distance of 5 m. At the most southern part of the spit the rover unit lost connection with the base station, resulting in an error margin for the precision of the GPS of 2m in north-south direction and 3m in east-western direction at most.

In order to analyze and find trends of an ongoing coastal evolution the recorded shoreline was compared with historical shoreline positions of the coast. The historical shorelines used for comparison were collected

from Google Earth satellite images between the years of 2003 and 2014 and an aerial photo over the northern part of the peninsula from 1979.

7.2.3 Sediment sampling and analysis

The shoreline and profile is under constant change due to forces acting on the beach zone from both the ocean and from weather phenomenas. The sediment composition in the beach zone could indicate the level of stability of the shoreline. A granulometric analysis of the grain size distribution is therefore of high interest in order to determine the condition and likeliness of change of the beach (Morang, Larson, & Gorman, 1997).

Sediment samples were collected at four locations for each cross-shore profile. The sampling points were chosen based on beach features in order to document all major morphological changes of the profile. Samples were taken at the breaker zone, swash zone, berm and foredune respectively. Moreover samples were taken at the swash zone at the tip of the spit on both riverside and seaside. At the two most narrow sections complimentary samples for analysis were taken from the river dune and riverbed.

The grain size distribution analysis was carried out by the US standard sieve analysis method. In order to evaporate all water from the samples the collected sediment samples were dried in an oven at 100℃ for around 24h. For each dry sample 200g was used for sieving analysis. The new sample was weighed and thereafter added at the top of a sieving column. The sieving column was shaken by a machine for 5min and thereafter the content of each tray was weighed. The finest sieve was not part of the column but hand shaken separately.

The sieve column consisted of 9 trays with different mesh size according to US. Standard sieve series. The A.S.T.M specifications and corresponding mesh size in mm are presented in Appendix I.

7.2.4 Bathymetric measurements

Waves propagating towards shore are highly dependent on the bathymetry. The wave transformation, breaking regions and sediment transport are all reliant on the seafloor topography.

The bathymetry outside Macaneta was measured with an echo sounder, Figure 22. The mapping was carried out from the vicinity of the beach at

a minimum depth of 2m to about 2km offcoast along the same latitude. The accuracy of the rover used together with the echo sounder had an error margin of 2m in north-south direction and 3m in east-western direction. The error margin of the echo sounder at a typical depth of 10m was 20cm according to manual.

Figure 22. Echo sounder used during field investigations.

The survey covered a longitude distance of 15km stretching from about 2km north of section A down to 2km south of the tip of the spit. The mapping along the latitude lines was measured for every 250m around the area of section A and around the tip of the spit while the remaining part of the spit was measured for every 500m. The recording pattern for the survey is displayed in Figure 23. Mapping of the bottom was possible to a minimum depth of approximately 2m to prevent the boat from run aground. At the tip of the spit a sand bank is reaching in southeastern direction from the spit with shallow depth less than 2 meter, as a consequence bathymetric survey of that location was not possible to obtain.

A grid of the collected bathymetric data was created with consideration to the tidal variation during the survey. The resulting bathymetry after interpolation in ArcGIS is presented according to mean low sea water level in Figure 23.

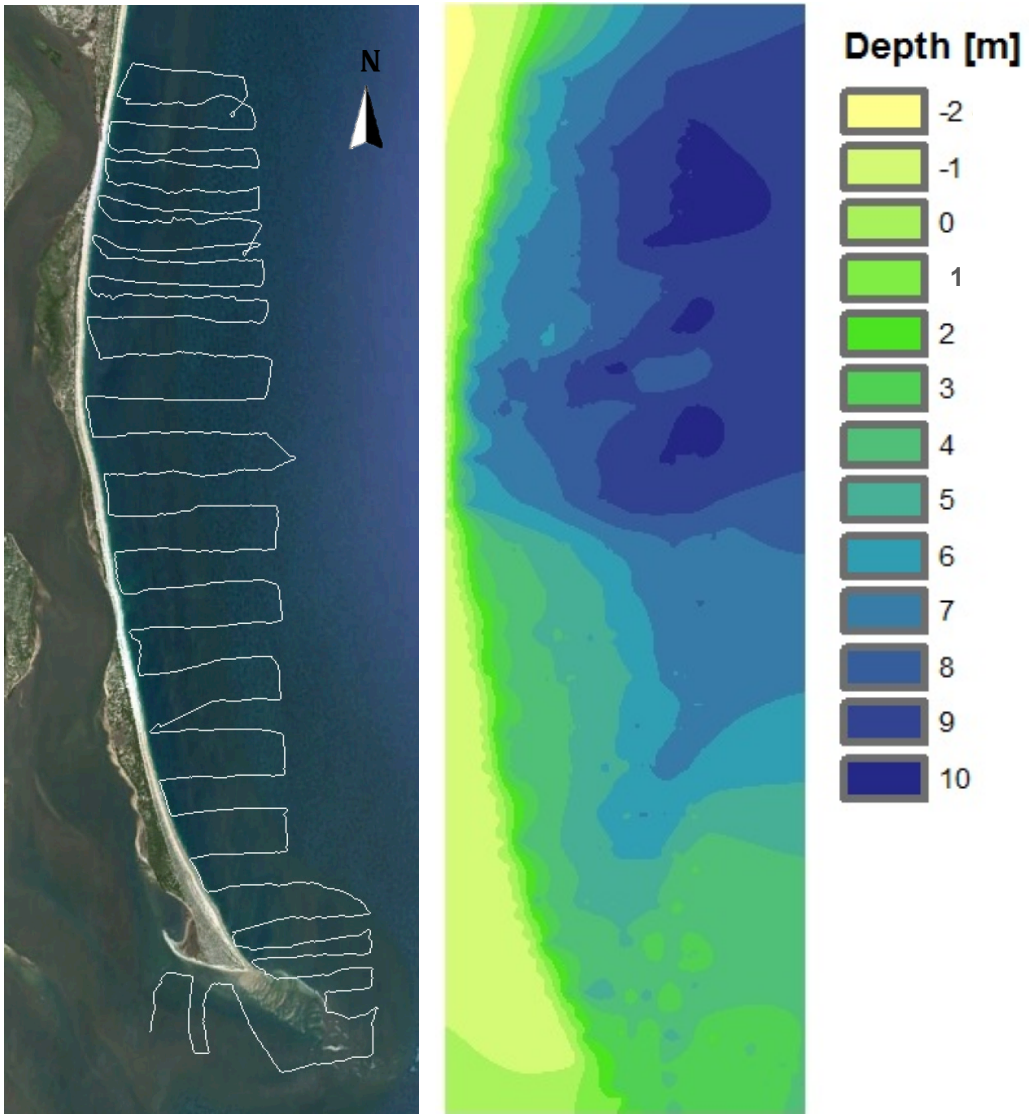

Figure 23. A satellite image of Macaneta spit (left). The white line displays the position of the bathymetric survey (Google Earth, 2014). Generated depth with reference to low sea water level on the seaside of Macaneta spit (right). The northern part of Macaneta spit have a steeper bottom profile close to the beach than the southern parts of the spit.

The bathymetric survey was conducted as a compliment to bathymetric data collected from the National Institute for Hydrography and Navigation (INAHINA – Instituto Nacional de Hidrografia e Navegacao). Bathymetric data from INAHINA was given in the form of a nautical chart and based on data collected from bathymetric surveys in Maputo Bay, see Appendix IV. The data collected with the echo sounder was then used to verify the data from INAHINA by comparing the depths at corresponding locations.

7.3 Tidal data

A tidal record was provided for the years 2005 to 2015 by WXTide32, a software that features tidal observations of sea stations worldwide (WXTide32, 2015). The tidal records obtained were from Durban, South Africa, but with a correction added to give values reasonable for Maputo Bay. However, the magnitude of the tidal range provided did not match previous studies in the region of Macaneta. The range between lowest and highest water level was 4m according to WXTide32 while earlier reports state it to be in the range of 3m (de Boer, Rydberg, & Saide, 2000; DHI, 2013). Subsequently the tide series was scaled by a factor of 0.75 to match earlier studies.

The datum of the tidal record referred to lowest sea level. The wave propagation software EBED does not account for tidal variation, consequently a mean sea level was used when conducting the modeling. The mean water level was computed from the tide series. The bathymetry used in the wave propagation modeling was provided by INAHINA. The reference level in the nautical chart referred to low sea level hence the computed mean sea level was used to calculate a new bathymetric profile.

7.4 Data collected and their properties

7.4.1 Cross-shore profiles

Below are the cross-shore profiles presented for the sections A-F. The profiles are presented from north to south along the spit, see Figure 20. The most narrow stretches are represented by the sections of A and E, while the widest section is found at section B.
The datum is defined as mean sea level based on the tide positions for the year of 2005-2015, given by WXTide32.

7.4.1.1 Section A

The section is the most northward section surveyed. Located at the beginning of the spit and with the narrowest cross-shore profile of the entire peninsula and a beach face facing east-southeast, ESE. In Figure 24 the view of the site together with the location of the section is displayed and in Figure 25 the measured profile is presented.

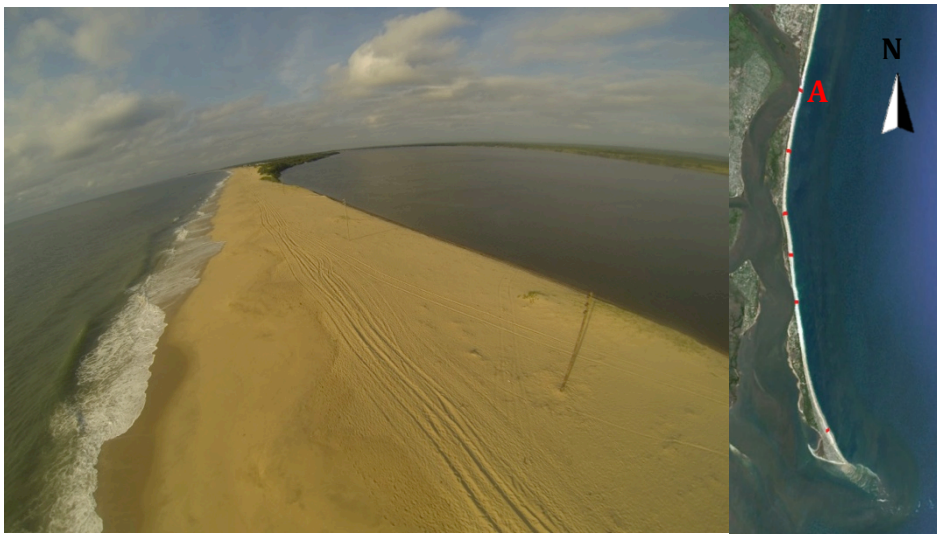

Figure 24. Photo of section A taken above the berm facing south. Displayed is also a map showing the location of the section.

The cross-shore profile was measured during low tide; the tide at Maputo port was reported as 0.74m above low water level. (Instituto Hidrografico, 2015). The breaking zone was located far out on the tidal plane and the swash merely reached the beach face. The profile was measured from breaker zone to the water edge of the Incomáti River. The cross-shore profile lacks a foredune and no vegetation were found at this section.

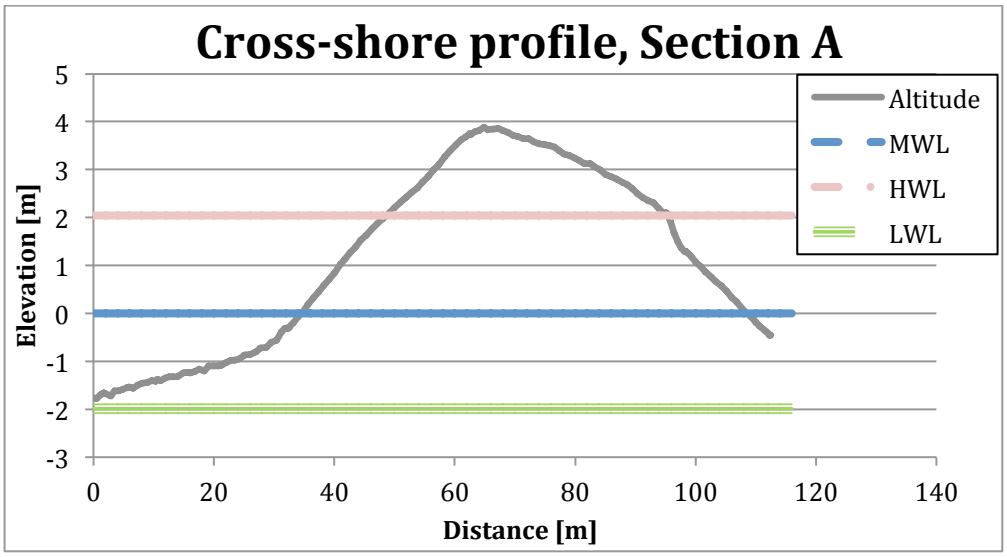

Figure 25. The cross-shore profile at section A. The profile is recorded from breaker zone on the seaward side (left) until the water edge of the river (right). The horizontal lines represent water level at high, mean and low tide. The datum is defined as the mean water level. (MWL – mean water level; HWL – high water level; LWL – low water level).

The berm of the section is located 3.7m above the mean water level and the highest point of the profile is found 3.8m above mean water level. Since the spring tidal range varies between 2-3m, there is only a barrier with a height of 1-2m separating the two sides during high tides. Assuming the river surface reaching the same level the width of the isthmus will be around 40-60m.

In Figure 25, five almost linear slopes can be identified and their slopes easily calculated. The slopes from left to right in the figure; tidal plane approximately 3%, beach face 12%, river dune -5%, river scarp -26% and river bed -12%.

7.4.1.2 Section B

The section is the widest section surveyed. Located 2km down the spit, facing ESE. In Figure 26 the view of the site together with the location of the section is displayed and in Figure 27 the measured profile is presented.

Figure 26. Photo of section B taken on the berm in southward direction, displayed is also a map showing the location of the section.

The cross-shore profile was measured during low tide, the tide at Maputo port was prognosed to be 0.49m one hour later (Instituto Hidrografico, 2015). The breaking zone was located far out on the tidal plane and the swash merely reached the beach face. The profile was measured from breaker zone up to the dense vegetation line on the dune.

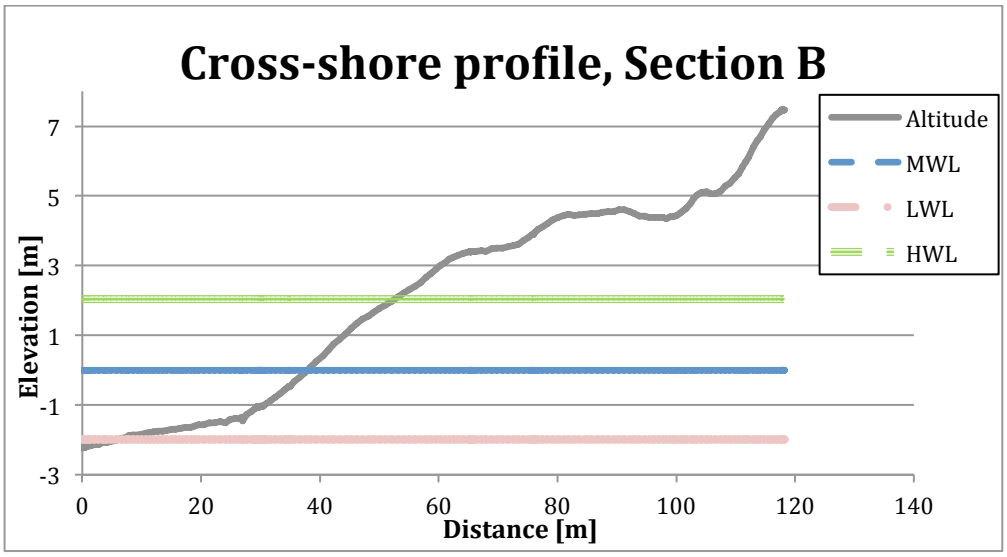

Figure 27. Cross-shore profile at section B. The profile is recorded from breaker zone on the seaward side (left) to dense vegetation line on the dune (right). The horizontal lines represent water level at high, mean and low tide. The datum is defined as the mean water level. (MWL – mean water level; HWL – high water level; LWL – low water level).

In Figure 27, the tidal plane and the beach face can be identified as almost linear slopes. Calculated by linear equation the slopes are 3% and 12% respectively. The berm of this section is found 3,4m above the mean water level.

7.4.1.3 Section C

The section is located about 4km down the spit, facing NEE. In Figure 28 the view of the site together with the location of the section is displayed and in Figure 29 the measured profile is presented.

Figure 28. Photo of section C taken on the beach face in northward direction, displayed is also a map showing the location of the section.

The cross-shore profile was measured during low tide, the tide at Maputo port was prognosed to be 0.74m above low water level one hour later (Instituto Hidrografico, 2015). The breaking zone was located far out on the tidal plane and the swash merely reached the beach face. The profile was measured from breaker zone up to the dense vegetation line on the dune.

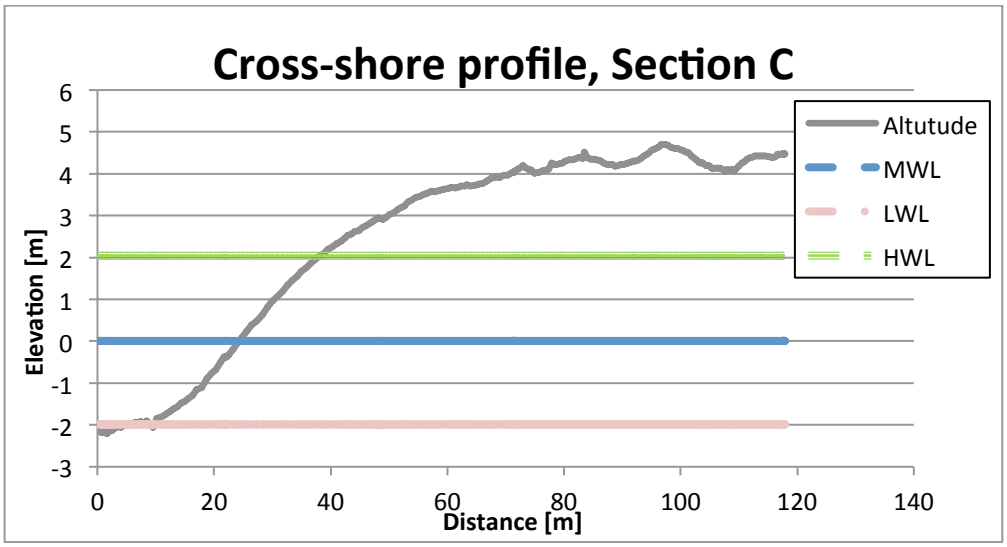

Figure 29. Cross-shore profile at section C. The profile is recorded from breaker zone (left) on the seaward side to dense vegetation line on the dune (right). The horizontal lines represent water level at high, mean and low tide. The datum is defined as the mean water level. (MWL – mean water level; HWL – high water level; LWL – low water level).

In Figure 29, the tidal plane and the beach face can be identified as almost linear slopes. Calculated by linear equation the slopes are 3% and 13% respectively. The berm of the section is found 2.9m above the datum.

7.4.1.4 Section D

The section is located about 5.5km down the spit, facing the direction of NEE. In Figure 30 the view of the site together with the location of the section is displayed, in Figure 31 the measured profile is presented.

Figure 30. Photo of section D taken from the vegetation line in northward direction, displayed is also a map showing the location of the section.

The cross-shore profile was measured half an hour after the lowest tide position, lowest tide at Maputo port was prognosedto be 0.74m above low water level (Instituto Hidrografico, 2015). The breaking zone was located far out on the tidal plane and the swash merely reached the beach face. The profile was measured from breaker zone up to the dense vegetation line on the dune.

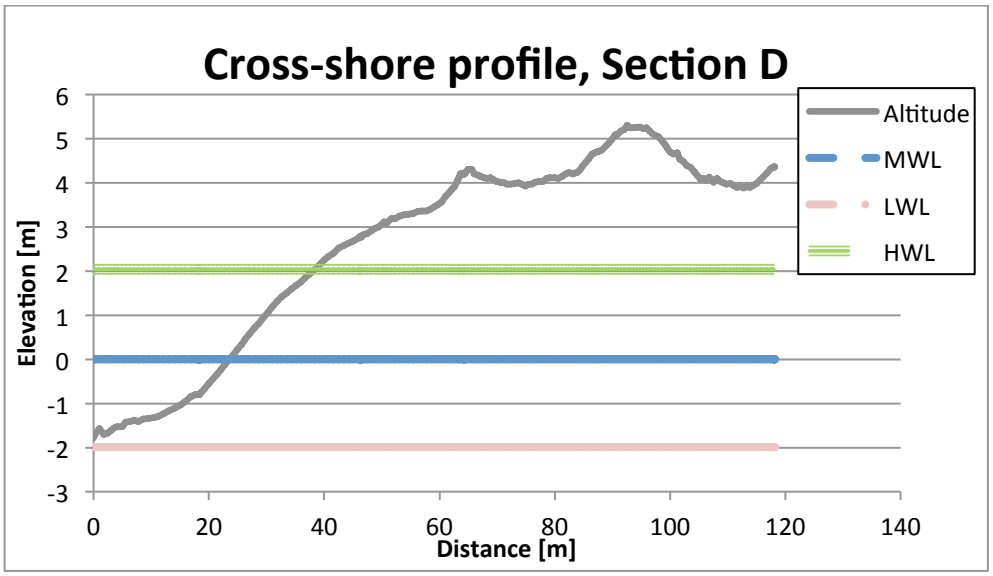

Figure 31. Cross-shore profile at section D. The profile is recorded from breaker zone on the seaward side (left) to dense vegetation line on the dune (right). The horizontal lines represent water level at high, mean and low tide. The datum is defined as the mean water level. (MWL – mean water level; HWL – high water level; LWL – low water level).

In Figure 31, the slope of the tidal plane and the beach face can be assumed almost linear. Calculated with linear equation the slopes are 5% and 12% respectively. The berm of the section is found 2.8m above the datum.

7.4.1.5 Section E

The section is located about 7km down the spit, facing the E direction. It is the second most narrow section of Macaneta spit and was measured from ocean to river. In Figure 32 the view of the site together with the location of the section is displayed and in Figure 33 the measured profile is presented.

Figure 32. Photo of section E taken at the highest point of the dune in southward direction, displayed is also a map showing the location of the section.

The cross-shore profile was measured one and a half hour after the lowest tide position, lowest tide at Maputo port was prognosed to be 0.74m above low water level (Instituto Hidrografico, 2015). The breaking zone was located far out on the tidal plane and the swash reached a couple of meter up the beach face. The profile was measured from breaker zone and cross the dune and vegetation to the water edge of the river.

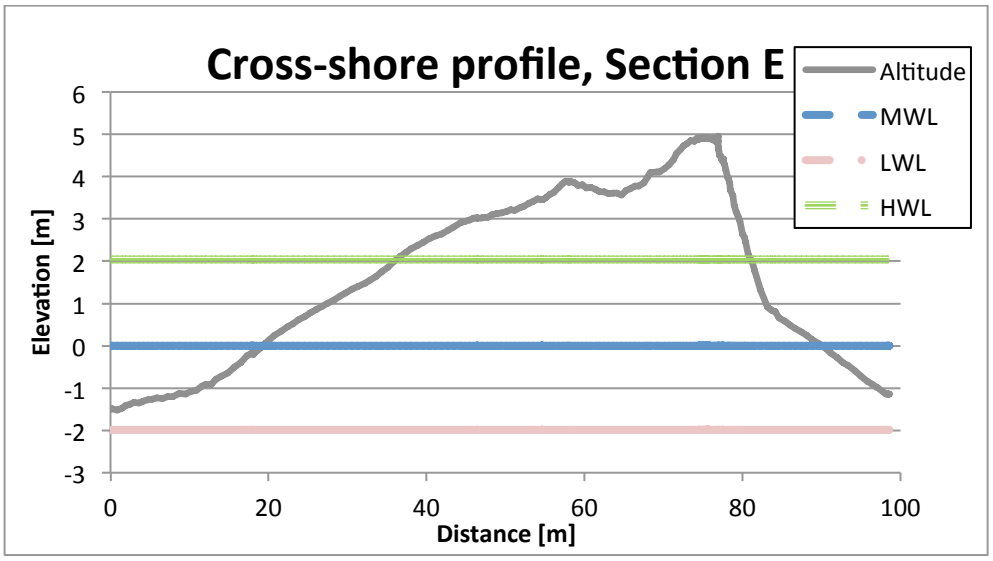

Figure 33. Cross-shore profile at section E. The profile is recorded from breaker zone on the seaward side (left) until the water edge of the river (right). The horizontal lines represent water level at high, mean and low tide. The datum is defined as the mean water level. (MWL – mean water level; HWL – high water level; LWL – low water level).

The berm is located 3.0m above the datum and the highest point of the profile is found 4.9m above the mean water level. Assuming the river surface reaching the same level as the ocean during high spring tide the width of the section will be around 40-60m.

In Figure 33, four sections where the gradient is almost constant are found; the tidal plane, beach face, river dune scarp and river bed. From the linear equation the slope of the tidal plane was approximated to 5%, the slope of the beach face to 12%, the slope of the river scarp to -69% and the slope of the river bed to -13%.

7.4.1.6 Section F

The section is located about 10.5km down the spit only 1km from the tip, with the shoreline facing NE. In Figure 34 the view of the site together with the location of the section is displayed and in Figure 35 the measured profile is presented.

Figure 34. Photo of section F taken at the vegetation line in northward direction, displayed is also a map showing the location of the section.

The cross-shore profile was measured at an incoming tide, two and a half hour after the lowest tide position. The lowest tide at Maputo port was prognosed to be 1.07m above low water level (Instituto Hidrografico, 2015). The breaking zone was located just off the beach face on the tidal plane and the swash reached a couple of meter up the beach face. The profile was measured from breaker zone and far enough to get a representation of the dune.

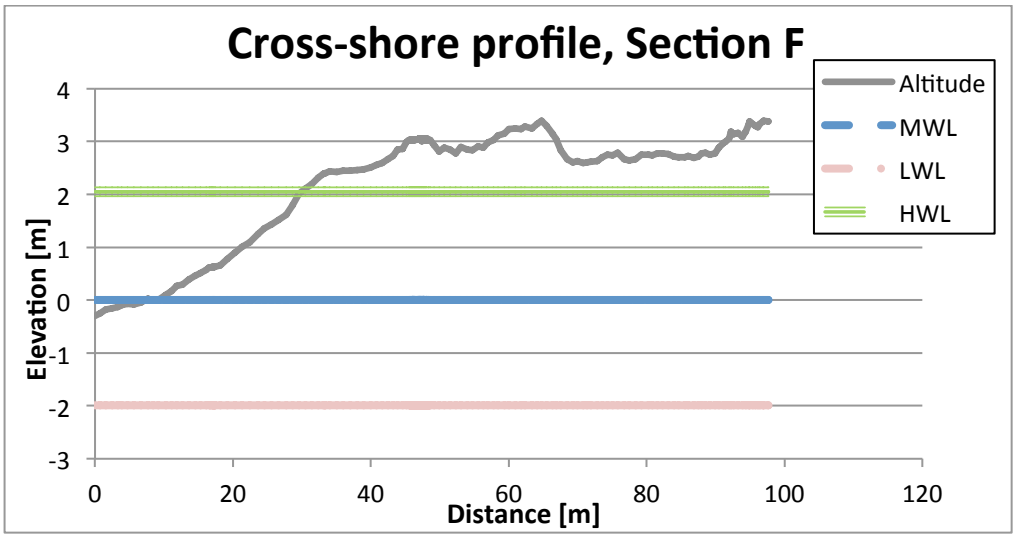

Figure 35. Cross-shore profile at section F. The profile is recorded from breaker zone on the seaward side (left) and up on the dune (right). The horizontal lines represent water level at high, mean and low tide. The datum is defined as the mean water level.

In Figure 35, the slope of the tidal plane and the beach face can be assumed to have a constant gradient. Calculated with linear equation the slopes are 4% and 10% respectively. The berm of the section is found 2.4m above the datum.

7.4.2 Sediment analysis

From the result of the sieving analysis it can be seen that the sediment distribution changes along the coastline of Macaneta. A median grain size, d_{50}, of each sample was determined by linear equation based on mesh size and weight of sediments on the trays in the sieving where 50 weight percent of the sample had passed the certain tray, see Appendix I for graphs and calculations. The d_{50}-values are presented in Table 1, sorted by each cross-shore profile. The results of the additional samples analyzed are presented in

Table 2.

Table 1. Median grain size $\boldsymbol{d_{50}}$ based on measurements for each beach feature on every cross-shore profile. Grain size in [mm].

Cross-shore profile	A	B	C	D	E	F
Foredune		0.68	0.62	0.36	0.29	0.26
Berm	0.72	0.84	0.57	0.33	0.70	0.29
Swash zone	1.10	1.17	1.20	0.91	1.11	0.26
Breaker zone	0.34	0.25	0.27	0.29	0.78	0.32

From the results presented in Table 1 it is seen that the beach section at the southern part of the spit, represented by section F, contains finer sediments than at the beach sections further up the spit. Results for each cross-section are presented in graphs in the Appendix. The foredune of section B and C contain very coarse sediment for a dune making it possible to assume that the dune is affected by cross-shore transport. Another interesting grain size is for the breaker zone at section E. Most likely an error in the sampling procedure is responsible for the divergent result. From the result it is also possible to make the statement that grain size distribution differ over the cross section. The finest sediments are, with the exception of section E, found in the breaker zone while the coarsest sediments are found primarily in the swash zone, see Table 1.

Table 2. $\boldsymbol{d_{50}}$-values for the additional samples sorted by location and beach feature. Grain size in [mm].

Additional samples	$\boldsymbol{d_{50}}$
Section A, river dune scarp	0.88
Section A, river bed	0.88
Section E, river dune scarp	0.75
Section E, river bed	0.29
Tip of spit, eastern swash zone	0.24
Tip of spit, southern swash zone	0.97

From

Table 2 it is seen that the mean grain size at the dune scarp of the river side at location E are bigger than at the river bed at the same section. This is naturally since at the river bed sediments get to settle at a gentle slope while the dune scarp is steep and the river only reaches this point during events of high discharge. However, this is not the case at location A where the grain size distribution of the dune scarp is similar to the one found at the river bed. This might indicate that there are overwash present at this section or that the longshore current in the river prevents finer sediment to settle.

Another interesting result is that the grain sizes are considerably larger at the southern tip of the spit, facing the Maputo bay, compared to the sediments found in the swash zone on the eastern side, facing the Indian ocean, see Figure 36 for location of sample points. This would indicate that the waves and current acting on the southern side are stronger than at the eastern side. A reason could be the diffraction of Inhaca and the shoaling of Danae shoal sheltering the peninsula from high waves and limits the wave force from east while the outlet of Incomáti and waves within Maputo bay have a stronger effect on the south side.

Figure 36. Sediment sampling points at the tip of Macaneta spit (Google Earth, 2014).

7.4.3 Shoreline positions

From the GPS survey of Macaneta spit the entire seaside shoreline from the tip up to the Macaneta Holiday Resort was recorded. By comparing the recorded positions with historical shorelines, longshore evolution trends can be detected. In Figure 37 to Figure 40, parts of the recorded shoreline from the field survey are displayed together with historical shoreline positions. Three areas of interest are chosen for analyze. The first one is the narrow isthmus at the northern part of the spit represented by section A, the second the southern isthmus located at section E and the last location of interest is the tip of the spit. Both section A and E are located at points where the Incomáti river bend to the west creating high flows close to the isthmus banks and thereby generate high risk of erosion of theses sections (Madsen, 1995).

In Figure 37 and Figure 38 the shoreline and riverbank are displayed for cross-section A, the most narrow isthmus of the spit. To determine the position of the shoreline at the section the berm position has been used. In the case for the tip of Macaneta spit, displayed in Figure 40, there is no berm present and the vegetation line has been chosen to indicate the shoreline position. In Figure 39 shoreline and riverside positions at section E are presented determined from satellite images. The vegetation line has been used to identify the shore position. An image of the entire shoreline is presented in the Appendix III.

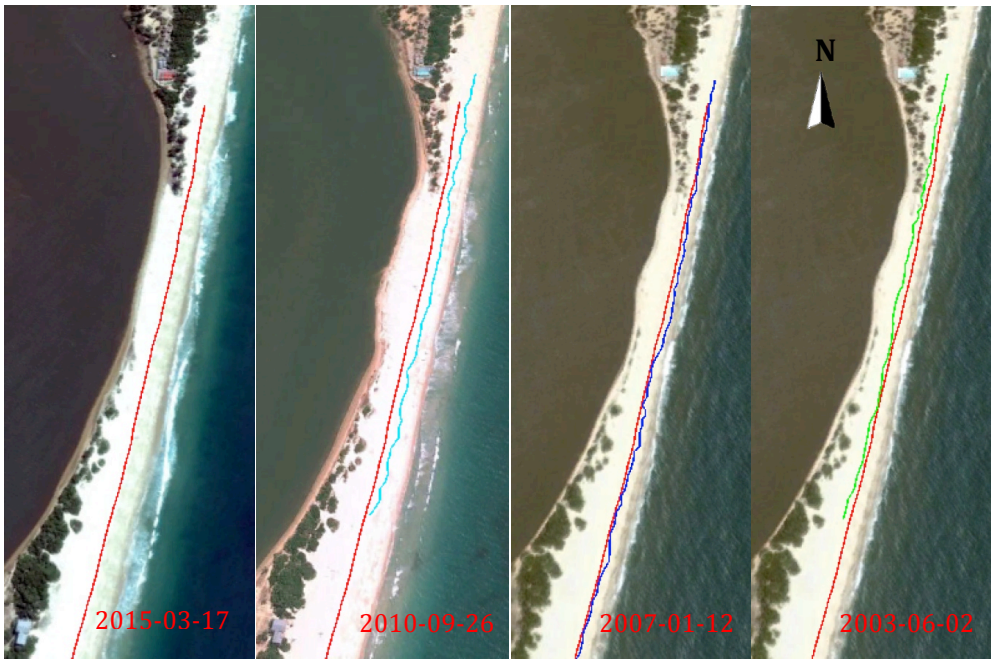

Figure 37. The recorded shoreline position (red line) from 2015-03-17 displayed together with historical shoreline positions on old satellite images (Google Earth, 2014). From the left: Recorded shoreline displayed on a satellite image from 2014-08-30, recorded shoreline together with shoreline position from 2010-09-26, recorded shoreline and shoreline position of 2007-01-12 and finally recorded shoreline and shoreline position from 2003-06-02. All images are captured at an altitude of 1km above MSWL.

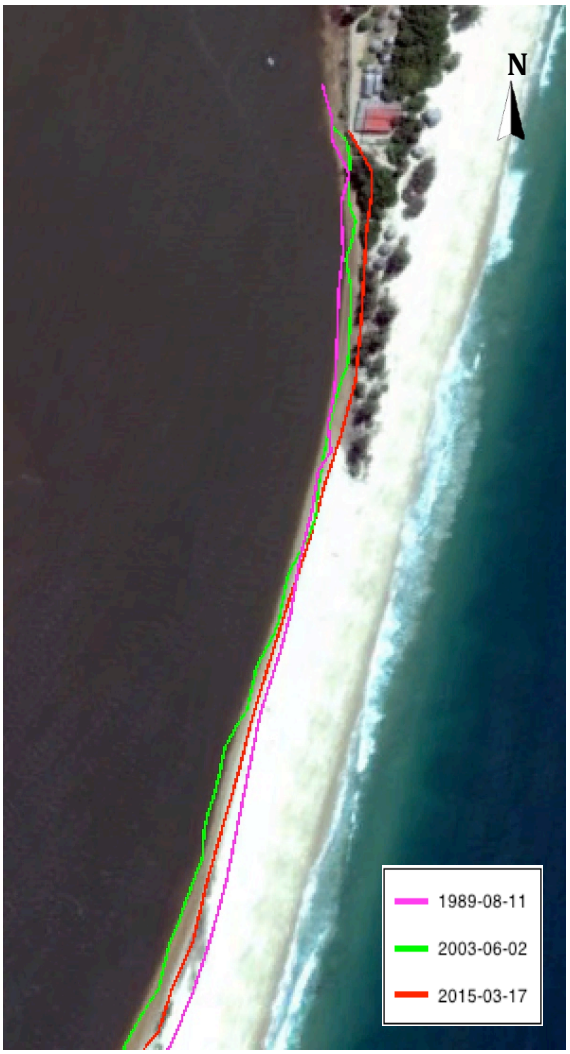

Figure 38. Satelite image from 2014-08-30 displaying the position of the riverbank for the years 1989, 2003 and 2015.

The shoreline positions recorded in Figure 38 do not show any historical trend of migration of the isthmus, but rather a yearly variation due to cross-shore influence at the time. Apart from the analysis based on historical satellite images an aerial photography from the 11th of August 1989, obtained from The National Center for Cartography and Remote Sensing (CENACARTA), was consulted to estimate migration of the shoreline at the isthmus. By geo-referencing with permanent structures in the region from before 1989 the photography was compared with the recent satellite image from 2014-08-30. No apparent change of shoreline position was detected between 1989 and today. Even though no migration of the dune seawards was identified it is obvious that there is

ongoing erosion on the riverside at Macaneta Holiday Resort, just north of section A, Figure 38. In the figure it is stated clear that the riverbank at Macaneta Holiday Resort has been eroded considerably during the last 25 years. From estimations the riverbank just south of the resort has withdrawn with about 20m between the years 1989 and 2015. On the slope facing the river at Macaneta Holiday Resort a simple revetment of dumped old construction material have be been created in an attempt to slow down the erosion. However while protecting the resort the revetment built risk to only move the erosion problem southwards, as it interfere with the littoral drift. At the non-vegetated isthmus a trend of erosion is harder to detect. The river bank position has historically been moving both towards east and west during different time periods. The growth and retraction of the riverbank could instead indicate that overwash events take place at the isthmus, transporting sediments from seaside to riverside. Although the erosion problem of the riverbank north of section A should be acknowledged focus of the study is to understand and quantify the coastal processes affecting the coastline.

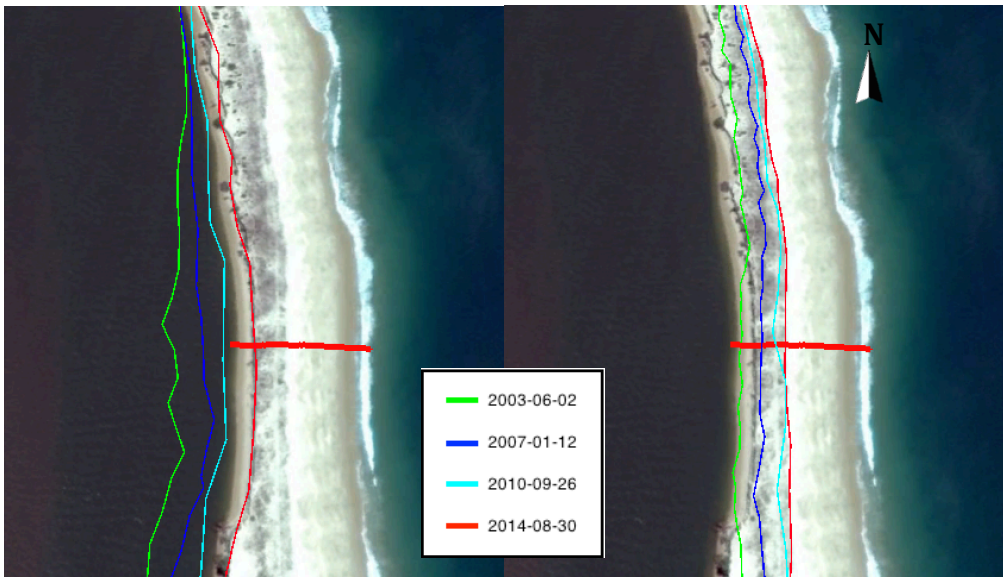

Figure 39. Satellite image from 2014-08-30 displaying the position of the vegetation line at section E; towards the river (left) and towards the ocean (right) for the years 2003, 2007, 2010 and 2014.

Figure 40. Surveyed shoreline position (2015-03-17) together with historical shoreline positions of the tip of Macaneta spit, displayed on old satellite images (Google Earth, 2014). From the top left to lower right: Surveyed shoreline printed on satellite image from 2014-08-30, Surveyed shoreline together with shoreline position from 2010-09-26, surveyed shoreline and shoreline position of 2007-01-12 and finally surveyed shoreline and shoreline position from 2003-06-02. All images are captured at an altitude of 1.32km above MSWL.

In Figure 39 it is clearly shown that the isthmus at section E is migrating eastwards. However, the riverbank is eroding at a higher pace than the migration thus the isthmus is narrowing. The vegetation line riverwards has moved 50m since 2003 while the vegetation line seawards has only moved 20m.

From the shoreline postions in Figure 40 it is possible to see that the tip of the spit has a historical trend of migrating to southeast. The shoreline seawards rather indicate seasonal trends in shoreline position than a significant ongoing trend over longer time. The trend of the shoreline position on the southern and western side of the spit is easier detected. As can be seen a natural cove has been formed towards northwest probably as a result of episodes of sediment transport in this direction. Moreover downdrifting sediments are trapped in the cove which forms a natural groin. Since the groin prohibit further downdrift transport the southwestern shoreline of the cape continue to erode and sediment is transported to the tip which explain the trend of the spit to extend more and more in southeast direction while the southern shoreline is withdrawing, creating a more cusped shape.

In summary, during the last decade the southern part of the Macaneta spit has slowly been migrating eastwards. The rate of movement differs along the spit. At section A the shoreline is considered at equilibrium and no trend of eastward migration is discovered and the same applies down to section C. At section C it can be seen that the coastline orientation change significantly and at the same time a more distinct migration is observed. The migration is even more significant closer to the tip of the spit but declines at the very tip. In section 10.2 the observed processes are compared with calculated littoral drift.

The river composes as a major threat to the isthmus at section A and E. At the Macaneta Holiday Resort just north of section A the owner has built a simple revetment to protect the property from erosion, at the surveyed section a trend of erosion is however hard to detect. For section E the erosion is very prominent and the riverbank has moved 50m during the period from 2003 until 2014.

7.4.3 Bathymetry

Data gathered during the bathymetric excursion and data obtained from INAHINA, was used to mapping of the ocean floor. While the bathymetric survey covered the nearshore region up to 2km offcoast bathymetric data from INAHINA was used for the rest of the region.

In order to quicken the modeling of nearshore wave conditions a coarse grid was employed to represent the bottom profile. Due to the poor resolution wave action in the surf zone cannot be modeled to satisfactory. The extraction points from the simulation carried out with EBED were therefore located about 5-10km offshore Macaneta spit. Consequently the topography was used from INAHINA alone and to a depth of 10m. The bathymetric was processed in ArcGIS and exported as a raster with a grid size of 200m by 200m with the most eastward and southward cell corresponding to a point east of Inhaca island where the depth exceeded 100m, Figure 41.

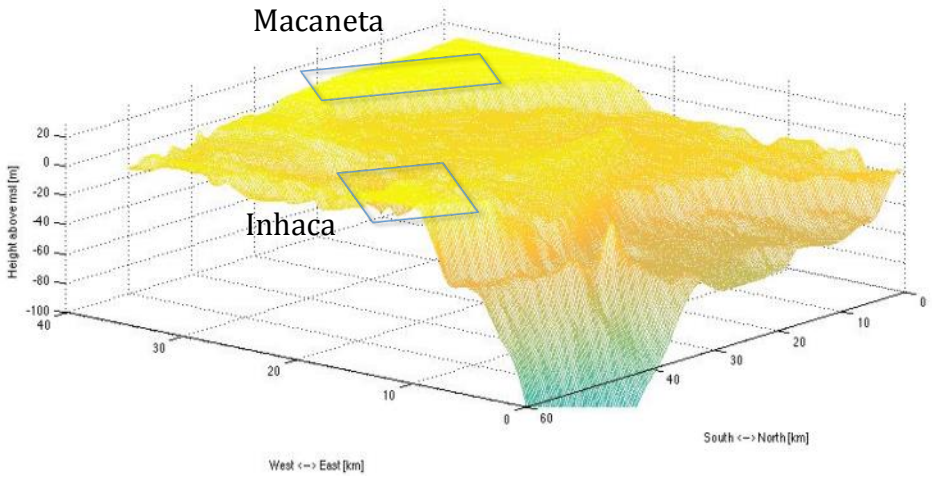

Figure 41. Displaying the bathymetry around Macaneta. The bright yellow parts are above sea level and the color mapping is getting darker with the depth. The upper rectangle display the location of Macaneta and the lower box show the location of Inhaca.

Among the landmasses above sea water level Macaneta spit is located on the western ridge in the figure and in south the northernmost part of Inhaca island is found. In the figure depths up to 100m are displayed. However, the greatest depths within the grid, found east off the coast of Inhaca, measure down to 248m.

8. Data analysis

8.1 Wave data

The wave data modeling was carried out implementing numerical modeling software EBED. Input to the numerical model are wave data reanalysis from WW3 including; significant wave height, wave direction and wave period and bathymetry from nautical chart provided by INAHINA. In the absence of locally measured wave data for the region of Maputo reanalysis hindcast data obtained from the NOOA Wave Watch III (WW3) model (NWS, 2010), developed by the U.S. National Center for Environmental Prediction (NCEP) was used for the study at Macaneta spit.

The extracted WW3 data downloaded covered the period from the first of February 2005 until the last of December 2014. The model generating the data from WW3 is based on a 0.5° by 0.5° grid with model outputs generated every three hours for the entire period.

The coordinates of extraction for modeling in EBED was determined by locating the nearest position, corresponding with WW3 output coordinates, off the coast of Macaneta with a depth larger than 100m. Three coordinate positions were located, see Figure 42. Data was downloaded for all three locations and by analyzing the prevailing wave directions and the topography of the region it was concluded that the coordinate with best representation was found at -26.0 N, 33.5 E.

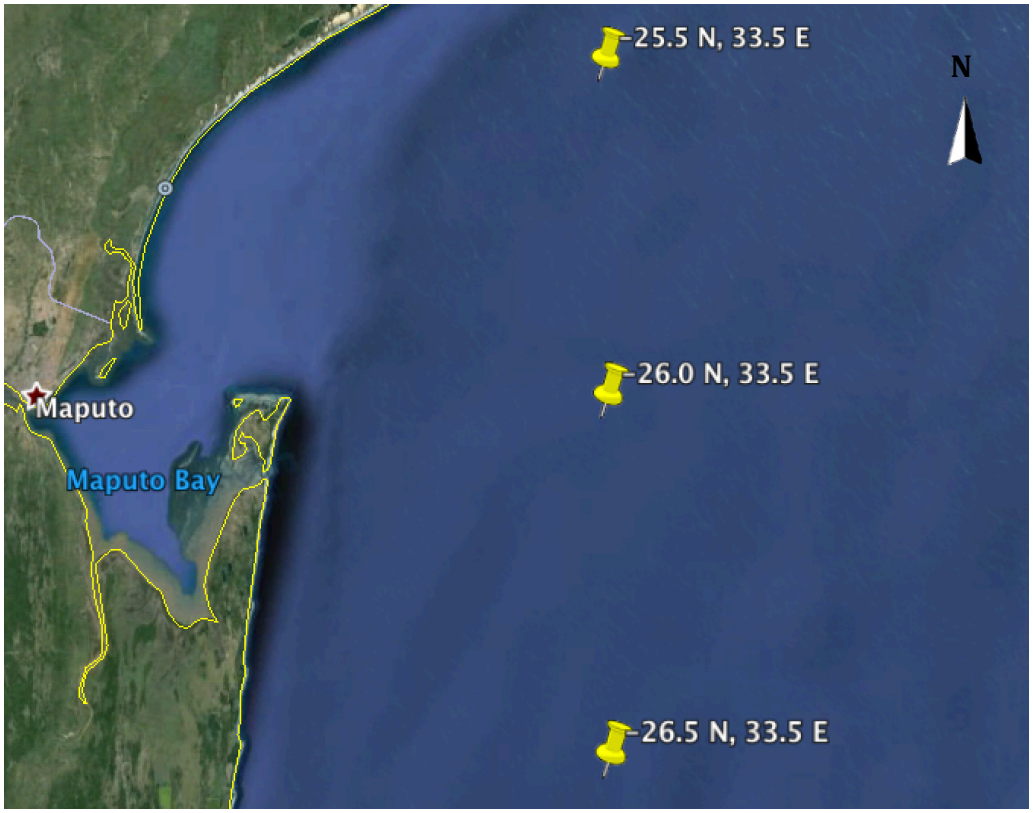

Figure 42. Three possible GPS positions for wave data extraction. The latitudal distance between each 0.5° is approximately 55km. From analysis of wave direction and topography -26.0 N, 33.5 E was chosen as the coordinate to extract the data from.

From the wave data extracted a wave rose was created based on the significant wave height and direction of the offshore data for the years 2005-2014, see Figure 43.

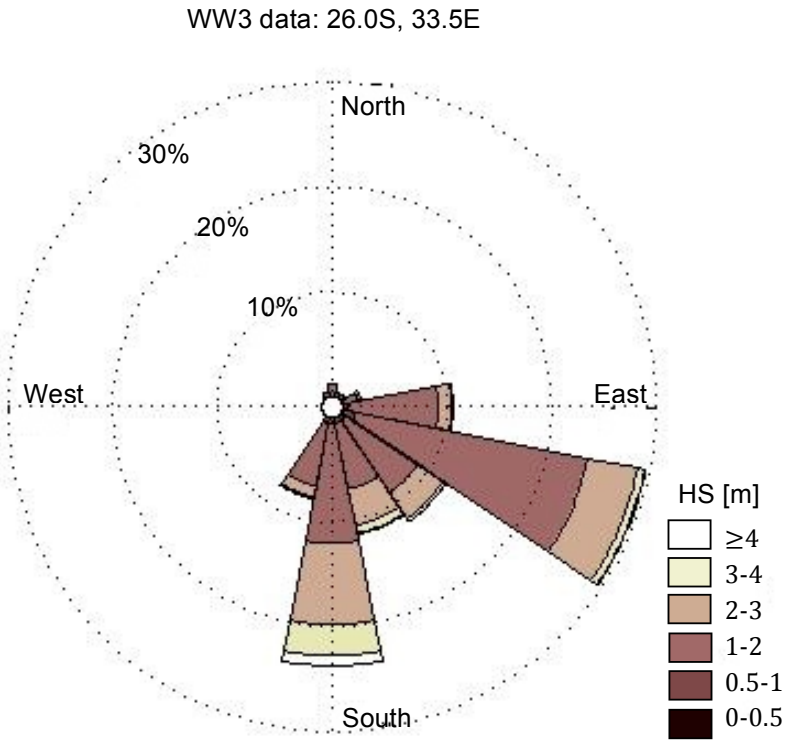

Figure 43. Wave rose presenting the wave conditions extracted from Wave Watch III at a point - 26.0N, 33.5E offshore Macaneta.

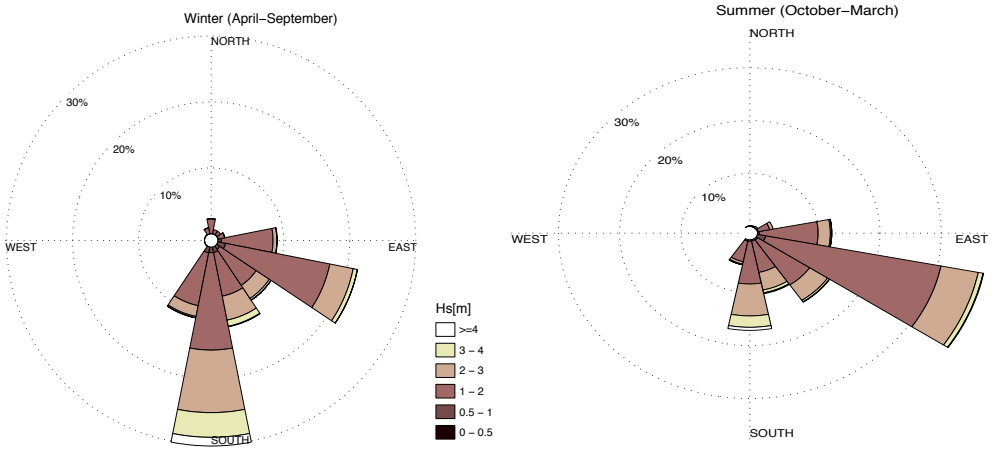

Figure 44. Wave roses displaying seasonal variation of the waveclimate offshore Macaneta, extracted from Wave Watch III. The left figure display direction and significant wave height during the winter season between April and September and the right figure display the summer conditions between October and March.

As seen in Figure 43, the wave directions offshore Macaneta are found in the directions of origin between south and east. The waves with highest significant wave height origin from south were approximately 4% of the waves exceed 3m. In line with prior studies of the coast (Young, 1999), the highest significant wave height of the waves off coast Macaneta are generated during the winter and the prevailing direction of propagation is northwards, Figure 44. Verifying the statement by the *Jury and Pathak* (1991) easterly to southeasterly waves are prominent throughout the year but strongest during the southern hemisphere summer.

8.2 Coastal profile at equilibrium

8.2.1 Equilibrium profile fitting

With the equilibrium profile equation deduced by Bruun (1954), Dean (1977) and Moore (1982) is it possible to link the beach profile with the grain size at the beach. The equation was evaluated by analyzing a wide variety of beaches all over the world and compering the slope and grain size.

Equilibrium profile equation:

$$D = A\, y^{2/3} \qquad (8.1)$$

D = depth in the equilibrium profile [m]
y = distance offshore [m]
A = empirical scale parameter

$A = 0{,}41 * {d_{50}}^{0{,}94}$ $\quad d_{50} < 0{,}4$
$A = 0{,}23 * {d_{50}}^{0{,}32}$ $\quad 0{,}4 < d_{50} < 10{,}0$

One disadvantage with the equilibrium profile equation is that it does not take into consideration the appearance of bar formations. However, the concept of an equilibrium profile is easy and useful for investigation in a coastal area. The equation is commonly used for simulation of coast evolution where the beach profile needs to be represented e.g. in *GENESIS* (Hanson & Kraus, 1989).

The theoretical beach profile might differ from the measured profile and there can be several reasons why there is a difference. The theoretical beach profile gives an average profile and do not include seasonal variation or storm variation. Small variant between the theoretical beach

profile and measured might be due to the seasonal or storm variation but higher variation could indicate that changes in the coastal climate or that the sediment transport at the beach are affecting by external obstacle or processes.

The theoretical equilibrium beach concept can also explain why erosion take place during storm events and storm surges in coastal areas where equilibrium is already established. In these events the increased water level will move the position of the equilibrium profile and both depth relationship and slopes will change. A deeper and steeper profile will be compensated by removing sand from the beach and transport it to the ocean until slope and depth corresponds to the equilibrium profile for the high tide. The offshore transport off sediment will cause the shoreline retreat and if the beach is not wide enough sand will be taken from the cliff or the dunes. After the storm most of the sand will slowly be transported back to the beach, extreme storm event might however result in permanent offshore losses of material.

8.2.2 Result from the survey at Macaneta

During the survey at Macaneta beach six cross-shore profiles were measured. From this profile is it possible to determine a theoretical mean grain size, d_{50}. These value can then validate the slope of the beach profile below mean low water line. The slope from each section was plotted from tidal plane, approximately 0.2 m, above mean water line towards breaker zone against the equilibrium profile equation, eq 8.1. The different d_{50} where then used to iterate the best mean square error fit. The d_{50} with the best fit was then considered to be the d_{50} of the section.

All plots and tables from the determination of d_{50} for each section can be found in the Appendix II. As an example the cross-shore profile A is plotted against eq 8.1 in the Figure 45 below. After iteration of different values for d_{50} the best match was a d_{50} of 0.23mm with a mean square error of 0.107 m.

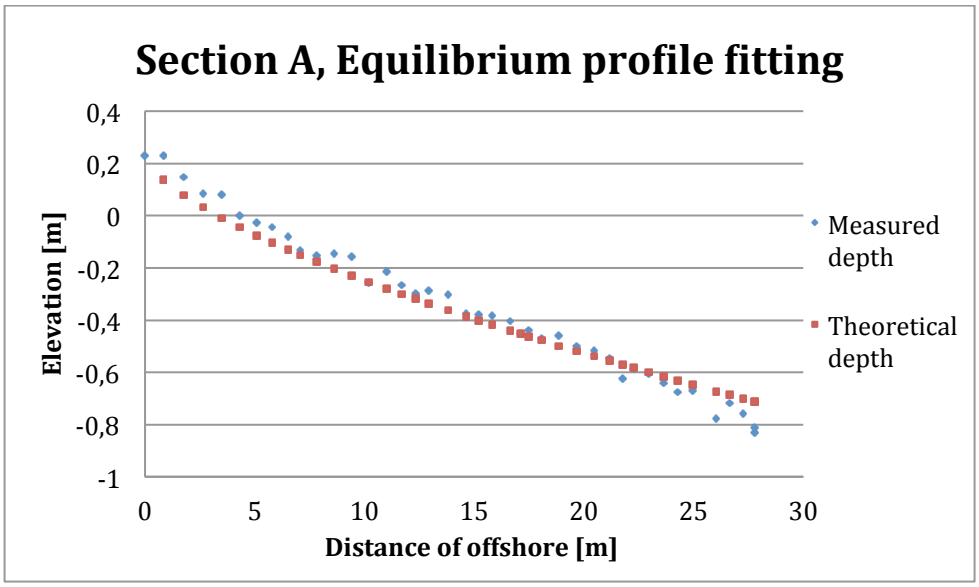

Figure 45. Adjusted theoretical depth against the measured depth at section A. The theorethical depth correspond to a d_{50} of 0.23mm.

From Table 3 is it possible to see the difference between measured d_{50} and a theoretical d_{50} based on eq. 8.1. There are no clear differences between the measured values and the theoretical values. Apart from section E is the difference between measured and theoretical d_{50} at most 0.12mm. The theoretical d_{50} should be used with care as the length of the bottom profile was short. When the d_{50} is determined from the cross-shore profile it is desirable to have data continuing deeper and further offshore than what was possible to collect during this survey. Even the low value of the mean square error, 0.107 m^2 for section A, could indicate lack of data as this corresponds to a mean difference of only 1cm between the measured profile and the theoretical.
However, Table 3 indicates that the measured values can be considered correct thus used when modeling the cross-shore processes, section 11.2. Due to a deviating measured d_{50} at section E, the theoretical value of 0.29mm was used when modeling this section.

Table 3, Measured and theoretical d_{50} and mean square error for each section.

Section	**A**	**B**	**C**	**D**	**E**	**F**
Measured d_{50} in breaker zone	0.34	0.25	0.27	0.29	0.78	0.32
Mean square error	0.107	0.163	0.163	0.053	0.025	0.379
Theoretical d_{50}	0.23	0.25	0.30	0.29	0.29	0.20

9. Mathematical modeling of nearshore waves

The wave climate of a coastal system is of uttermost importance when studying the evolution of a coastal zone. Sediment transport is very much influenced by the nearshore waves and dissipation of wave energy from breaking waves has a mayor effect on the form of the coastal profile. By modeling the waves approaching Macaneta spit it is possible to get an understanding of the forces acting on the beach, the nearshore direction field and significant wave heights.

Due to the complexities of morphology in different coasts, there is no universal model for analyzing and predicting coastal evolution and physical processes for the complete set of spatial and temporal scales (Hanson et al., 2003)

The model used in this study was a modification by Nam (2010) of the random wave model EBED, developed by Mase (2001). The EBED is a prediction model of multi-directional wave transformation for calculation of waves in the nearshore. It is based on the energy balance equation for conservation of wave energy flux and include terms for energy dissipation and diffraction (Mase, 2001). The model has the ability to handle complex topographic conditions, especially for cases where diffraction is prominent. In the case of Maputo the shadowing effect of the Inhaca Island is significant for the southeast waves and diffraction will affect the wave angle. Apart from diffraction the model also has the ability to handle shoaling, refraction, and breaking, all which have major influence on the waves in terms of wave height and wavelength. The model does not consider reflection.

9.1 Background and theoretical formulation

The modified model developed by Nam and Larson (2010) approaches the problem with frequently overestimated wave heights in the surf zone. A problem addressed by adjusting the algorithm for wave energy dissipation caused by wave breaking (Nam & Larson, 2010). The modified-EBED employed in this study is thereby able to genereate more accurate input for numerical models used to simulate the nearshore currents, determine the sediment transport and morphological evolution.

The original EBED model with terms for wave dissipation and diffraction is the basis of the modified-EBED, the energy balance equation is presented in (eq 9.1).

$$\frac{\partial(v_x S)}{\partial x} + \frac{\partial(v_y S)}{\partial y} + \frac{\partial(v_\theta S)}{\partial \theta} = \frac{\kappa}{2\omega}\left\{\left(CC_g \cos^2\theta S_y\right)_y - \frac{1}{2}CC_g \cos^2\theta S_{yy}\right\} - \varepsilon_b S \qquad \text{(eq 9.1)}$$

where S is the angular-frequency spectrum density, (x, y) are the coordinates, where the x axes is directed longshore and y axis in the cross-shore direction, θ is the angle measured counterclockwise from x axis; v_x , v_y , and v_θ are propagation velocities in resepective coordinate direction, ω is the angular frequency, C and C_g are the phase speed and group speed respectively, κ is defined as an independent coefficient to be optimized in order to change the degree of diffraction effect, and finally ε_b is a dissipation coefficient.

The first term on the right side of the equal sign describes the diffraction effect of the propagating waves and the second term describes the dissipation, later modified by Nam and Larson (2010). The final equation after modification is expressed as (Equation 2):

$$\frac{\partial(v_x S)}{\partial x} + \frac{\partial(v_y S)}{\partial y} + \frac{\partial(v_\theta S)}{\partial \theta} = \frac{\kappa}{2\omega}\left\{\left(CC_g \cos^2\theta S_y\right)_y - \frac{1}{2}CC_g \cos^2\theta S_{yy}\right\} - \frac{K}{h}C_g S\left\{1 - \left(\frac{\Gamma h}{H_s}\right)^2\right\} \quad \text{(eq 9,2)}$$

where h is still water level and K and Γ are non-dimensional experimental coefficient calculated as, (Equation 3):

$$\begin{cases} \Gamma = 0.45, K = \frac{3}{8}(0.3 - 19.2m) & m < 0 \\ \Gamma = 0.45 + 1.5m, K = \frac{3}{8}(0.3 - 0.5m) & 0 \le m \le 0.6 \end{cases} \qquad \text{(eq 9.3)}$$

where; m is the bottom slope (Nam & Larson, 2010).

Input to EBED consists of bathymetry of the region together with offshore wave data including height, period and direction. The bathymetry file for Macaneta has a mesh size of 200x200m. The direction of the x-axis is defined positive from deep water (offshore) towards shallow water (shoreline) in western direction with the total length of around 30km and the y-axis is defined positive in north direction with the total length of around 55km. Resulting in a total grid with more than 51 000 grid cells to represent the bathymetry of the coastal stretch.

9.2 Model implementation

Based on offshore wave data, provided by WW3, along with bathymetry, from the naval chart created by INAHINA, the EBED simulation was carried out. The number of time steps for simulation was limited by the input data from WW3, consequently the simulation was run from 2005-02-02 up to 2015-01-01 with wave data for every 3h.

The modeled output were significant wave height, wave period and wave direction at 6 points along the coast. The points were chosen to coincide with the latitude of the surveyed cross-shore sections and were chosen as the point nearest shore with a depth exceeding 12m below mean sea water level. The points were also given the same name as the sections, starting with A up north and ending with F in the south.

9.3 Result of nearshore simulation

An isolated timestep at 2012-01-16 at 09.00 was simulated to generate the wave climate with wave height and associated direction field for the modeled region. The offshore wave direction at the timestep presented in Figure 46 is from south-southeast, which represents the abundant wave direction offshore Inhaca Figure 43. The wave heights at Macaneta for this timestep are among the largest for the entire simulation period, with a significant wave height largest at point A with 2.09m and lowest at point F corresponding to 1.67m.

In Figure 47 wave roses along the Macaneta peninsula, displaying direction and wave height of nearshore waves between the years 2005-2015, are presented. Each wave rose corresponds to its geographic location.

The modeled wave climate, as seen in Figure 46 show that the waves tend to approach the coastline of Macaneta at almost perpendicular angle, resulting in a sediment transport of a more limited nature (further explained in section 11.2). The reason of this behavior, see Figure 46, are the shadowing effect of Inhaca island and the shallow region of Danae shoal north of Inhaca island, which reduce the waves and deflect them to west.

The shallow area of Danae shoal could even pose as a breaker zone in some cases. During low spring tides the depth at the most shallow part only measure 3.5m (INAHINA, 2010). As seen in Figure 46 the wave energy is highly dissipated when crossing the shoal resulting in significantly lower wave heights west of Danae shoal.

It must be stressed that the presented result is merely a model of the reality, some variables are overlooked and others not calibrated. The EBED model does not take into account the tide nor the storm surges effect on the sea water level. A fixed mean sea level was used in the model, calculated based on the tidal variation over the last 10 years. Consequently the model does not catch the difference in energy dissipated over Danae shoal between high and low tide. In reality waves breaking at Macaneta tend to be smaller during low tide and bigger during high tide as a result of the present water depth at the shoal.

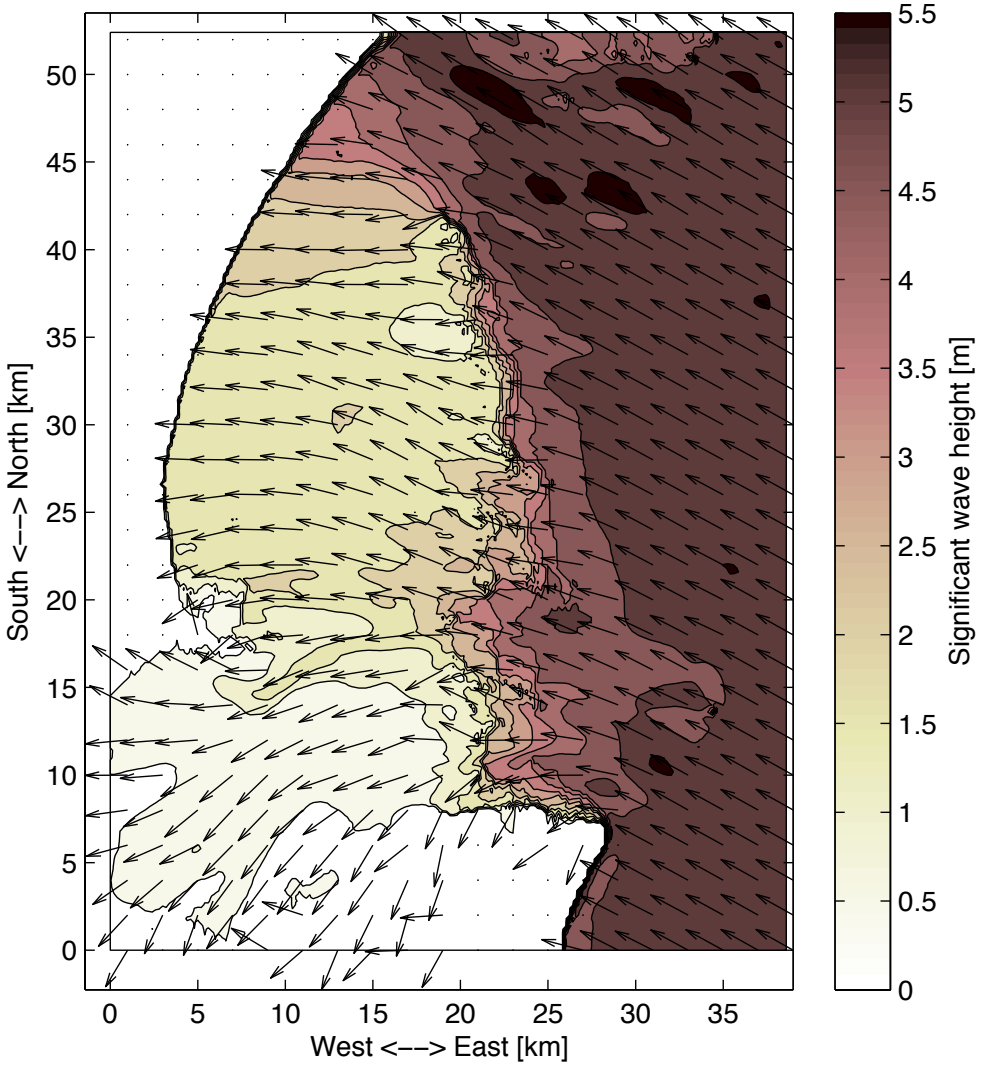

Figure 46. Modeled nearshore wave conditions during a large SSE swell at 09.00 the 16th of January 2012. Waves offshore have a wave height of 5.47m and a direction of 120° from true north.

By comparing the offshore wave input with the resulting waves at the coast of Macaneta, it is seen that the wave height are considerably reduced and the directions deflected to the west. Through a comparison of wave height between offshore and nearshore Macaneta the mean wave height nearshore Macaneta was calculated as 1.1m while the reported mean wave height off the coast of Inhaca was above 1.7m.

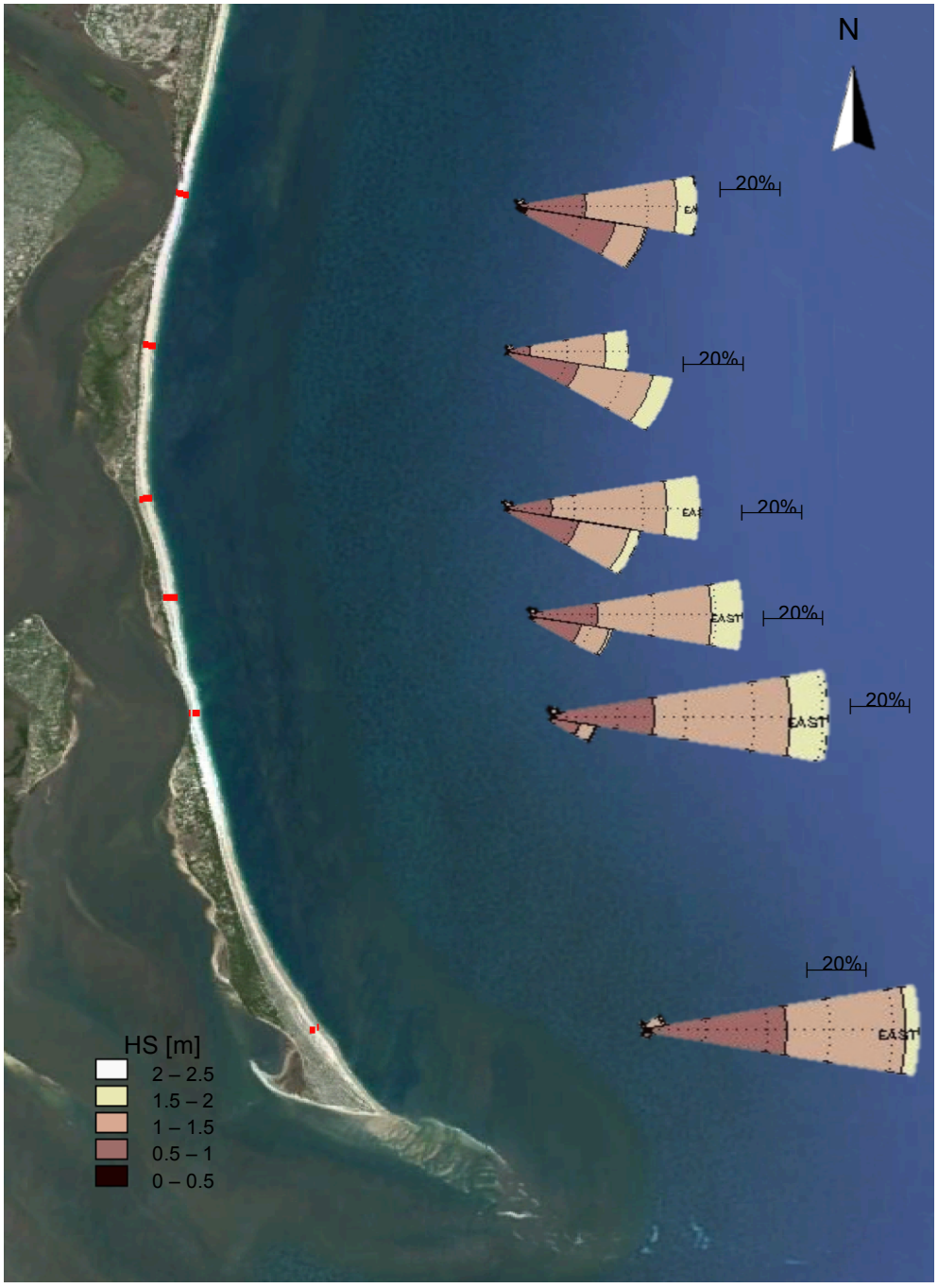

Figure 47. Wave roses displaying the modeled wave conditions along the Macaneta peninsula. Red markings along the shoreline display the sections for the cross-shore survey.

From calculations of the mean wave height and wave direction from true north respectively following values for the extracted locations in EBED are determined:

- Location A: 0.99m and 98.5°
- Location B: 1.15m and 102.0°
- Location C: 1.12m and 98.3°
- Location D: 1.10m and 95.3°
- Location E: 1.10m and 92.0°
- Location F: 1.00m and 84.5°

Although the mean wave height at location A are the smallest for Macaneta spit, the point is also subject to the highest incoming waves along the spit. According to the simulation performed, the only point with wave heights exciding 2m for the simulated period. The distribution of the wave heights at this point is presented together with the offshore wave heights in Figure 48. The wave heights at point A vary between 0.3-2.1m, however 80% of the waves have wave heights varying between 0.7-1.3m. Only about 3% of the waves reach a wave height above 2m. The offshore waves have a stronger variation in wave height indicating that the propagation towards shore even out and reduce large wave heights significantly and that Danae shoal has a major effect in extreme events.

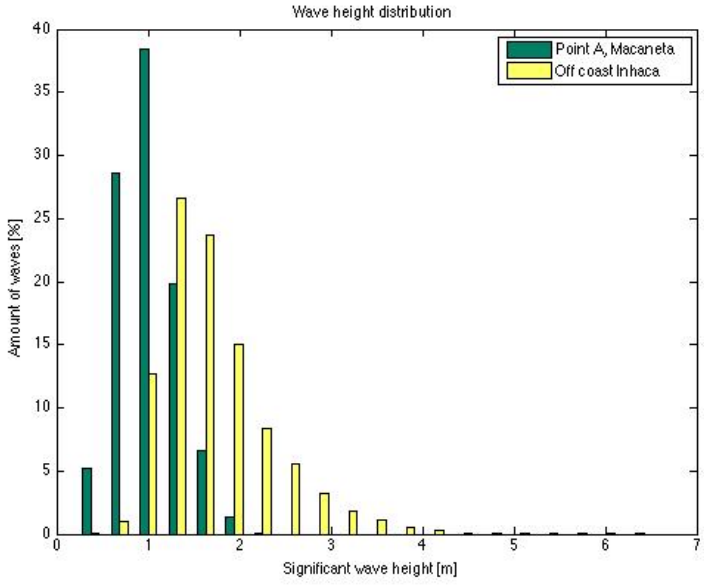

Figure 48. Histogram displaying the wave height distribution between input values offshore and the resulting values for point A at Macaneta.

The highest significant wave heights both offcoast and nearshore were found the 3rd of March 2012. This date correspond with the time of when the tropical storm Irina, responsible for causing a lot of damages and death during the hurricane season of 2012, struck the region of Maputo (DLR, 2012; NASA, 2012). At this date waves offcoast reached to 6.27m and modeled nearshore waves at point A and point F corresponded to 2.13m and 1.74m respectively. The direction of origin of the waves was from the east, thus limiting the diffracting effect of Inhaca. Moreover, making it even more obvious that Danae shoal act as a protecting barrier of ingoing waves.

At storm surges the water will rise above the normal high tide level (Pugh, 1996) and since storm surges are an indication of an incoming storm the sea rise is often accompanied by high waves. The increase in sea level will allow waves crossing Danae shoal to maintain higher energy and accordingly give an increase in wave height at Macaneta. The combined effect of high water levels and strong waves, storm surges have great importance and are most likely possible reasons for the occurrence of overwash events. At the time when the tropical storm Irina hit the south coast of Mozambique storm surges between 1.2 and 1.5m were assumed (DLR, 2012), of which are not accounted for in the model. However, the storm occurred during neap tide with a highest tide position of about 0.5m above mean sea level. Consequently, the storm event of 2012-03-03 had a water level at most 2m higher than modeled in EBED.

10. Modeling of longshore processes

The longshore current, heavily determined by the angle of breaking incident waves, has a major role controlling the eroding and accreting processes as a result of littoral drift over time (CEM, 2008).

For modeling the longshore transport the version of the Coastal Engineering Research Center (CERC) of the U.S. Army Engineer formula presented by Halcrow was employed (Halcrow, 2014). The CERC formula was first presented in the *Shore Protection Manual* (CERC, 1984) and is the most frequent used method to calculate total sediment transport. A variety of versions employing the CERC formula are available with some minor changes in the treatment of the variables. In the version used in this study, eq 10.1, the value of the transport coefficient has been changed compared to the original CERC formula.

$$Q_s = \frac{0.023 g^{1/2} {H_b}^{5/2} \sin(2\alpha_b)}{s-1} \; [m^3/s] \qquad (10.1)$$

where
Q_s = sediment transport rate integrated across the surf zone, volume of sediment per unit time.
g = gravitational acceleration.
H_b = significant wave height at breaker line.
α_b = angle between wave crest and shoreline at breaker line.
s = relative density of sediment

10.1 Model implementation and simulation

The CERC formula was employed in a software to calculate the longshore sediment transport. The model computes longshore transport from time series with significant wave height, wave period and incoming wave angle. The transformation of wave data is calculated from a stated reference depth.

The model considers shoaling and refraction phenomena and assumes the depth profile slope is constant and perpendicular to the beach face. The generalization works fine in the case of Macaneta, since there are no

coastal constructions interacting with the waves and cause diffraction and from the bathymetric study the contour lines for the depth profile along the spit are almost parallel to the shore at an similar interval, Figure 23. However, further down the spit become more unreliable. The depth profile deviates more from the simplified profile and waves from Maputo Bay together with current from Incomáti River might interfere with the longshore processes caused by the ocean waves.

The model uses the angle of the shoreline compared to incoming waves, in order to calculate the attack angle of the waves. No exact angles were known; instead these have been estimated from satellite images of the area (Google Earth, 2014). The shoreline orientation related to true north is presented in Figure 49 and **Fel! Hittar inte referenskälla.**.

Table 4. Shoreline orientation at the surveyed sections along Macaneta spit.

Section	**A**	**B**	**C**	**D**	**E**	**F**
Shoreline orientation (degrees)	98	94	76	79	77	58

The simulation was computed with nearshore wave data provided by the EBED model for the locations A-F. The wave data contained wave height, period and direction for the significant wave every 3h for the years 2005 to 2015.

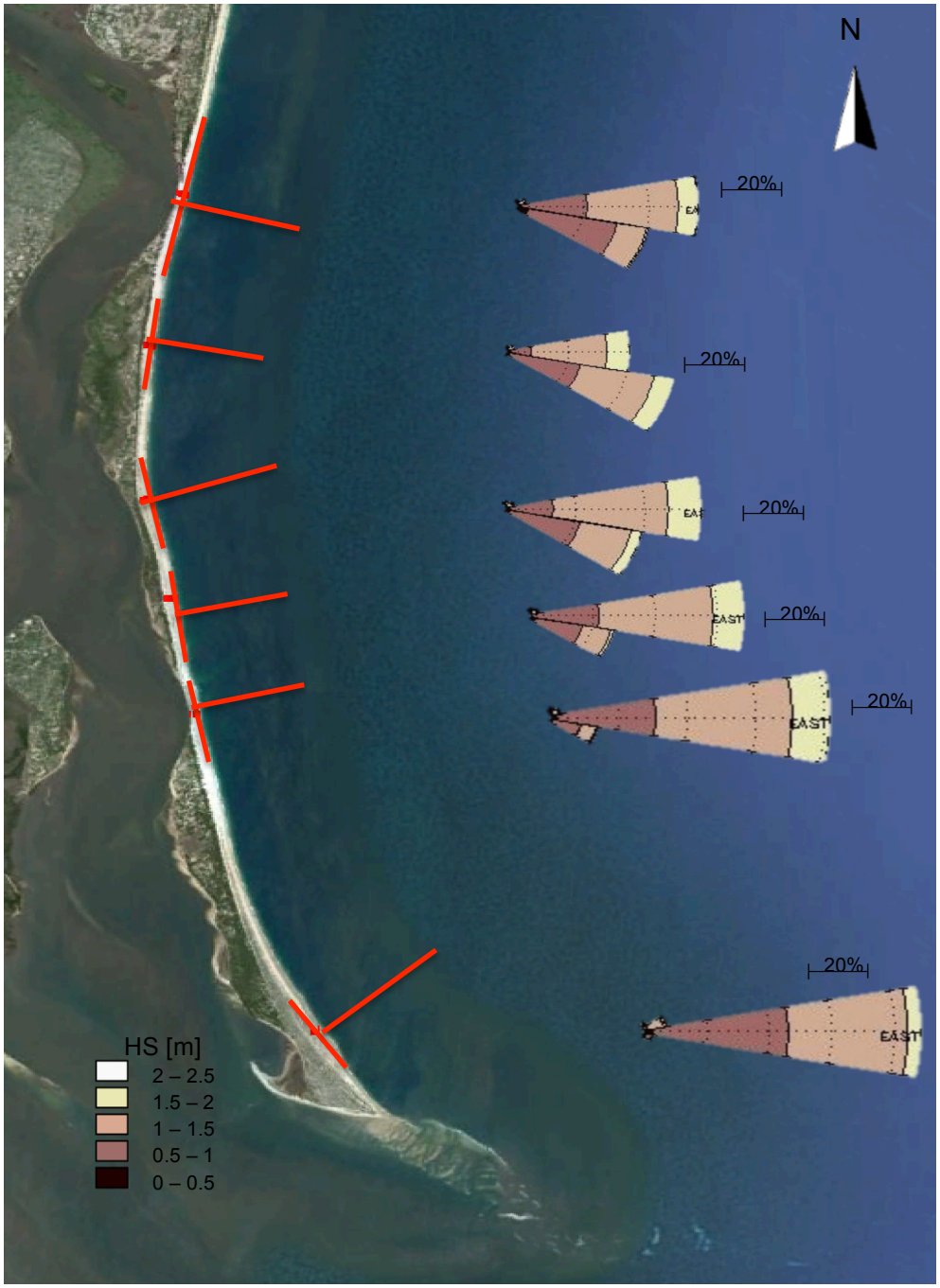

Figure 49. Each section with its normal perpendicular to the shoreline and the wave roses representing the wave during the simulation period for respective section. Long red line indicates true North and is used as reference to get an angle between normal and true North.

10.2 Result from longshore simulation

The results generated contain values of the yearly gross and net transport volumes for the 6 locations, see Figure 50 and Figure 51.

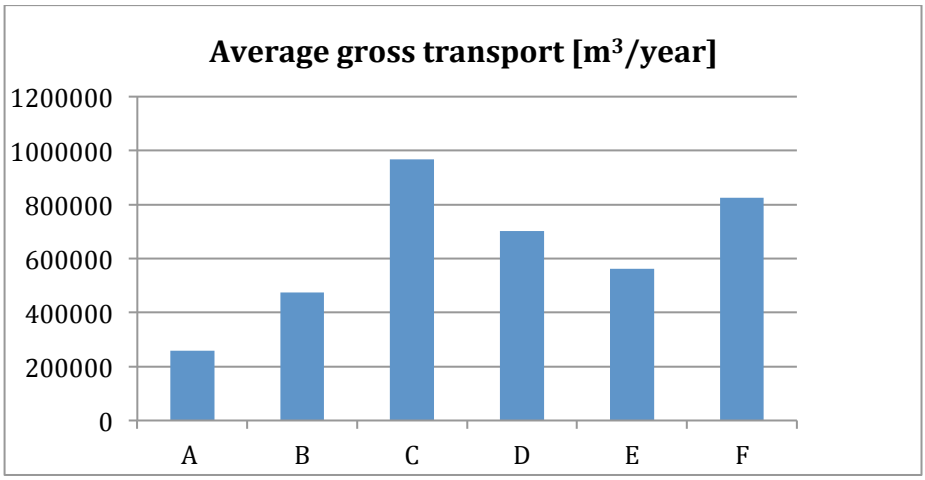

Figure 50. The average yearly gross transport for each section at Macaneta spit during the simulation period of 2005-2014.

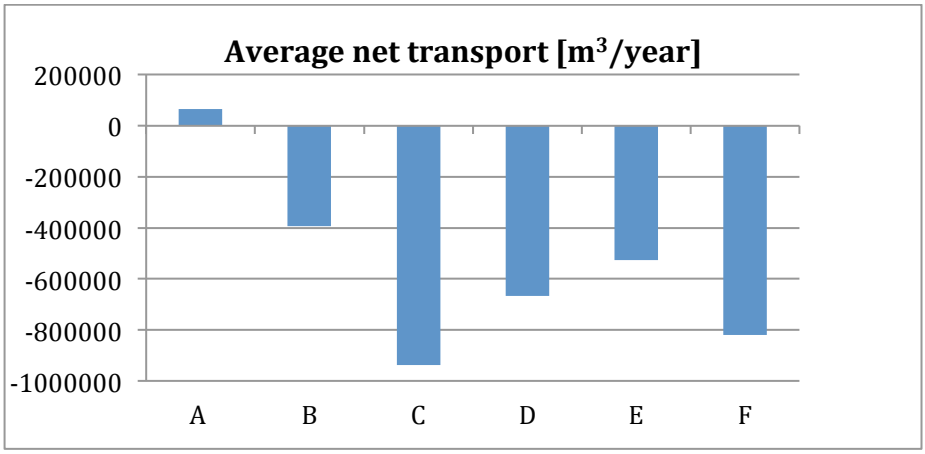

Figure 51. The average yearly net transport for each section at Macaneta spit during the simulation period of 2005-2014. Positive value represents a southern transport and negative value is a transport in northern direction.

The transport rates are high for a sheltered and protected coastline like Macaneta. Durban in South Africa, located 500km south of Macaneta and has a longshore net sediment transport of 300 000 m3/year (Komar P. D., 1988). The Macaneta spit, which is much more sheltered, has net transports at some sections more than twice of the transport rate at Durban. This illustrates the uncertainties in the simulation hence the magnitude of the transport is considered unreliable.

Some uncertainties when employing the model are; input data from the EBED model that was utilizing reanalysis data from WW3, estimations of the coastline orientations made from satellite images and empirical constants for calculations at the region are not known. With reference to these uncertainties a table presenting an equilibrium coastline orientation, which corresponds to zero net yearly sediment transport was made, Table 5.

Table 5. Shoreline orientation at the surveyed sections along Macaneta spit together with the equilibrium shoreline orientation corresponding to zero net yearly sediment transport.

Section	**A**	**B**	**C**	**D**	**E**	**F**
Shoreline orientation (degrees)	98	94	76	79	77	58
Equilibrium shoreline orientation (degrees)	96	102	98	94	91	83
Difference between measured shoreline and equilibrium shoreline (degrees)	2	-8	-22	-15	-6	-25

In Figure 52 the net longshore sediment transport are presented with arrows for direction and relative magnitude for each section.

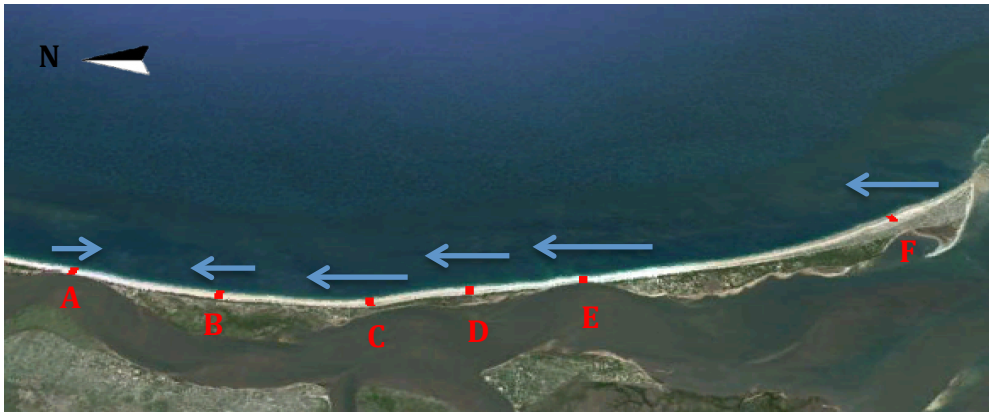

Figure 52. The net average yearly longshore transport with direction and relative magnitude along Macaneta spit, for the years 2005-2015.

The resulting average yearly net longshore transports indicate that direction of the littoral drift varies along the spit. There is a little southward littoral drift at the north part of the spit and northward littoral drift at the rest of the spit. Moreover the resulting directions correspond with the result from a survey conducted earlier (DHI, 2013).

Apart from varying directions, the transport rates do also vary. The transport in north going direction at, for example section B is considerably smaller than at section C. The differences in transport rate between the sections indicate that some areas lose sediment while others gain. The area around section C loose much sediment to northward drift while there is less influx of sediment taking its place, meaning that the beach section is eroding. Dissimilar conditions exist at the area between section A and B where counter directed transports meet consequently feeding a growing shore.

Based on the data from the GPS survey of Macaneta and the comparison of historical shoreline position at section A no yearly accretion at the section was discovered, section 8.3.3. Assuming that the longshore modeling is correct a reason could be that deposited sediment is transported cross-shore, both deposited at the dune, overwashed to the riverside and transported offshore. The overwashed sediments could maintain an equilibrium of the shoreline by counteract the erosion from Incomáti river.

The northward sediment transport does not necessarily mean that the tip of the spit is eroding. The sediment transported could origin from offshore or from sediment washed out by the Incomáti river. As described in section 8.3.3 the tip of Macaneta spit has a trend to extend in southeast direction with erosion taking place at the southwestern side of the tip. The eroded sediment seem to be deposited in the shallows just southeast of tip and could serve as the bar feeding the littoral drift along the spit.

From Figure 49 it is seen that the incoming waves propagate almost perpendicular to the beach face, in Table 5 it is presented how many degrees the coastline orientation has to be altered to reach an equilibrium orientation with a yearly net transport equal to zero.
The calculated equilibrium orientations of the shoreline differ substantially from the actual orientation at many sections emphasizes the northward littoral drift along the spit.

During the field investigation of the site a simple experiment of longshore drift was conducted by letting a floating object get transported by the currents during a limited time interval. The result from the experiment indicated a southward littoral drift along the spit. Although the test was carried out at the northern part of the spit, observations during the cross-shore measurements indicate a southward littoral drift present at the southern parts of the spit as well.

The section F is located close to the end of the spit, where currents and waves from the Incomáti river, Maputo Bay and the Indian ocean meet. The littoral drift is therefore very hard to model correctly and other processes excluded in the longshore model influence the sediment transport.

Although the findings should be acknowledged uncertainties in the result are significant and sources of errors could make up a major part of the degrees differing the actual coastline from the calculated equilibrium. Major sources of error for the shoreline orientation are the wave directions generated by EBED. Wave data was extracted off Macaneta Peninsula at locations where the depth profile exceeded 12m, which corresponded to a distance of about 5 -10km off the coast, closer to the coastline in north and further out in south, see nautical chart in Appendix IV. At this depth the refraction effect from the spit is very limited. As the longshore model assume the bathymetric contour lines parallel to the coastline orientation resulting littoral transport at especially section F will be of a big uncertainty do to the complex bathymetry offshore the section. The longshore model might work fine in the northern part of the spit, but with less satisfaction in the southern part, section 7.3.4.

11. Modeling of cross-shore processes

By modeling the cross-shore processes of the surveyed beach sections at Macaneta spit it is possible to simulate the shoreface profile evolution and discover scenarios and events when the spit integrity is at risk. The computation was conducted in order to simulate the cross-shore response of the spit barrier to wind, waves, and water level. Output wave data from EBED was used for wave height and period in the simulation. The water level was represented by tidal data extracted from WXTide32, software featuring information of sea stations worldwide. Wind-data could not be obtained for the area, therefore a coefficient to represent the wind action of the region was determined empirically to match the present state of the beach.

The model used for simulation of cross-shore response originates partly from models describing the subaerial and subaqous portion of the beach profile (Hansson, Larson, & Kraus, 2010; Larson, Hansson, & Palalane, 2013) complimented by a model for overwash (Larson, Donnelly, Jiménez, & Hanson, 2009). The model focuses on simulating the cross-shore movement of predefined positions for the berm (y_B), dune seaward (y_S) and dune landward (y_L) due to cross-shore material exchange. The cross-shore profile has a predefined appearance, schematized as in Figure 53; with a subaqueous slope determined by a Dean equilibrium profile and the material for transport stored in a bar with volume (V_B).

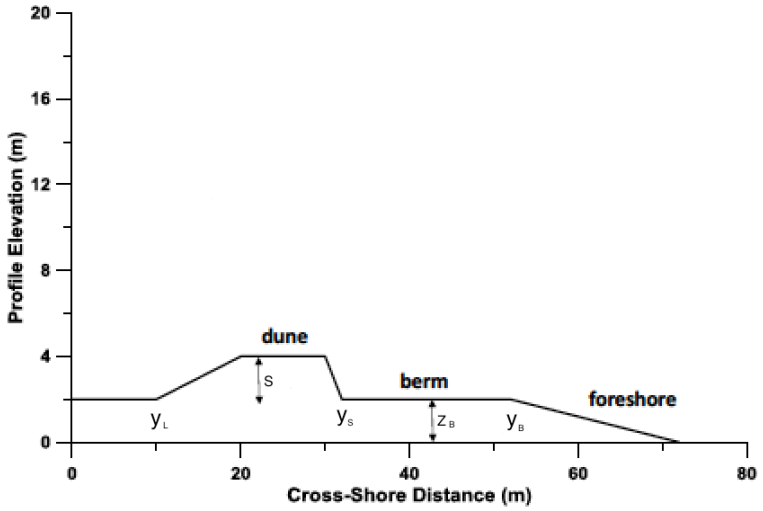

Figure 53. Schematized cross-shore profile used in the model.

11.1 Theoretical formulation

The model considers dune erosion and accretion of the dune seawards and landwards, both as a result of transport due to impact of incoming waves as well as wind-blown sediment.

Dune erosion due to uprushing waves is calculated using the impact model (Overton & Fisher, 1988) modified as formulated in (Larson, Erikson, & Hanson, 2004):

$$\Delta V_E = 4A(R - z_B)^2 \frac{\Delta t}{T} \qquad (11.1)$$

where:
ΔV_E = eroded volume sediment during a specific time [m^3/m].
R = Runup height [m].
z_B = height of berm above mean sea level [m].
Δt = time [s]
T = wave period [s]
$A = 2{\times}10^{-4}$, empirical dune impact coefficient.

The erosion of the dune is governed by the size difference of R and z_B. For a runup not reaching over the berm ($R < z_B$) there will be no dune erosion, while a runup larger than the height of the berm ($R < z_B$) will cause erosion. In the case of a runup larger than the height of dune foot

and dune combined ($R > s + z_B$) an overwash event occur. The height of the runup is determined by:

$$R = C_R\sqrt{H_0 T} \tag{11.2}$$

where:
C_R = 0.158, empirical coefficient.
H_0 = significant wave height [m].

In the case of an overwash event a portion of the uprushing wave will pass over the dune to the landside. The eroding effect of such event will therefore be reduced according to:

$$\Delta V_E = 4A(R - z_B)\frac{\Delta t}{T} \tag{11.3}$$

The volume of sediment transported over the dune (ΔV_L) and the volume transported offshore (ΔV_S) are expressed as:

$$\Delta V_L = \frac{\Delta V_E}{1+\alpha} \tag{11.4}$$

$$\Delta V_s = \alpha\frac{\Delta V_E}{1+\alpha} \tag{11.5}$$

where:
α = a coefficient expressing the portion of material overwashed, determined by following equation:

$$\alpha = \frac{\frac{R-z_B}{s}-1}{A_{over}} \tag{11.6}$$

where:
A_{over} = an empirical constant. Based on a study of field data it was approximated to 3 (Larson, Donnelly, Jiménez, & Hanson, 2009).

The constructing process of the dune is given by wind-blown sand. The resilience of the dune is determined by the size of the wind-blown transport rate. For the case at hand wind speed and other wind properties are unknown and therefore the wind-blown transport rate is given an empirical value to reflect the conditions at Macaneta in best possible way.

Erosion and accretion of the dune are to counteracting forces working in order to maintaining a balance. For some areas the eroding force might be stronger and breaching of the cross-shore profile will occur. In the model, breaching of the profile due to overwash and erosion refer to the volume of the dune and breaching is considered to occur when 90% of the dune has eroded away (Larson, Donnelly, Jiménez, & Hanson, 2009).

11.2 Model implementation and simulation

Time series of wave height, wave period and water level for every third hour were used as input to the model. For the wave heights and periods the output from the wave propagation model EBED was used. Tidal data was extracted from WXTide32, a software featuring information of sea stations worldwide. The tidal data available represented the conditions for Maputo bay and was scaled by a factor of 0.75 in order to match earlier studies in the region of Macaneta (de Boer, Rydberg, & Saide, 2000; DHI, 2013). Consequently the tidal variations considered in the model fluctuated between -1.46m and +1.52m with reference to mean sea water level. It could be discussed how accurate the assumption of scaling the tidal series with a factor 0.75 is, however it should be noted that the tide levels provided by WXTide32 are not observed either. The values are calculated based on tidal positions at Durban, South Africa. By comparing with both previous studies and existing tidal forecasts of Maputo it was decided that a tidal range of about 3m gave a better representation than a range of 4m. Other assumed values together with measured input values of the profiles and calculated values when running the model are presented in the Appendix V.

The simulation was computed for the two most narrow sections A and E, where the risk for breaching was considered the highest. Results from the EBED model at offshore points corresponding to these two sections were used as wave data input.

The model utilizes a schematized profile of the cross-shore, featuring berm and dune. When schematizing section A, which is lacking a dune, an assumed profile based on the measurements surveyed was created. Figure 55 present the schematized profiles used in the model.

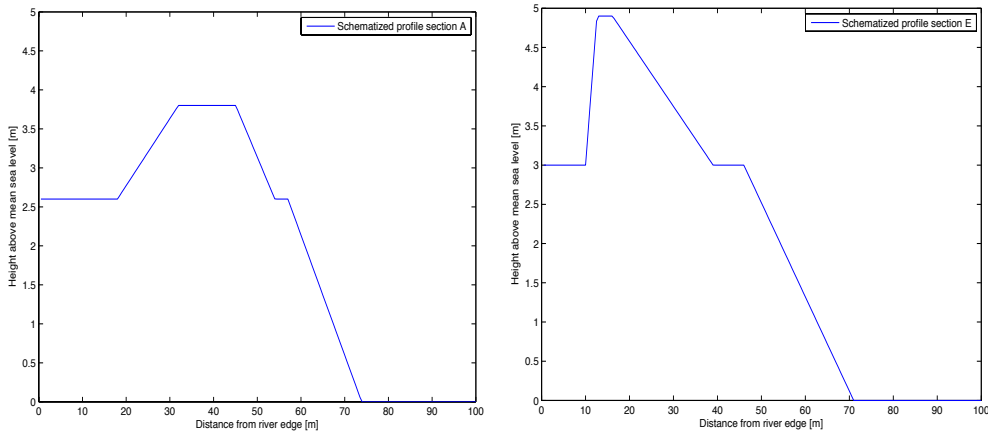

Figure 54. Schematized cross-shore profiles for section A (left) and E(right). The datum used represent the mean sea level.

The positions of the dune foot landwards in the schematized profiles do not reflect the reality. However, the position is used solely to describe slope and width of the dune and variations of the dune foot position confirms that sediment has been transported across the dune, which gives is an indication and quantification of overwash events.

The cross-shore sediment transport was calculated for the years 2005 to 2015 with focus on monitoring the horizontal movement of berm, dune foot on landside and dune foot on seaside. The results generated contain values of the volume flux of dune and bar over time together with the migrating dune position. In Figure 55 and Figure 56, representing section A and E respectively, the dune foot fluctuations on both seaside and landside together with berm migration are presented for the years 2005-2015. Also displayed in the figures are overwash events for the time period.

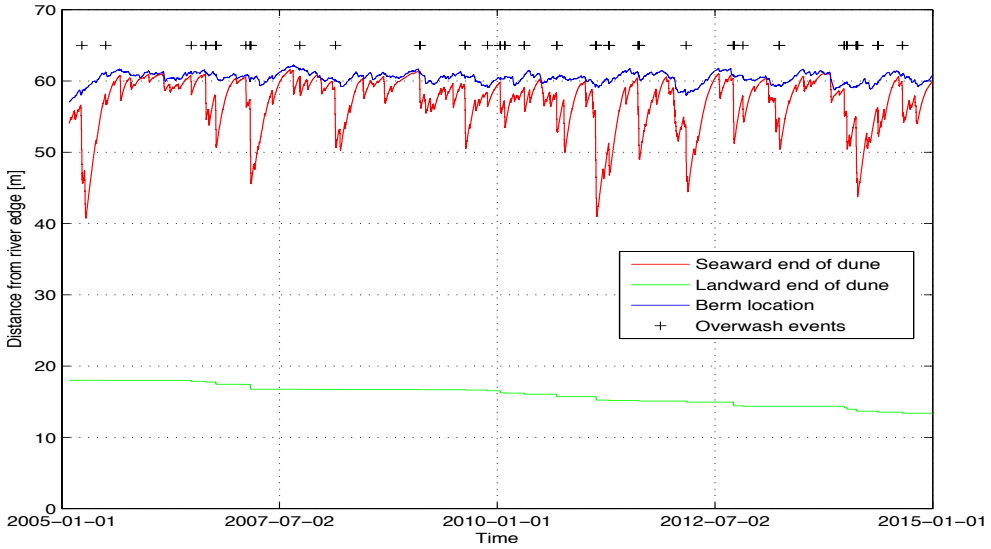

Figure 55. Displayed are the migration pattern of the dune and berm at section A for the years 2005-2015. Marked along the time line with plus-marks are overwash events.

From the graph in Figure 55 it is seen that the position of the berm and dune are in constant change and that incoming waves and wind-blown sediment both carry away and deposit sediments, affecting both slope of the beach and width of the berm and dune. The accreting and eroding processes at both berm and dune seem to be in equilibrium and the position of the beach features are oscillating around a standard state.

No less than 67 overwash events were modeled to occur at section A during the 10 years simulated timeseries. However, the amount of overwashed sediments during the events is low with a total volume of 5,5 m^3/m during the simulated period. The results are indicating a slow successive migration of the landward end of the dune towards the riverbank.

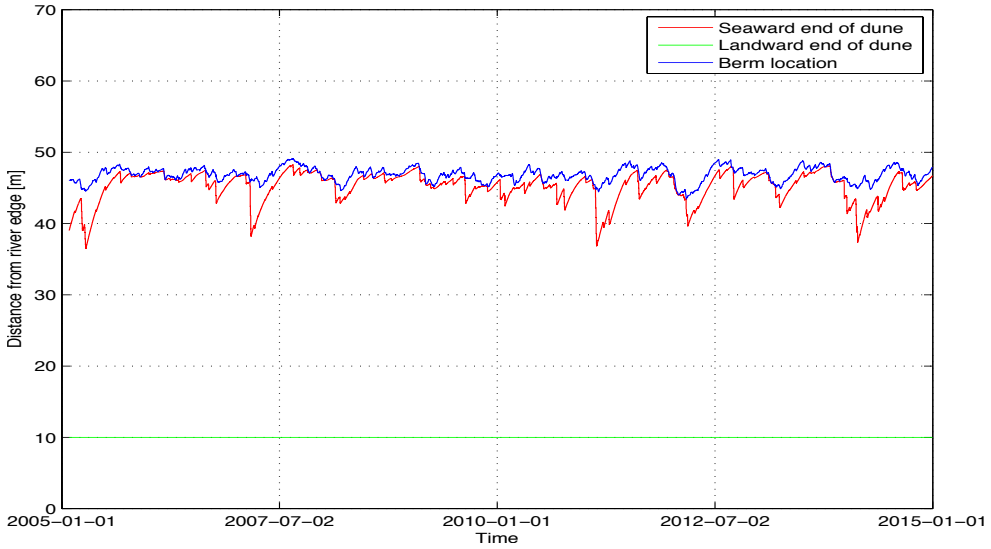

Figure 56. Displayed are the migration pattern of the dune and berm at section E for the years 2005-2015. No overwash events occurred during the simulated period.

As in the case of section A the dune and berm position at section E are in constant change but seem to be oscillating around an equilibrium. At the section no overwash events occurred, leaving the position of the landward end of the dune unaffected.

By comparing the migration pattern of both sections it can be seen that dune erosion at the two sections coincide in time. Although, erosion at section A is significantly stronger than at section E, possibly explained by a higher wave climate at section A together with a lower located dune.

An interesting observation is detected when comparing profiles and number of overwash events with satellite images. Section A, more prone to overwash, according to the cross-shore model has a dune continuously extending towards the river while at section E the dune foot riverwards is constant. However, by looking at satellite images with focus on the dune scarp at the riverside, section A has no trend of continuous dune migration while section E has migrated around 50m towards east during 2003 until 2014. This could be explained by the fact that the model does not take into consideration the effect of the Incomáti River flowing on the backside of the spit. It could be assumed that the overwashed sediments at section A do not feed an expanding isthmus riverwards but rather counteracts erosion from the river at the site. Overwashed sediment gets transported away and the position of the riverbank maintains an equilibrium position. Nevertheless, this

reasoning should imply that the beach would erode due to loss of sediments. According to analysis of satellite and aerial images no indications of erosion is seen. The probable reason is that the amount of sediment transported by littoral drift is much larger than what is being lost to the river, and will re-establish the beach. At section E no sediments are transported cross the dune towards the river, thus the isthmus lack a counteracting process and erosion take place.

Since no monitoring of the beach profile at Macaneta exist it is hard to calibrate a model to represent the reality. It is very difficult to know if overwash events take place on a regular basis, if they are rare or even non-existent. From the sediment analysis collected at section A it was nevertheless found that the sediment distribution at the river bed contained mainly sand and corresponded well with the grain size distribution of samples taken at the dune and beach of the section. Moreover from satellite images it was observed that what appears to be overwashed sediments were seen on the river bank at section A during several occasions between the years 2003 and 2015. Subsequently it can be assumed that there is a significant supply of sediments from the seaward side to the riverward side at the section, which could indicate the occurrence of overwash events at the site. Moreover, according to statements from local residents interviewed by DHI (2013) there have been some episodes of overwash of the isthmus, which may occur several times some years while during other years be completely absent.

The Runup-coefficient (C_R) used in the model, regulating the friction acting on an uprushing wave, was determined by laboratory studies and field data. The value was determined from cases with waves with significantly shorter wave periods prominent than at Macaneta. Since the runup height is influenced by the wave period, equation 11.2, the value of the coefficient might not correspond to the situation at Macaneta and thereby result in more overwash events than what is actually the case.

12. Discussion

12.1 Longshore evolution and coastline orientation

The waves approaching the Macaneta Coastline mainly derive from south to southeast, section 9.1. As the waves pass Inhaca Island, move across Danae shoal and propagate into shallow water the waves are diverted to the west and the wave height decreases significantly, section 9.3. According to longshore modeling of the nearshore waves the incident waves at Macaneta spit create a northward littoral drift up to section A, section 10.2. It can be argued whether or not this result is reliable, in an earlier study the coastline orientation was considered at equilibrium and during the field investigation of the site a southward littoral drift was identified. The wave data results from EBED could pose a significant uncertainty since the resulting waves are extracted from a coarse 200x200m grid and 5-10km off the coast where refraction has little impact on the directions. Furthermore the simplified bathymetric profile linearly decreasing perpendicular to the coastline orientation, which is used in the longshore transport model, is not in conformity with the reality and the EBED model does not take storm surges and tidal variations into account. A constant sea level result in less dissipation of energy at Danae shoal at high tide and more energy dissipated during low tides.

Analyses of the shoreline position from satellite images over time indicate that Macaneta Spit has been migrating eastwards during the last decade, section 8.3.3. The movement is largest in the south, decline further north and is considered non-existent in the northernmost parts.

12.2 The risk of permanent breaching of the spit

The cross-shore model did not result in any breaching events at the most narrow sections of the spit, section A or E .The risk of a permanent breaching is however imminently and should be considered as a possible scenario in the future.

According to observations of satellite images, sediment distribution analyses and the cross-shore model overwash events occur frequently at the northern isthmus, section A, and that the dune of the section is in a

stable equilibrium, neither migrating nor eroding, section 12.2. Even though the overwash events at section A seem to maintain a stable equilibrium with the riverbank evolution, the conditions could change in the future and the risk of breaching is therefore significant. The survey focuses on the coastal processes of the ocean and therefore the overwash of seawards waves are in focus when analyzing the risk of breaching, however it should be acknowledged that overflow of the Incomáti River during high discharges or continuous erosion of the riverbank at the isthmus also poses major treats to breaching of the spit.

Although overwash events have occurred during a series of occasions at section A no overwash has created washover channels deep enough to create a permanent connection between sea and river. Shortly after the overwash events have occurred the channels have been filled up by sediment. An overwash event where the washover channel extends below the water level would create a continuous flow of water between sea and river. As observed during the field investigation the water level between river and sea do not agree thereby a gradient is created inducing a strong current across the isthmus, causing the breakdown of the isthmus to accelerate and rapidly erode the sides causing it to widen and form a permanent linkage of the two water bodies.

The condition posing as the highest threat for a breaching event is tropical storms. Even though regular storms generate sever wave conditions offshore, the sheltering effect of Danae shoal maintain a more calm wave condition at Macaneta spit, section 10.3. During a tropical storm surges will be generated, thus raising the seawater level allowing waves crossing Danae shoal to maintain higher energy and accordingly give an increase in wave height at Macaneta. Naturally, tropical storms generate severe wave conditions. The highest waves offshore, exported from the WW3 reanalysis model occurred during the tropical storm of Irina in 2006. In the case of a storm surge occurring during high spring tide the combined effect of high water levels would form a condition most likely to cause breaching of the isthmus.

It is hard to determine the probability of such extreme overwash event caused by tropical storms since no reliable data is available regarding storm surges in the region. The cross-shore model indicated that overwash events occur frequently at the isthmus. Since the height of the waves are underestimated for high water levels this would suggest that

the risk of a critical overwash event resulting in a permanent breaching of the isthmus is significant.

Another section subject to the risk of breaching is section E. The survey indicate that the southern isthmus at section E is subject to massive erosion from the Incomáti River, the width of the vegetated part of the dune has decreased with 30m during the last decade, section 8.3.3. There is an associated risk that the isthmus in the future will form a similar cross-shore profile as for section A. As the isthmus is narrowing due to erosion the dune height probably will decrease, thereby causing overwash events from ocean waves that will decrease the slope of the river dune. Risks of a permanent breakthrough are present at section E in the same way as for section A. The ongoing erosion is especially alarming, if retraction of the riverbank is progressing in the same pace as during the last decade the dune of the isthmus will be gone in the next decade. Consequently there are high risks of breakthrough events at section E if no equilibrium position is found.

12.3 Increased anthropogenic pressure

When the bridge is constructed and the access to the spit increase it is essential to monitor the effects of a higher number of tourists in the area. It is hard to predict the consequences from more tourists in the area, but more activities like launching of boats and vehicles driving along the beach could damage the vegetation and alter the natural sediment movement at the beach and cause new or severe existing erosion problem. The bridge will also make it easier to transport construction material to Macaneta and the development of holiday houses and resorts will probably increase with a higher anthropogenic pressure on the beach. With more tourism in the area there might be suggestions to construct a jetty or similar construction at the beach. This kind of construction should be handled with great concern as they could disturb the longshore transport of sediment, which according to the study seem to be of great importance to prevent permanent overwash channels.

12.4 Future recommendation

With reference to the conducted study further studies of the area are highly recommended, in particular for coastal sections evidently more prone to the risk of breaching.

It is strongly recommended that the Coastal Zone Management unit, CZN, in Maputo closely observe the evolution of the spit. Few studies of the area are carried out and consequently little is known about the evolution of the spit. There are some theories, as presented in the study but these have to be further investigated before being accepted. Regular studies comparing the present state with previous would be of great benefit for the understanding and conservation of the region.

It is of uttermost importance to start with monitoring of the beach as soon as possible, in order to be able to observe trends due to increased tourism pressure in connection with the opening of the bridge. If negative trends are observed due to the impact of a higher tourist concentration in the area protective measures has to be taken immediately.

In order to early detect changes of the conditions at the northern narrow isthmus and take action if necessary, an idea is to install some form of monitoring device to create a record of overwash events. It is most probable that overwash events take place at the isthmus, sometimes even several times per year. However records of the events are scares with the latest during year of 2001 or 2002 and a continuous monitoring would give a better understanding of the overwash events, trends and the associated risk.
If overwash of the spit becomes more frequent the risk of permanent breaching will increase and some kind of protection might be evaluated. However, for the present situation with a stable condition of sediment transport at the isthmus no protection is considered required.

13. Conclusions

Based on the findings during the study it has been concluded that:

- The southern part of the spit is migrating eastwards.

- The shadowing effect of Inhaca and the sheltering effect of Danae shoal has major effects in directing the waves westwards and maintaining a moderate wave climate nearshore Macaneta spit respectively.

- There are several overwash events occurring at the northern isthmus of Macaneta spit, according to observations from satellite images and at site. However no permanent connection between sea and river has been made and the width of the section is considered as in a stable equilibrium. The risk of a permanent breaching is however imminently and should be considered as a possible scenario in the future if no precautions are taken.

- The isthmus at section E is eroding and if progressing at same pace as up to today the vegetated dune of the isthmus will be gone in the next decade. Consequently followed by high risk of breaching.

- Modeled results indicate a strong northward littoral drift along Macaneta spit up to section A where a counteracting longshore transport exists. The findings regarding the littoral drift should be acknowledged but uncertainties in the result are significant, both prior research and several other observations are conflicting with the findings.

With reference to the conducted study further studies of the area are highly recommended, in particular for coastal sections evidently more prone to the risk of breaching. Regular studies comparing the present state with previous would be of great benefit for the understanding and conservation of the region. Especially when an increased tourism pressure in connection with the opening of the bridge, could have negative effects of Macaneta spit.

Bibliography

Aerts, J., Hassan, A., Savenije, H., & Khan, M. (2000). Using GIS tools and rapid assessment techniques for determining salt intrusion: STREAM, a river basin management instrument. *Physics and Chemistry of the Earth* (25), p. 265-273.

Böhlmark, J. (2003). *Meretrix meretrix as an Indicator of Heavy Metal Contamination in Maputo Bay.* Uppsala Universitet, Department of Earth Science, Uppsala.

Bird, E., & Lewis, N. (2015). *Beach Nourishment.* (Springer, Red.) Australia.

Brockway, R., Bowers, D., Hoguane, A., Dove, V., & Vassele, V. (2006). A note on salt intrusion in funnel-shaped estuaries: Application to the Incomáti estuary, Mozambique. *Estuarine, Coastal and Shelf Science* (66), p. 1-5.

Canhanga, S., & Dias, J. M. (2005). Tidal characteristics of Maputo Bay, Mozambique. *Journal of Marine Systems , 58*, p. 83-97.

CEM. (2008). *Engineer Manual - EM 1110-2-1100.* (D. o. Army, Red.) Qashington DC, USA.

CERC. (1984). *Shore Protection Manual.* The Coastal Engineering Research Center (CERC) of the U.S. Army Engineer .

Chemane D, Motta H, Achimo M. (1997). Vulnerability of costal resources to climate changes in Mozambique: a call for integrated coastal zone management. i *Ocean & Costal Management, Vol 37* (p. 63 – 83).

CIA. (20/6 2014). *Central Intelligence Agency - World Factbook*. Retrieved from: https://www.cia.gov/library/publications/the-world-factbook/geos/sw.html, at 18/10 2014

Climatemps. (2015). Retrieved from Climatemps: http://www.maputo.climatemps.com/ at 28/1 2015

de Boer, W. F., Rydberg, L., & Saide, V. (2000). Tides, tidal currents and their effects on the intertidal ecosystem of the southern bay, Inhaca Island, Mozambique. *Hydrobiologia , 428*, p. 187-196.

de Freitas, A. J. (1984). The Penaeoidea of Southeast Africa. I. The Study area and key to the southeast African species. *South African Association for Marine Biological Research, Investigational Report No. 56*.

DHI. (2013). *Macaneta, Coastal and river bank erosion.*

DLR. (2/2 2012). *Center of Satellite Based Crisis Information.* Retrieved from Geographic Reference Map - Overview - Maputo - Mozambique: http://www.zki.dlr.de/map/2200 at 15/5 2015

European Commission. (22/1 2015). *European Commission, Enviromment*. Hämtat från European Commission, Enviromment: http://ec.europa.eu/environment/iczm/home.htm at 30/1 2015

Fanos, A. M. (1995). The Impact of Human Activities on the Erosion and Accretion of the Nile Delta Coast. *Journal of Coastal Research , 11* (3), p. 821-833.

Google Earth. (30/8 2014). *Google Earth Pro 6.1.2.2041 (beta)* . Retrieved from Maracuena Region, Maputo Mozambique. 25° 50'S, 32° 44'E: http://www.google.com/earth/index.html at 22/3 2015

Halcrow. (2014). *SANDS - software description version 7.2*. Retrieved from Sediment transport rates: http://www.halcrow.com/sands/documents/manuals/html/index.html?kamphuistransportrates.htm at 7/5 2015

Hanson, H., & Kraus, N. C. (1989). *GENESIS: GENERALIZED MODEL FOR SIMULATING SHORELINE CHANGE.* Washington, DC: US Army Corps of Engineers.

Hansson, H., Larson, M., & Kraus, N. (2010). Calculation of beach change under interacting cross-shore and longshore processes. *Journal of Coastal Engineering , 57*, p. 610-619.

Herrington, T. (2012). *All about waves.* Stevens – New Jersey Sea Grant Coastal Processes Cooperative Extension.

Hoguane, A. M. (2000). Salt intrusion in the Incomáti River. In: Proceedings of the Second National Conference on Coastal Zones Research. Maputo, 29th of September 2000. *CDS-ZC/MICOA/ SEACAM/UEM* , p. 29-35.

Hoguane, A., & Meulen, F. v. (2010). Incomáti delta. i M. M. Tom Bucx, *Comparative assessment of the vulnerability and resilience of 10 deltas.* Deltares.

INHANINA. (2010). Hydrographic map of Maputo Bay. Maputo, Mocambique.

Instituto Hidrografico. (2015). *Previsão de Marés - Porto de Maputo*. Retrieved from http://www.hidrografico.pt/mocambique.php?prodarea=6&prodid=10 at 31/3 2015

Johansson, L. (1997). *Coastal Management - Coastal Sector Coordination and Intergrated Coastal Area Planning.* Stockholm: The Sida Marine and Coastal Initiative.

Jury, M. R., & Pathack, B. (1991). A Study of Climate and Weather Variability over the Tropical Southwest Indian Ocean. *Meteorology and Athmospheric Physics , 47*, p. 37-48.

Khalili, B. (2007). *Monitoring of Incomáti River Basin with Remote Sensing.* Division of Water Resources Engineering and Department of Building and Environmental Technology. Lund Univesity.

Komar, P. (1976). *Beach processes and sedimentation.* Englewood Cliffs, NJ, USA: Prentice-Hall, Inc.

Komar, P. D. (1988). *Beach Processes and sedimentation.* New Jersey, USA: Prentice- Hall.

Kraus, N. (1999). Analytical model of spit evolution at inlets. *Proceeding Coastal Sediments* , p. 1739-1754.

Langa, J. V. (2007). Problemas na zona costeira de Moçambique com ênfase para a costa de Maputo. *Revista de Gestão Costeira Integrada , 7* (1), p. 33-44.

Larson, M., Donnelly, C., Jiménez, J., & Hanson, H. (2009). Analytical model of beach erosion and overwash during storms. *Journal of Maritime Engineering , 164*, p. 115-125.

Larson, M., Erikson, L., & Hanson, H. (2004). An analytical model to predict dune erosion due to wave impact. *Journal of Coastal Engineering , 51*, p. 675-696.

Larson, M., Hansson, H., & Palalane, J. (2013). Simulating cross-shore material exchange in long-term coastal evolution models. *Proceeding of Coastal Dynamics , 2013*, p. 1037-1048.

Lutjeharms, J. R., & da Silva, A. J. (1988). The Delagoa Bight eddy. *Deep-Sea Research , 35* (4), p. 619-634.

Madsen, B. (1995). *Danish Watercourses - Ten Years with the New Watercourse Act.* Atmark: Ministry of Environment and Energy.

Magos, M. (2002). *Erosão costeira de Maputo e arredores: O exemplo da Macaneta.* Licenciatura Thesis, Universidade Eduardo Mondlane. .

Makoye, K. (at 31 January 2012). Salty soils drive Tanzanian farmers into forest reserve. *Thomson Reuters Foundation* .

Mangor, K. (2004). *SHORELINE MANAGEMENT GUIDELINES.* Hørsholm, Atmark: DHI Water & Environment.

Mase, H. (2001). MULTI-DIRECTIONAL RANDOM WAVE TRANSFORMATION MODEL BASED ON ENERGY BALANCE EQUATION. *Coastal Engineering Journal , 43* (4), p. 317-331.

Morang, A., Larson, R., & Gorman, L. (1997). Monitoring the Coastal Environment; Part III: Geophysical and Research Methods. *Journal of Coastal Research , 13* (4), p. 1064-1085.

Moreira, M. E. (2005). A dinâmica dos sistemas litorais do sul de Mocambique durante os últimos 30 anos. *Revista Finisterra* (79), p. 121–135.

Moreira, M. E. (2010). Mozambique. i E. C. Bird (Red.), *Encyclopedia of the world's coastal landforms.* London: Springer Science and Business Media.

Nagle, G. (2000). *Advanced Geography.* USA: Oxford University Prep.

Nam, P. (2010). *Numerical Model of Beach Topography Evolution due to Waves and Currents - Special Emphasis on Coastal Structures.* Water Resources Engineering. Lund: Lund University.

Nam, P., & Larson, M. (2010). Model of Nearshore Waves and Wave-Induced Currents around a Detached Breakwater. *J. Waterway, Port, Coastal, Ocean Eng , 136* (3), p. 156-176.

NASA. (2012). *Hurricane Season 2012: Tropical Cyclone Irina (Indian Ocean).* Retrieved from Hurricanes/Tropical cyclones - Latest storm images and data from NASA: http://www.nasa.gov/mission_pages /hurricanes/archives/2012/h2012_Irina.html at 15/5 2015

NWS. (2010). *National Weather Service*. Retrieved from Wave Watch III Model: http://polar.ncep.noaa.gov/waves/

Overton, M., & Fisher, J. (1988). "Laboratory investigation of dune erosion. *Journal of Waterway, Port, Coastal, and Ocean Engineering , 114* (3), p. 367-373.

Palalane, J., Larson, M., Hanson, H., & Juízo, D. (2015). Coastal Erosion in Mozambique: Governing Processes and Remedial Measures. *Journal of Coastal Research , In press*.

Portman, M. E., & Fishhendler, I. (2011). *Towards Integrated Coastal Zone Management: A Toolkit for Practitioners.* Jerusalem: Hebrew University.

Post, J. C., & Lundin, C. G. (1996). *Guidelines for integrated coastal zone management.*

Pugh, D. (1996). *Tides, Surges and Mean Sea Level.* Swindon, UK: John Wiley & Sons.

Quartly, D. G., & Srokosz, M. A. (2004). Eddies in the Southern Mozambique Channel. *Deep Sea Research II , 51* (1-3), p. 69-83.

Ruby, J., Canhanga, S., & Cossa, O. (2008). *Assessment of the Impacts of Climate Changes to Sea Level Rise at Costa do Sol Beach in Maputo – Mozambique.*

SADC. (2010). *Maputo River Basin Pilot report - Final report.* SADC Economic Accounting of Water Use Project . Produced by the project consultant Egis Bceom International.

Saetre, R. (1985). Surface Currents in the Mozambique Channel. *Deep-Sea Research , 32* (12), p. 1457-1467.

Saetre, R., & da Silva, A. J. (1984). The circulation of Mozambique Channel. *Deep-Sea Research , 31* (5), p. 485-508.

Schwartz, R. (1982). Bedform and stratification characteristics of some modern small-scale washover sand bodies. *Sedimentology , 29*, p. 835-849.

Sete, C., Ruby, J., & Dove, V. (2002). *Seasonal variation of tides, currents, salinity and temperature along the coast of Mozambique.* UNESCO (IOC) ODINAFRICA, CENADO.

Suoto, M. (2014). South West Indian Ocean Fisheries Governance and Shared Growth in Mozambique (SWIOFish) - Draft. Maputo: República de Mocambique Ministério das Pescas.

Sverdrup, H. U., Johnson, M. W., & Fleming, R. H. (1942). *The Oceans Their Physics, Chemistry, and General Biology.* New York: Prentice-Hall, Inc.

The Comet Program. (2012). *Rip Currents: Nearshore Fundamentals*. Retrieved from: http://www.meted.ucar.edu/marine/ripcurrents at 11/3 2015

Warwick. (24/11 2011). *Wave energy conversion*. Retrieved from http://www2.warwick.ac.uk/fac/sci/eng/meng/waveenergy/wind_waves.jpg at 23/2 2015

Windfinder. (2015). Retrieved from Windfinder: http://www.windfinder.com/windstatistics/maputo at 28/1 2015

Viola, C. N., Grifoll, M., Palalane, J., & Oliveira, T. C. (2014). Sea wave propagation from offshore to Maputo's coast. Application to longshore sediment transport assessment. *Water Science & Technology , 69* (12), p. 2438-2445.

World Bank and Sida. (1997). *The Journey from Arusha to Seychelles, Success and failures in integrated coastal zone management in Eastern Africa and island states.* Örebro: Graphic Systems AB.

WXTide32. (2015). *WXTide32 - a free Windows tide and current prediction program.* Retrieved from http://www.wxtide32.com/ at 27/4 2015

Young, I. (1999). SEASONAL VARIABILITY OF THE GLOBAL OCEAN WIND AND WAVE CLIMATE. *International Journal of Climatology , 19*, p. 931-950.

Appendix I – Sediment grain size distribution

Figures representing the measured grain size distribution for each cross profile section. In the table corresponding mesh size in mm are presented with US Standrard Sieve sizes.

Table 6. US Standard Sieve sizes presented with corresponding mesh openings.

US Standard Sieve size	Mesh opening (mm)
4	4,76
8	2,38
16	1,19
30	0,595
40	0,42
50	0,297
70	0,21
100	0,149
200	0,075

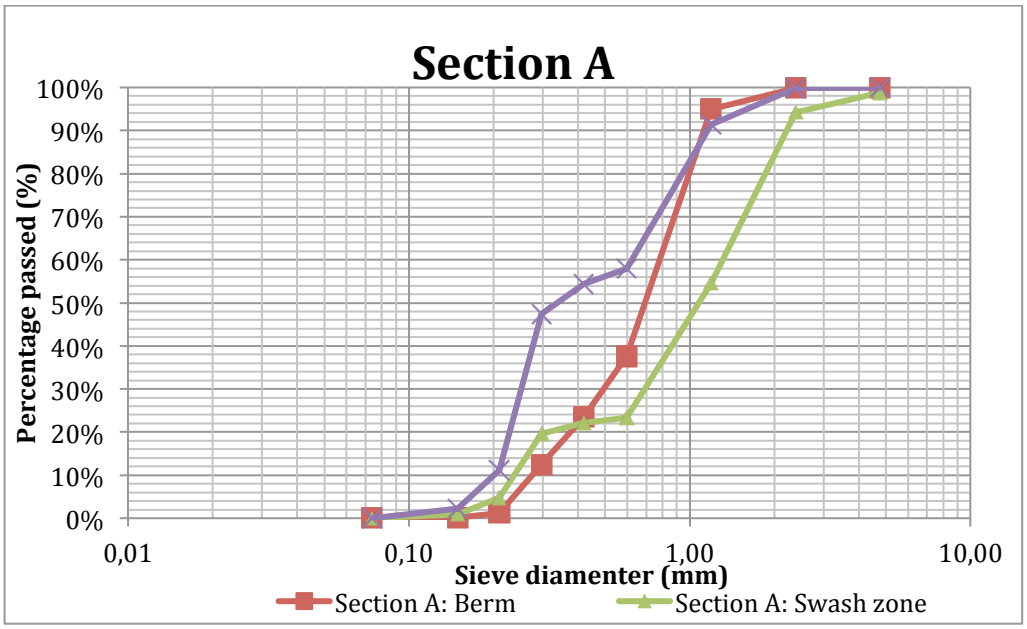

Figure 57. Grain size distribution for section A.

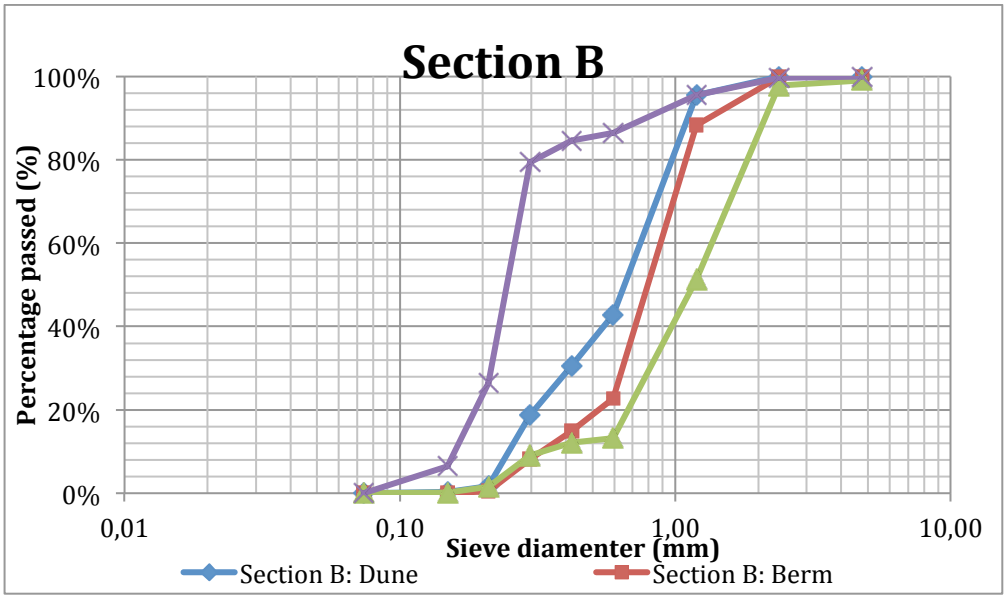

Figure 58. Grain size distribution for section B.

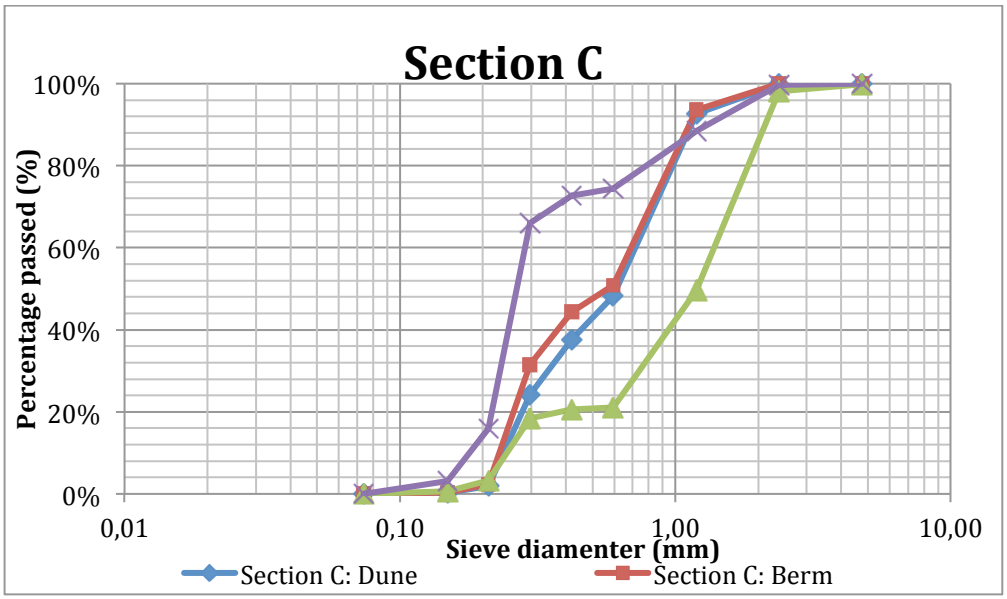

Figure 59. Grain size distribution for section C.

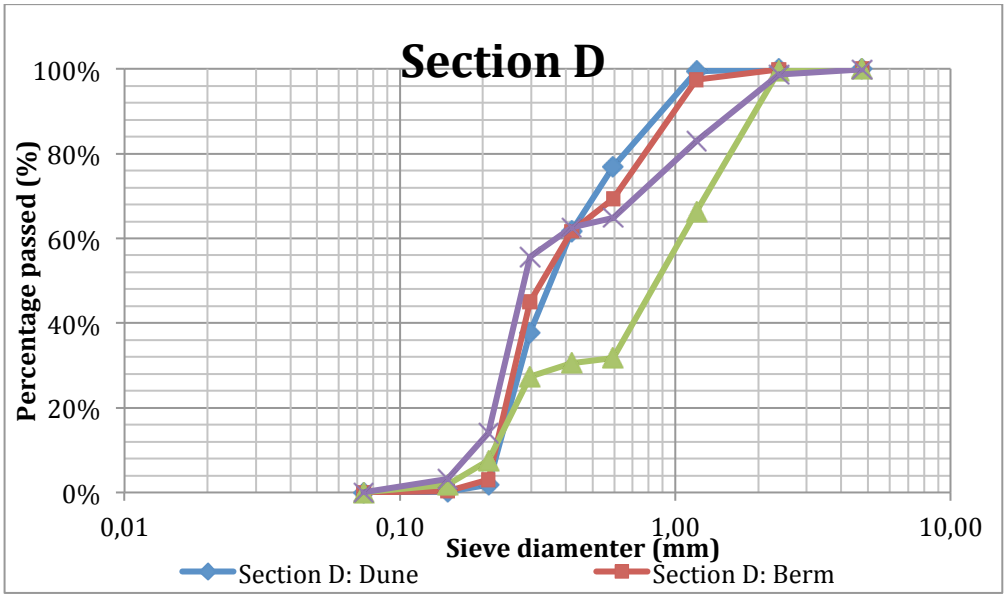

Figure 60. Grain size distribution for section D.

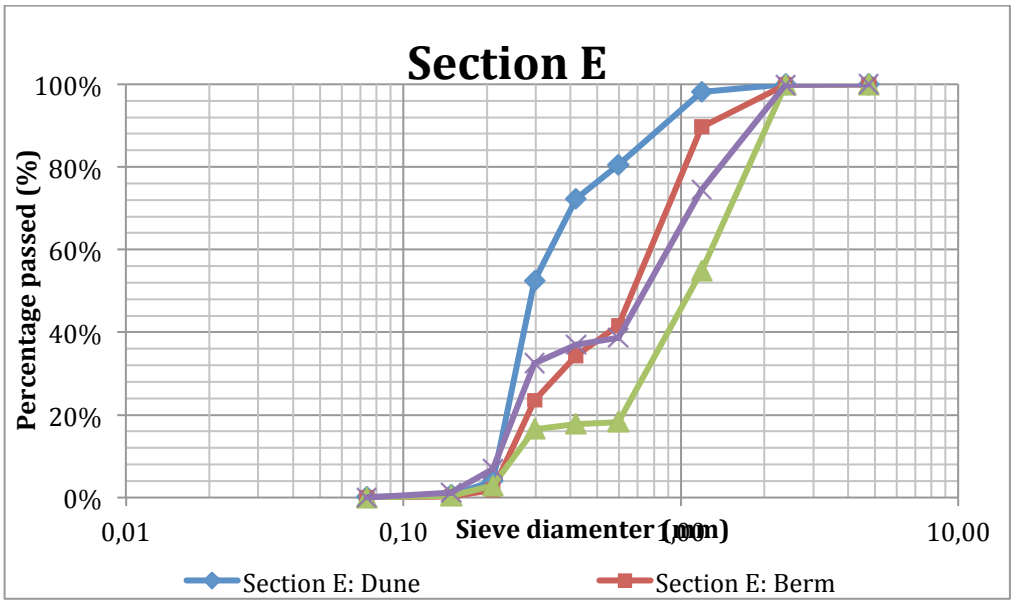

Figure 61. Grain size distribution for section E.

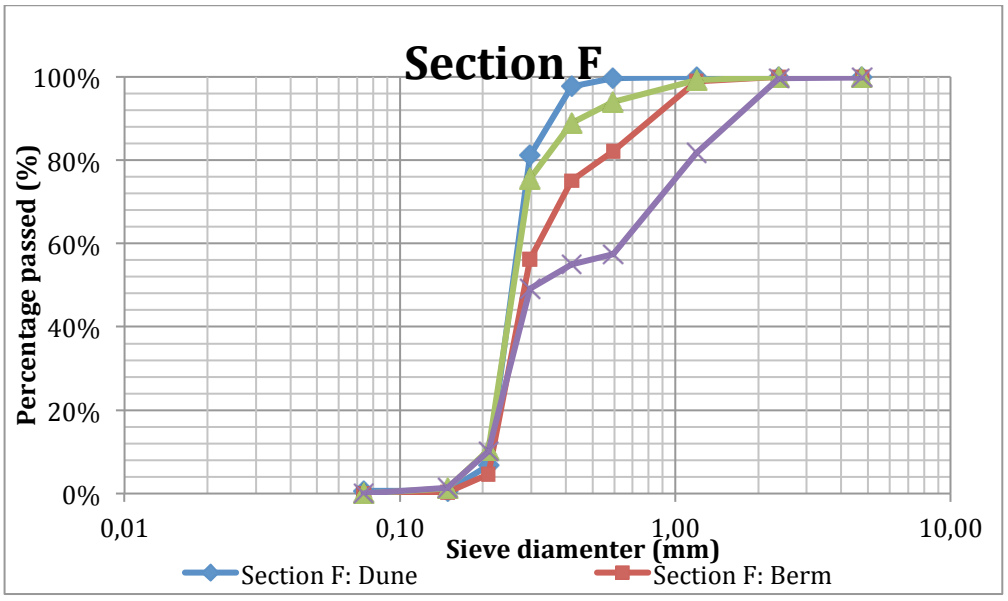

Figure 62. Grain size distribution for section F.

The d_{50}-value was calculated by linear equation in Matlab for points just before and after 50% of the total sediment had passed a certain mesh size:

```
MA =[0 0 0 0; 1.19 0.949 0.595 0.376; 1.19 0.546 0.595 0.234; 0.42 0.544 0.297 0.474]
MB = [1.19 0.955 0.595 0.428; 1.19 0.882 0.595 0.227; 1.19 0.512 0.595 0.131; 0.297 0.794 0.210
0.264];
MC = [1.19 0.926 0.595 0.482; 0.595 0.509 0.42 0.444; 2.38 0.981 1.19 0.496; 0.297 0.659 0.210
0.16];
MD = [0.42 0.616 0.297 0.378; 0.42 0.616 0.297 0.45; 1.19 0.664 0.595 0.317; 0.297 0.556 0.21
0.141];
ME = [0.297 0.524 0.210 0.04; 1.19 0.896 0.595 0.417; 1.19 0.547 0.595 0.182; 1.19 0.744 0.595
0.387];
MF = [0.297 0.81 0.210 0.067; 0.297 0.562 0.210 0.046; 0.297 0.756 0.210 0.105; 0.420 0.55
0.297 0.491];
MA_river = [1.19 0.841 0.595 0.19; 1.19 0.877 0.595 0.15]
ME_river = [1.19 0.898 0.595 0.354; 0.297 0.556 0.21 0.031];
TIP = [0.297 0.866 0.21 0.271; 1.19 0.69 0.595 0.169];
y=0.5
for i=1:4;
   VA=MA(i,:);
   VB=MB(i,:);
   VC=MC(i,:);
   VD=MD(i,:);
   VE=ME(i,:);
   VF=MF(i,:);
   A50(i)=(((y-VA(4))*(VA(1)-VA(3)))/(VA(2)-VA(4)))+VA(3);
   B50(i)=(((y-VB(4))*(VB(1)-VB(3)))/(VB(2)-VB(4)))+VB(3);
   C50(i)=(((y-VC(4))*(VC(1)-VC(3)))/(VC(2)-VC(4)))+VC(3);
   D50(i)=(((y-VD(4))*(VD(1)-VD(3)))/(VD(2)-VD(4)))+VD(3);
   E50(i)=(((y-VE(4))*(VE(1)-VE(3)))/(VE(2)-VE(4)))+VE(3);
   F50(i)=(((y-VF(4))*(VF(1)-VF(3)))/(VF(2)-VF(4)))+VF(3);
end
for i=1:2;
   VA_river=MA_river(i,:);
   VE_river=ME_river(i,:);
   VTIP=TIP(i,:);
   A50_river(i)=(((y-VA_river(4))*(VA_river(1)-VA_river(3)))/(VA_river(2)-
VA_river(4)))+VA_river(3);
   E50_river(i)=(((y-VE_river(4))*(VE_river(1)-VE_river(3)))/(VE_river(2)-
VE_river(4)))+VE_river(3);
   TIP50(i)=(((y-VTIP(4))*(VTIP(1)-VTIP(3)))/(VTIP(2)-VTIP(4)))+VTIP(3);
end
```

Appendix II – Equilibrium bottom profiles

Table 7 Measured cross-shore profile compared with theoretical depth described by eq 8.1

Section	A	B	C	D	E	F
A-value	0,102	0,113	0,133	0,125	0,128	0,093
Mean Square error [m²]	0,107	0,164	0,163	0,052	0,025	0,379
d_{50}mean [mm]	0,08	0,11	0,18	0,15	0,16	0,06

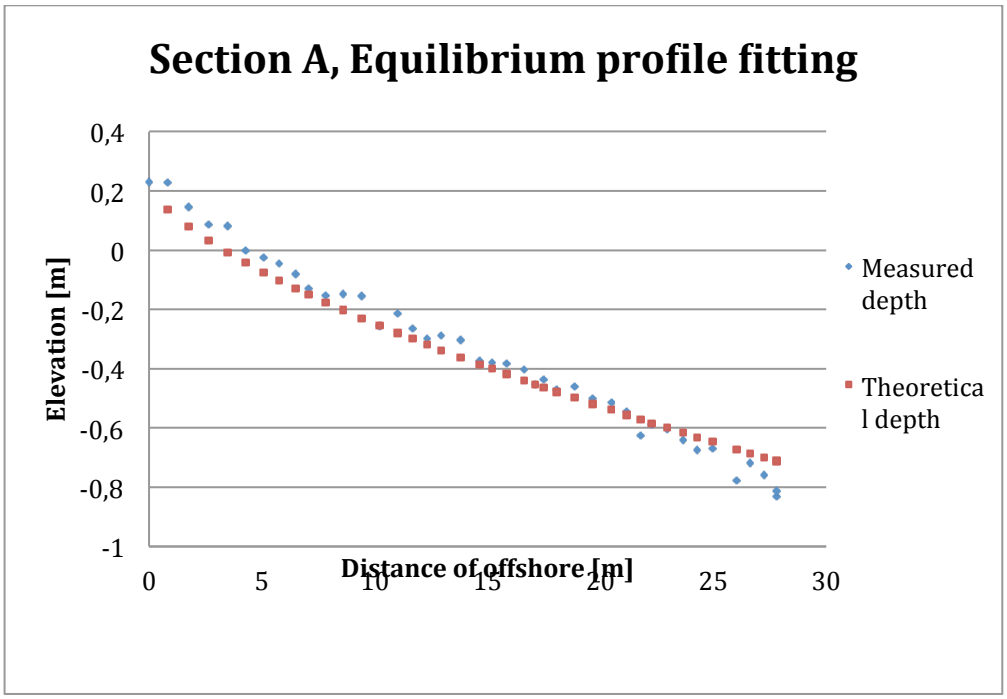

Figure 63 adjusted theoretical depth against the measured depth at section A

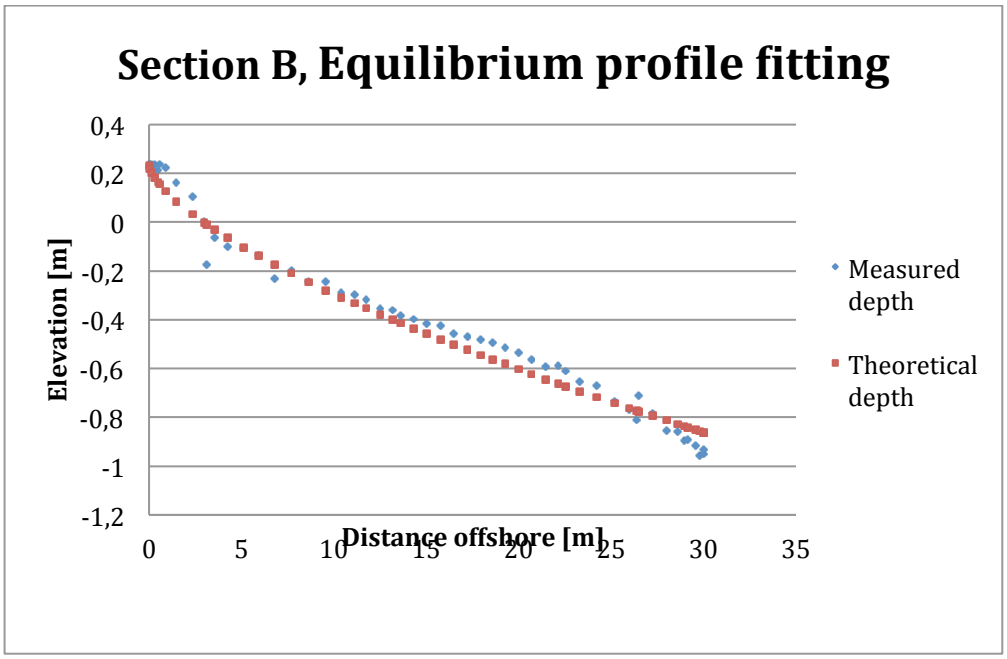

Figure 64 adjusted theoretical depth against the measured depth at section B.

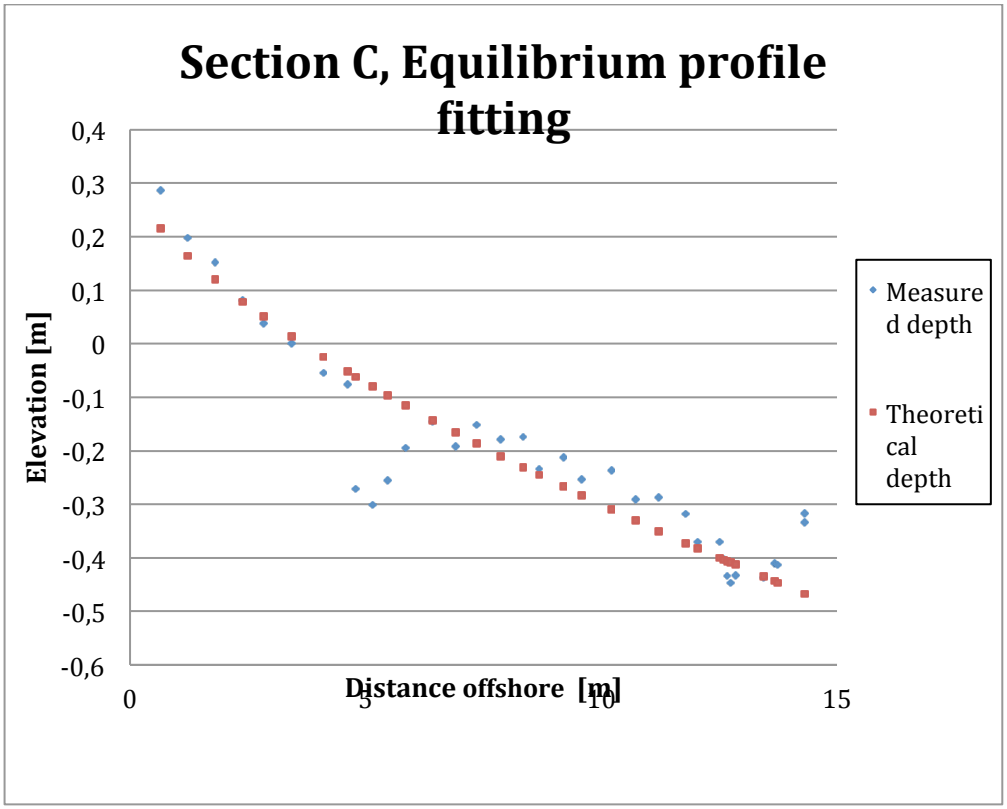

Figure 65 adjusted theoretical depth against the measured depth at section C.

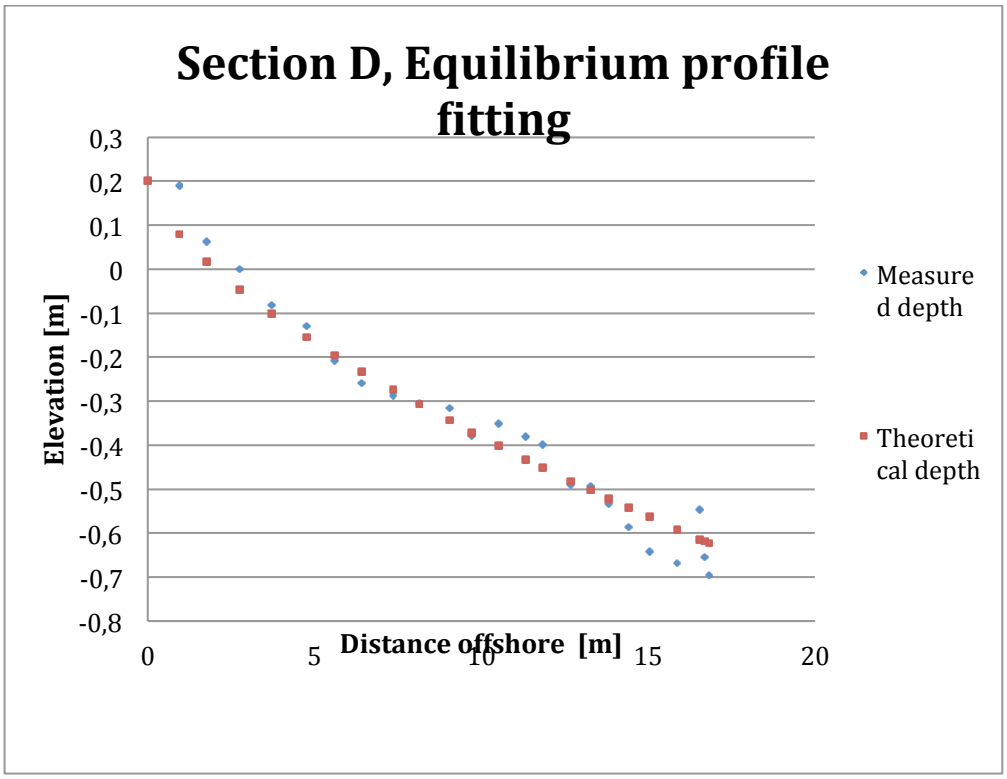

Figure 66 adjusted theoretical depth against the measured depth at section D

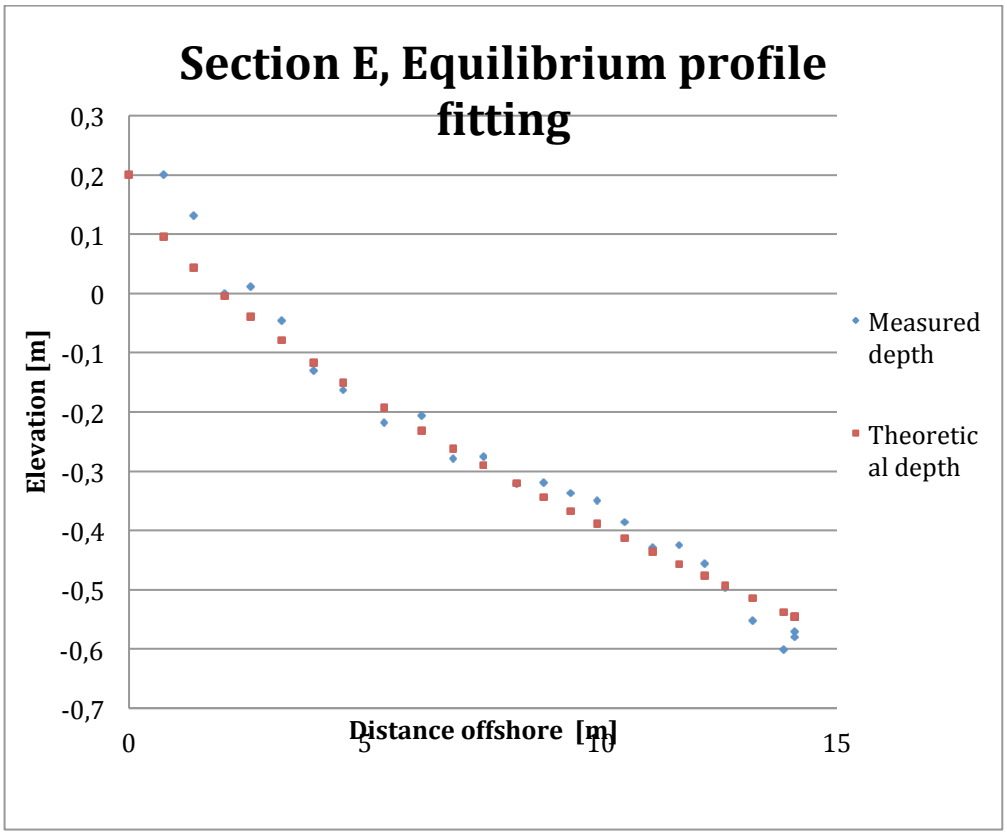

Figure 67 adjusted theoretical depth against the measured depth at section E

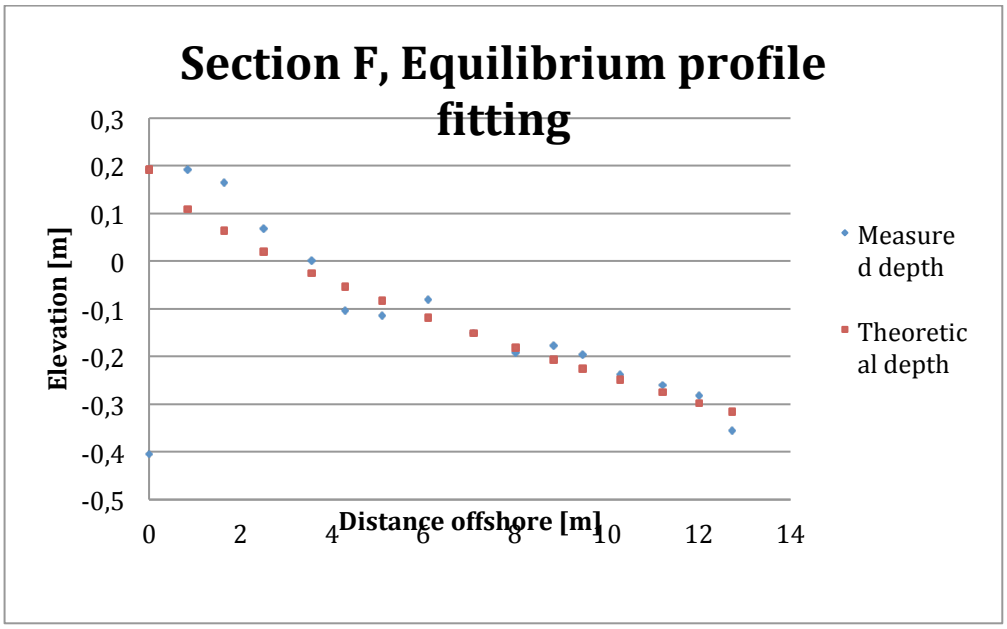

Figure 68 adjusted theoretical depth against the measured depth at section F

Appendix III - Measured shoreline position

The shoreline position measured on 2015-03-17 is presented in the map below.

Figure 69. The recorded shoreline position (red line) from 2015-03-17 displayed on a satellite image from 2014-08-30.

Appendix IV – Bathymetric chart of Maputo Bay

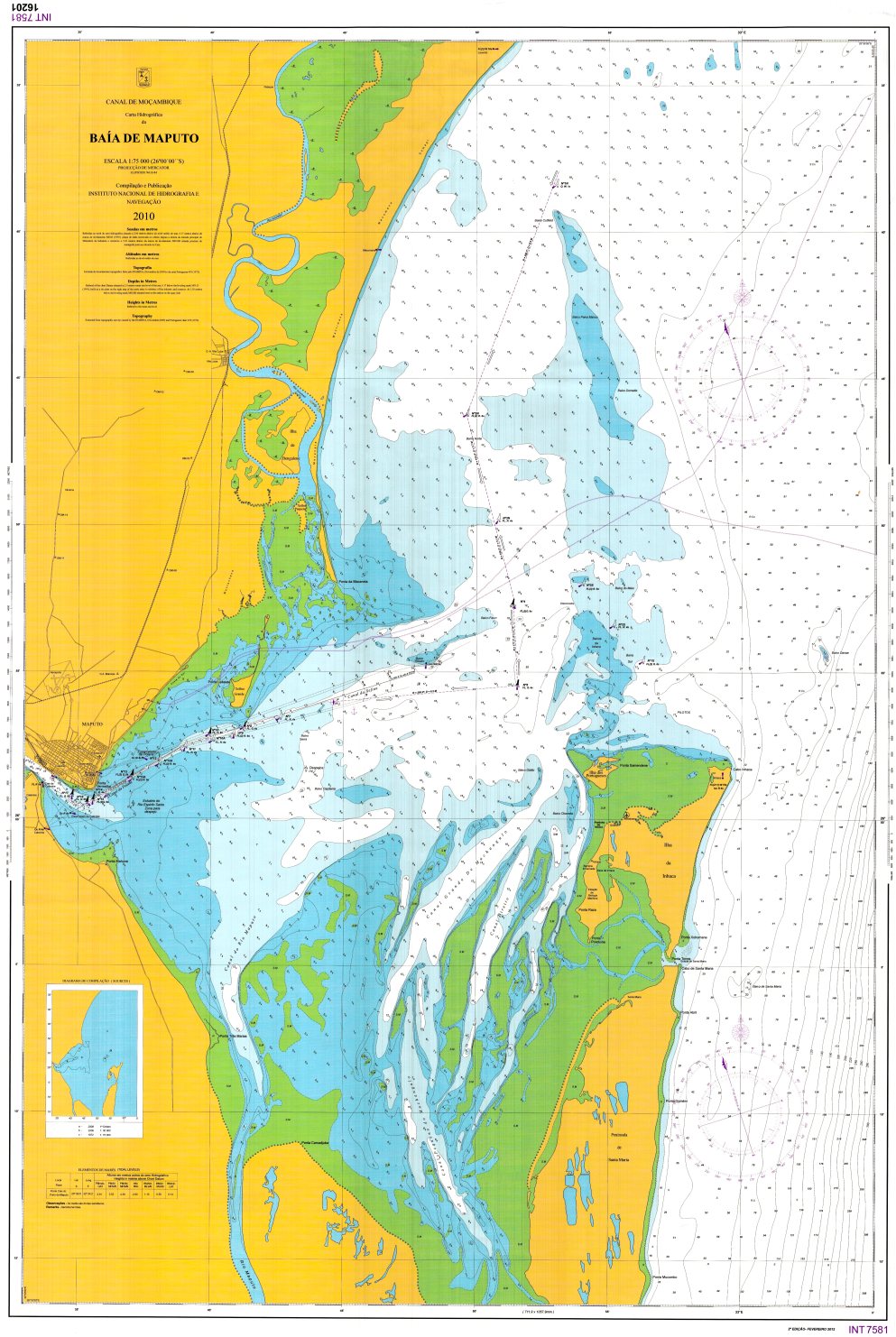

Figure 70 The nautical chart produced by INAHINA.

Appendix V –Cross-shore parameters

Table 8. Parameters used for cross-shore modeling.

Parameter	Value
Initial bar volume	70 m^3
Depth of closure	6 m
Spatial growth rate, wind transport	0.2
Constant wind transport	4 x 10^{-6}
Temperature	20°C